uOttawa

L'Université canadienne
Canada's university

Investigation of Biologically-Produced Solids in Moving Bed Bioreactor (MBBR) Treatment Systems

By

Mohsen Soleimani Karizmeh

Master of Applied Science Thesis

Submitted to the School of Graduate Studies and Research
in partial fulfillment of requirements
for degree of M.A.Sc in Environmental Engineering

Supervisors:
Dr. Robert Delatolla and Dr. Roberto M. Narbaitz

Ottawa-Carleton Institute for Environmental Engineering

Department of Civil Engineering

University of Ottawa

Ottawa, Canada

THE UNIVERSITY OF OTTAWA-FACULTY OF GRADUATE STUDIES

CERTIFICATE OF EXAMINATION

Examining Board

_____	_____
_____	_____
_____	_____

Advisors

Dr. Robert Delatolla and Dr. Roberto M. Narbaitz

The thesis by

Mohsen Soleimani Karizmeh

Entitled

Investigation of Biologically Produced Solids in Moving Bed Bioreactor (MBBR) Treatment Systems

is accepted in partial fulfillment
of the requirements of the degree of
Master of Applied Science (Environmental Engineering)
in the
Department of Civil Engineering

Date: _____ _____

Chairperson of Examining Board

Abstract

Lower production rate of solids in attached growth moving bed bioreactor (MBBR) systems as compared to conventional activated sludge (AS) systems makes them an attractive choice for municipal wastewater treatment (Ødergaard et al. 1994). However, the production of biologically-produced solids in MBBR systems is currently not well defined and requires additional investigation.

Three identical MBBR reactors were operated under the same dissolved oxygen (DO) concentration, influent pH and volume of Anoxkalnes media in two different experimental phases. In the first phase, the hydraulic retention time (HRT) kept constant in three reactors and SALR increased and in the second phase, the SALR was the constant parameter while HRT increased. These two phases were implemented to investigate the effect of variations in HRT and SALR on biologically-produced solids in MBBR reactors. This study demonstrated that HRT and SALR play an important role in settling characteristics of the biologically-produced solids in MBBR systems.

Acknowledgement

My first and foremost sincere thanks go to my primary supervisor Dr. Robert Delatolla for his support, guidance and help to complete this research work. Special thanks to my co-supervisor, Dr. Roberto M. Narbaitz for his valuable technical advices and the time that he spent for me to successfully complete this thesis. Also I would like to thank NSERC for partial financial support to this study. Moreover, I would like to thank Christine Séguin for all her efforts and helps during the project that created a better environment to perform my experimental works. Furthermore, I would like to thank my lab-mates, Bahman Banihashemi and Ali Sedigh, for their helps during this research work.

At the end, I would like to thank my family for all their great understanding and support.

Table of Contents

Abstract III
Acknowledgements IV
List of Figures VII
List of Tables X
List of Abbreviations XII
CHAPTER 1: Introduction 1
1.1 Background 1
1.2 Research Objective 6
1.3 Thesis Organization 7
CHAPTER 2: Literature Review 8
2.1 Introduction to Biological Wastewater Treatment 8
2.1.1 Suspended and attached growth biological treatment 9
2.2 Activated Sludge Systems 9
2.2.1 Factors affecting activated sludge performance 11
2.2.1.1 Effect of SRT 11
2.2.2 Settling characteristics and particle size distribution of AS systems solids 12
2.2.2.1 Impact of SRT 16
2.3 MBBR systems 17
2.3.1 Factors affecting MBBR performance 22
2.3.1.1 Carrier size and shape 22
2.3.1.2 Effect of percent fill 23
2.3.2 Biosolids characteristics of MBBR systems 24
2.3.2.1 Impact of HRT 24
2.3.2.2 Impact of SALR 26
2.3.2.3 Impact of aeration rate 28
2.3.2.4 Impact percent fill of carriers 29
2.4 Summary 29
CHAPTER 3: Experimental Plant, Materials and Methods 31
3.1 Experimental Plan 31
3.2 Inocculum Source for AS and MBBR Laboratory Reactors 31
3.3 Synthetic Wastewater 32
3.4 Activated Sludge 35
3.5 MBBR Reactors 40

3.6 Analytical Methods 43
3.7 Settleability and Particle Characteristic Methods 44
3.8 Particle Size Distribution Analysis 46
3.9 ESEM Analysis 52
CHAPTER 4: Effect of SRT on AS Biologically-Produced Solids 54
4.1 Operational Conditions of AS Reactors 54
4.2 MLSS and MLVSS of AS Reactors 56
4.3 Sludge Volume Index 60
4.4 Decantation Index 62
4.5 Particle Distribution Analysis 63
CHAPTER 5: Effect of SALR on MBBR Biologically-Produced Solids 74
5.1 Operational Conditions of the MBBR Reactors 74
5.2 Effluent TSS and VSS of MBBR Reactors 78
5.3 Sludge Volume Index 81
5.4 Decantation Index 82
5.5 Particle Distribution Analysis 83
5.6 ESEM of MBBR Carriers 94
5.7 MBBR and AS Biomass Yield and Solid Production Comparison 98
CHAPTER 6: Effect of HRT on MBBR Biologically-Produced Solids 100
6.1 Operational Conditions of the MBBR Reactors 100
6.2 Effluent TSS and VSS of the MBBR Reactors 102
6.3 Sludge Volume Index 104
6.4 Decantation Index 106
6.5 Particle Distribution Analysis 107
6.6 ESEM of MBBR Carriers 117
6.7 Biomass Yield and Solid Production Comparison in Two Different MBBR Experimental Phases 121
CHAPTER 7: Conclusions and Recommendations 122
7.1 Conclusions 122
7.2 Recommendations 124
References 126
Appendix A: Influent and Effluent COD Measurement 131
Appendix B: TSS Measurement 136
Appendix C: SVI and DI Measurement 138
Appendix D: Density of Biologically-Produced Solids Calculation 141

List of Figures

Figure 1.1 Canadian wastewater treatment-2004 4
Figure 2.1 Typical AS schematic 10
Figure 2.2 Flocculation and settling characteristics of AS as related to organic loading rate 14
Figure 2.3 A schematic of a two layer sludge floc 17
Figure 2.4 Carrier movements in aerobic and anaerobic MBBR 19
Figure 2.5 Typical moving bed biofilm process flow diagrams for BOD/COD removal 20
Figure 2.6 Obtainable COD removal rate versus COD loading rate 21
Figure 2.7 Carrier characteristics reported by manufacturer 23
Figure 2.8 Development of particle diameter as a function of HRT a) based on particle volumes; b) based on particle number 25
Figure 2.9 Particle size distribution in terms of volume percentage for MBBR reactor effluent 26
Figure 2.10 MBBR reactors particle size distributions in number and volume percentage–low loading rate COD 7 g $O_2/m^2 \cdot d$; a) differential distribution, b) cumulative distribution 27
Figure 2.11 MBBR reactors particle size distributions in number and volume percentage–high loading rate COD 24 g $O_2/m^2 \cdot d$; a) differential distribution, b) cumulative distribution 28
Figure 3.1 Experimental setup of laboratory porous pot reactor 36
Figure 3.2 Detailed schematic of a laboratory porous pot reactor 37
Figure 3.3 Experimental setup of laboratory MBBR reactor 40
Figure 3.4 Detailed schematic of a laboratory MBBR reactor 41
Figure 3.5 Schematic of DI aparaturs setup 46
Figure 3.6 Brightwell MFI 47
Figure 3.7 Size projection of HIACROYCO 9064 light-blocking particle counter 49
Figure 3.8 DPA images of particles showing sensitivity to string shaped particles (a) and (c) grayscale picture, (b) and (d) binary scale picture 50

Figure 4.1 MLSS and MLVSS concentrations in the AS reactors operated at different SRTs 57
Figure 4.2 Linear regression for finding b and Y of AS reactors at three SRTs 59
Figure 4.3 SVI values for the AS reactors operated at various SRTs 61
Figure 4.4 DI values for the AS reactors operated at various SRTs 62
Figure 4.5 DPA grayscale images of the AS reactors operated at different SRTs (a) SRT =5 days, (b) SRT =10 days and (c) SRT =15 days 64
Figure 4.6 Volume based particle size distributions of particles between 2-400 μm and > 400 μm for AS reactors operating at three different SRTs for mixed liquor samples (before settling) 67
Figure 4.7 Percent volume distribution of particles between 2-400 μm and > 400 μm before settling and after settling for the AS systems operating with SRTs of (a) 5 days, (b) 10 days, and (c) 15 days 69
Figure 4.8 Volume percentage removals of particles between 2-400 μm and > 400 μm for AS reactors operating at three different SRTs 70
Figure 5.1 TSS and VSS concentrations in the MBBR reactors operated at various SALRs 79
Figure 5.2 SVI values for MBBR reactors operated at various SALRs 81
Figure 5.3 DI values for MBBR reactors operated at various SALRs 83
Figure 5.4 DPA grayscale images of MBBR reactors operated at different SALRs (a) 9 g COD/m^2·d, (b) 32 g COD/m^2·d and (c) 64 g COD/m^2·d 84
Figure 5.5 Volume based particle size distributions of particles between 2-400 μm and > 400 μm for MBBR reactors operating at three different SALRs for effluent samples (before settling) 87
Figure 5.6 Percent volume distribution of particles between 2-400 μm and and > 400 μm before settling and after settling at (a) 9 gCOD/m^2·d, (b) 32 gCOD/m^2·d and (c) 64 gCOD/m^2·d SALRs 90
Figure 5.7 Volume percentage removals of particles between 2-400 μm and > 400 μm for MBBR reactors operating at three different SALRs 91

Figure 5.8 ESEM of MBBR reactors at various SALRs acquired at- 15x (a) 9 gCOD/m^2·d (b) 32 gCOD/m^2·d and (c) 64 gCOD/m^2·d 95
Figure 5.9 ESEM of MBBR reactors at various SALRs acquired at- 50x (a) 9 gCOD/m^2·d (b) 32 gCOD/m^2·d and (c) 64 gCOD/m^2·d 96
Figure 5.10 ESEM of MBBR reactors at various SALRs acquired at- 1000x (a) 9 gCOD/m^2·d (b) 32 gCOD/m^2·d and (c) 64 gCOD/m^2·d 98
Figure 6.1 TSS and VSS concentrations in the MBBR reactors operated at different HRTs 103
Figure 6.2 SVI values for MBBR reactors operated at various HRTs 105
Figure 6.3 DI values for MBBR reactors operated at various HRTs 106
Figure 6.4 DPA grayscale images of MBBR reactors at different HRTs (a) HRT= 1 hour, (b) HRT =1.5 hours and (c) HRT= 2 hours 107
Figure 6.5 Volume based particle size distributions of particles between 2-400 μm and > 400 μm for MBBR reactors operating at three different HRTs for effluent samples (before settling) 110
Figure 6.6 Percent volume distribution of particles between 2-400 μm and > 400 μm for before settling and after settling the MBBR reactors operated at (a) 1 hour, (b) 1.5 hours and (c) 2 hours HRT 113
Figure 6.7 Volume percentage removals of particles between 2-400 μm and > 400 μm for MBBR reactors operating at three different HRTs 114
Figure 6.8 ESEM of MBBR reactors at various HRTs acquired at- 15x (a) HRT 1 hour (b) HRT 1.5 hours and (c) HRT 2 hours 118
Figure 6.9 ESEM of MBBR reactors at various HRTs acquired at- 50x (a) HRT 1 hour (b) HRT 1.5 hours and (c) HRT 2 hours 119
Figure 6.10 ESEM of MBBR reactors at various HRTs acquired at- 1000x (a) HRT 1 hour (b) HRT 1.5 hours and (c) HRT 2 hours 120

List of Tables

Table 1.1 Categories and numbers of Canadian wastewater treatment plants-2003 5
Table 2.1 Distribution of AS floc..... 16
Table 3.1 Synthetic wastewater recipe-COD = 380 mg/L..... 34
Table 3.2 AS reactors operational conditions..... 38
Table 3.3 MBBR reactors operational condition - first experimental phase 42
Table 3.4 MBBR reactors operational condition - second experimental phase..... 43
Table 3.5 Calibration results..... 48
Table 4.1 AS steady state operating conditions..... 55
Table 4.2 MLVSS/MLSS for the AS reactors operated at various SRTs. 58
Table 4.3 Mean CC of the AS reactors operated at various SRTs..... 65
Table 4.4 Particle size distribution characteristics of AS reactors at different SRTs 71
Table 4.5 Percent number of particles in different ranges for AS reactors..... 72
Table 4.6 SVI, DI, percent volume and percent number removed that measured by DPA for AS reactors at different SRTs..... 73
Table 5.1 MBBR steady state operating conditions..... 75
Table 5.2 SRT and volumetric loading rate of MBBR reactors operated at various SALRs..... 77
Table 5.3 VSS/TSS ratio for MBBR reactors operated at various SALRs..... 80
Table 5.4 Mean CC of MBBR reactors operated at various SALRs 85
Table 5.5 Particle size distribution characteristics of MBBR reactors at various SALRs..... 92
Table 5.6 SVI, DI, percent volume and percent number removal for MBBR reactors at various SALRs 94
Table 5.7 Solid production and biomass yield of MBBR and AS reactors 99
Table 6.1 MBBR steady state operating condition 101
Table 6.2 SRT and volumetric loading rate of MBBR reactors operated at various HRTs 102
Table 6.3 VSS/TSS ratio for MBBR reactors operated at various HRTs 104
Table 6.4 Mean CC for MBBR reactors operated at different HRTs 108

Table 6.5 Particle size distribution characteristics of MBBR reactors operated at various HRTs 115
Table 6.6 SVI, DI, percent volume and percent number removal measured by DPA for MBBR reactors operated at various HRTs 116
Table 6.7 Solid production and biomass yield of MBBR reactors operated at various HRTs and SALRs 121

List of Abbreviations

AS	Activated Sludge
BOD	Biochemical Oxygen Demand
BAF	Biological Aerated Filter
CC	Circularity Coefficient
C.I.	Confidence Interval
CBOD	Carbonaceous Biochemical Oxygen Demand
COD	Chemical Oxygen Demand
DI	Decantation Index
DO	Dissolved Oxygen
DPA	Dynamic Particle Analyzer
ECD	Equivalent Circular Diameter
EDTA	Ethylenediaminetetraacetic Acid
EPS	Extracellular Biopolymer Substances
ESEM	Environmental Scanning Electron Microscope
F/M	Food over Microorganism
FSS	Fixed Suspended Solid
HRT	Hydraulic Retention Time
LPM	Litre per Minute
MBBR	Moving Bed Bioreactor
MFI	Micro Flow Imaging
MLSS	Mixed Liquor Suspended Solid

MLVSS	Mixed Liquor Volatile Suspended Solid
nbVSS	non biodegradable Volatile Suspended Solid
RBC	Rotating Biological Contactor
ROPEC	Robert O.Pickard Environmental Center
SALR	Surface Area Loading Rate
SEM	Scanning Electron Microscope
SRT	Sludge Retention Time
SVI	Sludge Volume Index
SWW	Synthetic Wastewater
TMP	Transmembrane Pressure
TN	Total Nitrogen
TOC	Total Organic Carbon
TSS	Total Suspended Solid
TSS	Thickened Waste Activated Sludge
VSS	Volatile Suspended Solid
WWTP	Wastewater Treatment Plant

Chapter 1

Introduction

This chapter provides a summary of wastewater treatment history and regulations in Canada with a focus on biochemical oxygen demand (BOD), total suspended solid (TSS), ammonia and chlorine treatment. A brief introduction to the different types of wastewater treatment plants (WWTPs) operating in Canada in 2003 will be presented with the objectives of the research being presented at the end of the chapter followed by a description of the thesis organization.

1.1 Background

Wastewater treatment plant effluent discharges represent one of the largest sources of pollutants in Canada with the harmful impact of these pollutants on the aquatic ecosystem being reported for over 20 years (Canada Gazette, 2010). Presently, municipal wastewater treatment ranges from very good in many areas of Canada to poor or even no treatment, especially at smaller sized coastal communities (Canada Gazette, 2010). Municipalities generally implement levels of treatment that are (i) financially sustainable and (ii) meet provincial permits which are based directly on the assimilative capacity of the receiving water. The greater the potential impact of the discharge on the river water the stricter the level of treatment that is required. Canadian natural water assimilates an estimated quantity of 6×10^{12} L/yr of treated wastewater and 150×10^{9} L/yr of untreated wastewaters.

In Canada, the environment is currently regulated by provincial jurisdiction. The federal government provides only wastewater treatment guidelines which are not legally enforceable. A new federal wastewater treatment regulation proposed in March 2010 (but yet to be implemented) would require many communities across Canada to increase the level of treatment they provide (Canada Gazette, 2010). The specific deleterious substances under the proposed federal regulations include BOD, TSS, total residual chlorine and unionized ammonia. Specifically the proposed regulations state that the carbonaceous biochemical oxygen demand (CBOD) average effluent concentrations must be less than or equal to 25 mg/L; the average effluent TSS concentration must be less than or equal to 25 mg/L; the average total residual chlorine effluent concentration must be less than or equal to 0.02 mg/L and the un-ionized ammonia effluent concentration must be less than or equal 1.25 mg/L of ammonia nitrogen at 15°C±1°C. These federal effluent standards would bring Canada in line with those in the European Union and the United States of America. These regulations have the potential to improve the effluent quality throughout Canada and to ensure that aqueous life and our water resources are preserved for the future.

Although numerous Canadian treatment systems would require upgrading to meet the proposed federal regulation, it should be noted that many wastewater treatment plant operating permits issued by provincial governments currently incorporate or exceed the proposed federal effluent regulation. Wastewater can be broadly categorized into three levels of treatment: primary, secondary and tertiary. These levels are almost always preceded by preliminary treatment units which serve to screen the large solids and debris from the wastewater and can include a grid removal unit prior to downstream mechanical

treatment. Primary treatment consists of the physical separation of settleable suspended solids from the wastewater. Secondary treatment often incorporates biological processes to remove dissolved and particulate biodegradable organic compounds. Tertiary treatment involves advanced processes to remove specific deleterious materials from wastewater to meet stricter effluent standards. The proposed federal standards will ensure a level of secondary wastewater treatment or equivalent at all Canadian WWTPs. It should be noted that primary treatment systems that are enhanced by chemical addition are often able to achieve effluent concentrations approaching those of secondary treatment.

In 2004 there were 28 million people living in 1294 Canadian municipalities with wastewater collection and treatment. Almost 68% of the population was receiving at least secondary treatment (47% secondary mechanical and 21% advanced treatment), 23% were receiving primary treatment and 6% of the population were served by stabilization ponds. For the remaining 3% of the population served by sewers there was no treatment provided prior to discharge. Hence, the level of treatment varies across Canada with higher treatment levels used for wastewater effluents discharged into inland fresh waters than those being released in coastal waters. As shown in Figure 1.1, 50% or less of the population in the three Atlantic Provinces and Quebec are served by secondary treatment. In British Columbia, approximately 36% of the population is served by wastewater treatment of less than secondary treatment. On the other hand, more than 89% of the population of Saskatchewan and Manitoba and greater than 82% of the population in Ontario receive secondary wastewater treatment or higher (Canada Gazette, 2010).

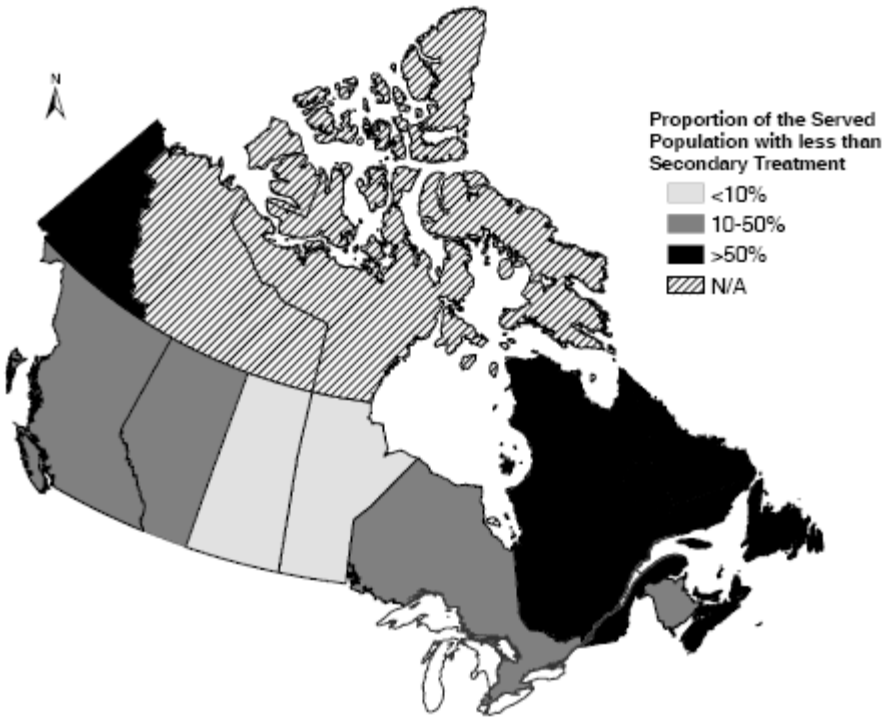

Figure 1.1 Canadian wastewater treatment-2004 (Canada Gazette, 2010)

Table 1.1 lists the number of municipal wastewater treatment plants in operation in 2003 in Canada. Most of the municipal wastewater treatments in Canada were providing secondary treatment. Only 72 attached growth biological treatment systems (i.e. rotating biological contactors (RBC), trickling filters and biological aerated filters) were operating in Canada in 2003 and they were treating less than 1% of the municipal wastewater by volume. Meanwhile, more than 1300 treatment plants were lagoons that served smaller communities and 494 treatment plants were activated sludge (AS) systems (conventional AS, high-rate AS, extended aeration and so on) that comprised 24% of wastewater treatment plants in Canada in 2003. Lagoons and AS systems are considered the conventional wastewater process in Canadian rural and urban communities, respectively.

Table 1.1 Categories and numbers of Canadian wastewater treatment plants-2003 (Environment of Canada, 2003)

Municipal wastewater treatment plants			Number
Primary treatment			90
Secondary treatment	Conventional facultative lagoons		762
	Low rate mechanical systems (i.e., aerated lagoons and aerated facultative lagoons		593
	High rate mechanical systems	Conventional activated sludge	212
		High rate activated sludge	11
		Extended aeration activated sludge	157
		Contact stabilization activated sludge	22
		Oxidation ditch	63
		Sequencing batch reactor (SBR)	23
		Membrane bioreactors (MBR)	4
		Rotating biological contactor (RBC)	34
		Trickling filter	29
		Biological aerated filter (BAF)	9
Total MWWTP's			2009

More recently the moving bed bioreactor (MBBR) as an attached growth treatment system has become increasingly popular in the world with 400 large-scale installations having been built in 22 countries around the world in the last 16 years (Rusten et al., 2006). In these systems microbes grow attached to carriers that are maintained in suspension in a well mixed basin (McQuarrie and Boltz, 2011).

The advantages of MBBR systems include a small footprint, low aeration requirement compared to other biofilm treatment systems due to high oxygen transfer rate through MBBR biofilms (Wessman et al., 2006), high level of treatment (Rusten et al., 2006), ability to perform at low temperatures (Wessman et al., 2006) and lower biological solids production (Åhl et al., 2006). These systems requires one-fifth to one-third of the footprint area that is necessary for an AS plant (Metcalf & Eddy, 2003).

The poorer settling characteristics of MBBR effluent observed at certain operational conditions are an important limitation of this process (Leiknes and Ødegaard, 2001).

Studies found that increasing the surface area loading rates (SALRs) have negative impact on settling characteristics of MBBR biologically-produced solids (Ivanovic and Leiknes, 2012) and shorter hydraulic retention times (HRTs) with higher SALRs results in poorer settling characteristics of these solids (Melin et al., 2005). The fundamental knowledge such as the particle size distribution and settling characteristics of the biologically-produced solids in MBBR systems at various operating conditions is currently not well defined and requires further study. Therefore, the current research investigate the effect of various operating parameters on the production of biologically-produced solids by MBBR reactors with the ultimate goal of optimizing MBBR operating conditions so as to improve MBBR solids settleability.

1.2 Research Objective

The main objective of this research is to investigate the particle size distribution and settling characteristics of biologically-produced solids in MBBR laboratory reactors. The specific objectives are as follows:

- Investigate the settling characteristics of biologically-produced solids in AS treatment systems at various sludge retention times (SRTs) as baseline results from conventional suspended growth treatment systems used in Canada
- Determine the particle size distribution of biologically-produced solids by AS treatment systems and the range of particles that shows poor settling characteristics at various SRTs
- Investigate the effect of organic SALR on the settling characteristics of the MBBR biologically-produced solids

- Determine the effect of organic SALR on the particle size distribution of MBBR biologically-produced solids and the particle ranges that show poor settling
- Investigate the effect of organic SALR on morphology and thickness of the biofilm on the carriers of MBBR reactors
- Investigate the settling characteristics of the MBBR biologically-produced solids at different hydraulic retention times (HRTs)
- Determine the particle size distribution of MBBR biologically-produced solids at different HRTs
- Investigate the morphology and thickness of the biofilm on the carriers at different HRTs in MBBR reactors

1.3 Thesis Organization

The second chapter of this thesis presents a literature review concentrating on the characteristics of biologically-produced solids by AS systems (as a conventional biological suspended growth process) and MBBR (as a biological attached growth process) systems. In Chapter 3, the materials and methods used to implement this experimental work will be discussed and information regarding the experimental plan will be presented. Chapter 4 presents the settling characteristics of the biologically-produced solids and their particle size distribution of laboratory AS reactors operating at different SRTs. Chapter 5 and 6 present the effect of organic SALR and HRTs of MBBR laboratory on the settling characteristics of the biologically-produced solids and their particle size distribution. Finally, conclusions and recommendations for future research are presented in Chapter 7.

Chapter 2

Literature Review

This chapter will provide a brief general introduction to biological wastewater treatment followed by a more detailed analysis of the AS process and MBBR systems. This will be followed by a discussion of the solids characteristics and the settling potential of these systems and the influence of different factors such as organic SALR, HRT and aeration rate on the systems solids.

2.1 Introduction to Biological Wastewater Treatment

Bacteria and other microorganisms in natural waters consume organic compounds as an electron donor (energy source) and substrate and produce new bacterial cells and by-products like carbon dioxide. When sewage is discharged into receiving water, the naturally present microorganisms often start to decompose the sewage organics relatively rapidly in the presence of oxygen. In the 1920s, these natural processes were used and accelerated in sewage treatment systems to remove biodegradable organic matter from wastewaters (US EPA, 2004). The main objectives of aerobic biological treatment include but are not limited to (i) oxidizing the dissolved and particulate biodegradable compounds into new products which are acceptable for treatment, (ii) capturing and assimilating the colloidal solids and particles that are nonsettleable into biological floc and biofilms, (iii) converting or removing nutrients like nitrogen and phosphorous and (iv) removing specific trace organic matters and compounds (Metcalf and Eddy, 2003).

2.1.1 Suspended and attached growth biological treatment

The biological processes that are being used in wastewater treatment can be classified into the two main categories of suspended growth and attached growth (or biofilm) processes. In suspended growth processes, the bacteria that are responsible for treatment are maintained in suspension in the liquid by various methods of mixing. Suspended growth processes in wastewater treatment supply air or dissolved oxygen (DO) for aerobic respiration and mixing. Anoxic and anaerobic processes use mechanical mixer to maintain the growth in suspension. The anaerobic reactors are often used for wastewaters with high organic concentrations and to treat organic sludge, where sludge refers to the residual that mostly contains solids that settled in clarifier in wastewater industries. The solids mainly consist of suspended solids that produced by biologically conversion of organic matters, inert solids from influent and solids precipitated after addition of chemicals to improve settlement (Metcalf and Eddy, 2003).

In attached growth systems, the bacteria and microorganisms for organic and nutrient removal are attached into inert biological carriers which can be plastic, rock, sand redwood or polymeric materials. The organic matter and nutrients are oxidized, reduced or accumulated by the attached microbes that form biofilms when attached to carriers. Examples of these processes include trickling filters, RBCs, BAFs and MBBR systems (Metcalf and Eddy, 2003).

2.2 Activated Sludge Systems

AS systems are one of the most widely used biological treatment processes for wastewater processing and is the conventional method of wastewater treatment in

Canada. This system was developed by Arden and Locket (EPA, 1997). The system incorporates an aeration tank for biological growth, a settling tank for the separation of the produced biomass, recirculation of biomass to the aeration basin (to maintain the proper micro-biological concentration in the aeration tank) and the removal of excess biomass (sludge) to maintain stable system performance (EPA, 1997). Figure 2.1 shows the schematic of a typical AS system. The liquid in the aeration basin, which eventually flows into clarifier, is called mixed liquor.

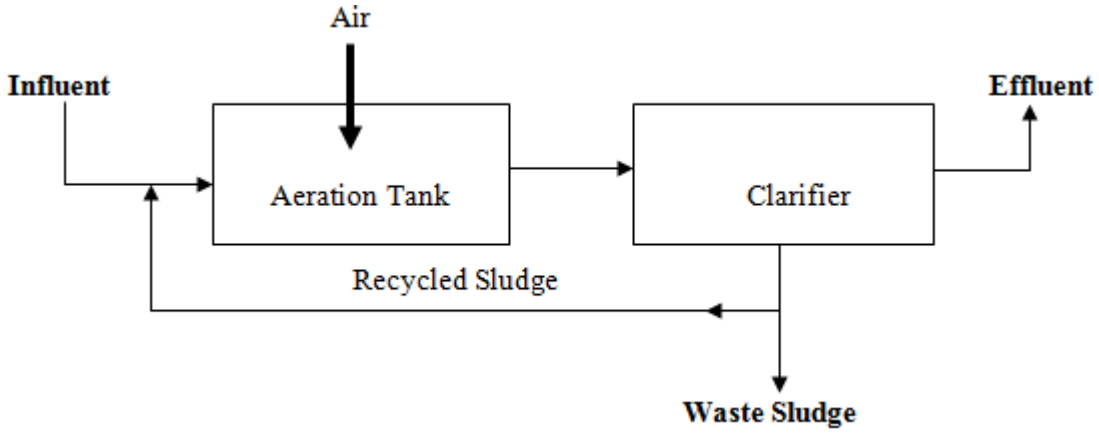

Figure 2.1 Typical AS schematic

AS systems are mainly used to oxidize the carbonaceous matter and remove TSS; they can also be designed to oxidize ammonia, remove the nitrogenous matter (nitrification and denitrification) and remove phosphorus. The organisms in the aeration tank remove the targeted contaminant from wastewater and produce well-settling biological flocs that separate from the liquid in the settling basin by gravity settling (Metcalf and Eddy, 2003).

2.2.1 Factors affecting AS performance

Efficiency of an AS plant may be considered as the removal rate of the pollutional matters. This is also known as the performance of a plant. However, insufficient removals of suspended solids by the final setting tank, is a critical factor to the performance of an AS plant (Stanley, 1949). In fact, the success of membrane bioreactors is in part due to their ability to reliably separate flocs from water. Several factors that affect the effluent quality of an AS system include influent BOD and SS concentration variability, environmental factors such as temperature and wind, biological and operational parameters such as food to microorganism (F/M) ratio and return sludge flow, settling characteristics (such as sludge volume index (SVI) and setteable solids), clarifier design, type of process and human factors (Niku and Schroeder, 1981).

In designing an AS system for proper treatment, influent carbonaceous constituents that can be measured as chemical oxygen demand (COD) or BOD, is very critical and can affect the performance of the process by affecting the pollutional matter removal rates and the size of basins significantly. Higher influent concentrations of biodegradable COD or BOD results in a larger aeration basin volume, greater aeration rate requirements and greater sludge production (Metcalf and Eddy, 2003).

2.2.1.1 Effect of SRT

SRT is an operational factor that controls the performance of AS systems. It is defined as the average period of time which the sludge remains in the system. Eckenfelder (1979) pointed out that as the SRT increased from 2 to 7 days the BOD removal changed significantly. He also found that an SRT of greater than 7 days provides essentially the

same BOD removal up to an SRT of 40 days. Barr et al. (1996), in another study, changed the SRT in the range of 5 to 15 days and they found no trend of improved removal in higher SRTs. However, other studies showed that variation of SRT can affect the concentration of volatile and suspended solids in an AS system. Bisogni and Lawrence (1971) operated a bench-scale AS reactor with HRT of 6 hours and then changed the SRT in the range 0.25 to 12 days; they demonstrated that increasing the SRT increased the mixed liquor suspended solid (MLSS) concentration from 81 mg/L to 2294 mg/L.

2.2.2 Settling characteristics and particle size distribution of AS systems solids

The characteristics of the solids that are produced in AS systems are very important for continuous operating of this system and the quality of the effluent. The solids in wastewater are mainly characterized as colloidal, dissolved, suspended and settleable particles. The removal of colloidal and dissolved particles by settling is more difficult than suspended and settleable solids and this is often achieved by different means such as chemical addition. The settleable particles that are produced in the AS process are removed by gravity settling, leaving a relatively clear liquid as the treated effluent. Typically, greater than 99% of the influent suspended solids can be removed in a gravity settling, clarification step. As discussed, to operate an AS system continuously, the flocs must be separated in the clarifier and a portion of them return to the aeration tank. Although the specific gravity of all the produced flocs are approximately 1.0, only well formed flocs will settle in clarifiers and non ideal flocs will remain in the effluent (EPA, 1997). Sludge bulking is a common cause for production of poor settling flocs and it is mainly due to excess growth of filametous bacteria (Guellil et al., 2001).

Filamentous growth appears in systems with an abundance of carbon source. The most common form of these aerobe bacteria is *Sphaerotilus natans* which consists of chains of rod-shaped cells. When the carbon source is exhausted in the system, the filamentous bacteria start to disappear. In general, the filamentous growth is favored by high substrate concentration, lack of DO, too high or low pH, wastewater with high temperature and when there are insufficient nutrients. Figure 2.2 shows the relationship between operational parameters in an AS system process and filamentous bulking. At lower F/M ratio due to lack of nutrients dispersed growth can occur. Low SVI which shows good settling characteristics is observed between sludge ages of 8 to 20 days and thus this range is suitable for designing a conventional AS system (Eckenfelder, 1979). SVI indicates the gravity settling properties of solids in wastewater system and a value of larger than 200 ml/g indicates that the solids have settling problems. On the other hand, low SVI values of 30-60 ml/g indicate good settling properties of solids in a system (Carnes and Eller, 1972; Janczukowicz et al., 2001).

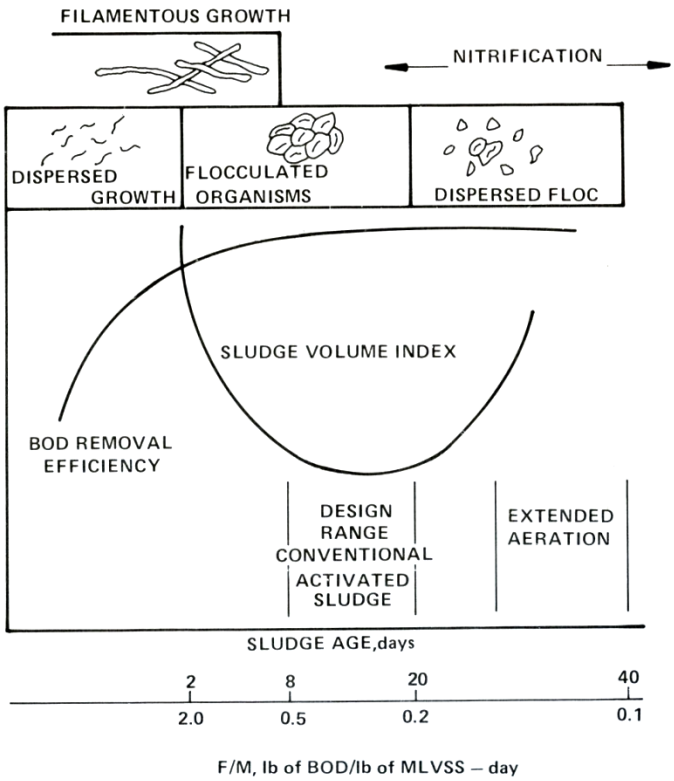

Figure 2.2 Flocculation and settling characteristics of AS as related to organic loading rate (Eckenfelder, 1979)

Moreover, Wanner (1994) observed slimy, jelly-like sludge with poor settling that was attributed to excess amounts of extracellular biopolymers (EPS) that occurs when F/M ratio or DO concentrations are very low (<0.5 mgO_2/L) (Metcalf and Eddy, 2003). In addition, straggler flocs can cause another type of non-filamentous bulking. These types of flocs are characterized by small, transparent and fluffy particles and are caused by over aeration and low MLSS concentrations (EPA, 1997).

Thus, there are lots of factors that could affect the settling characteristics of particles produced in an AS system. Tuntulaves et al. (1983) showed that an increase in sludge recycle ratio can cause a decrease in effluent suspended solids. Keefer and Miesel (1951) found that raising or lowering the pH from 7.0 will improve the settling characteristics of

solids. They also pointed out that the optimum suspended solid removal occurred at the pH of 7.0 to 7.5. Low aeration rates (i.e. 0.5-1.5 mgO_2/L) could also cause bulking in an AS reactor and it can be cured by increasing the DO concentration to >2.5 mgO_2/L (Palm el al., 1980); where the low DO concentration causes formation of flocs with poor settling mainly due to excessive growth of filament bacteria and porous flocs.

Li and Ganczarczyk (1991) analyzed the particle size distribution for a conventional AS by number, volume, area and mass. They measured the particles smaller than 10 μm by the frequency of occurrence with a Coulter counter, while the larger particles were measured individually by an image analysis system. As it is shown in Table 2.1, most of the particles by number are in the range of <2 to 16 micrometer, but this range is responsible for only 2-8% of the total mass of particles. On the other hand, most of the mass of particles is located in the range of 16-128 μm while the number percentage for this range is only 4% of the total numbers (Li and Ganczarczyk, 1991). Hilligard and Hoffman (1997) found a correlation between particle size distribution and SVI by analyzing the effluent of secondary clarifier of different wastewater treatment plants. They showed an increase in particle size when SVI increased. They also observed that sludges with an SVI greater than 100 ml/g had more particles larger than 100 μm (Hilligardt and Hoffmann, 1997). This may suggest that particles >100 μm could be responsible for poor settling ability of solids in AS systems. Andreakis (1993) found that most of the floc in an AS system to be in the 10 to 70 μm size range and increasing the mean floc size increased the SVI. Based on that correlation, larger floc sizes in AS decrease the settleability of the particles. Also, particles with higher volumes can affect its settling characteristics as, the relative density of the particle decreases and the setting

velocity will decrease and as a result the larger flocs leads to poor separation behaviour (Zaki and Richardson, 1954).

Table 2.1 Distribution of AS flocs (Li and Ganczarczyk, 1991)

Size (μm)	**Distribution (%)**			
----------	**By number**	**By Area**	**By Volume**	**By Mass**
<2	30-80	<2	Negligible	2-8
2-16	17-70	1-8	Negligible	5-28
16-128	1-4	20-70	10-80	50-80
128-256	<1	5-50	10-70	5-25
>256	Negligible	0-50	0-60	0-30

2.2.2.1 Impact of SRT

Liao et al. (2002) found that for SRTs between 16 and 20 days the floc strength was higher than those with SRTs between 4 and 9 days. That is because the sludge surface is more negatively charged at lower SRTs and which increases the repulsive electrostatic interactions between particles and makes them less stable (Liao et al., 2002). Their model of floc structure at high and low SRTs is shown in Figure 2.3.

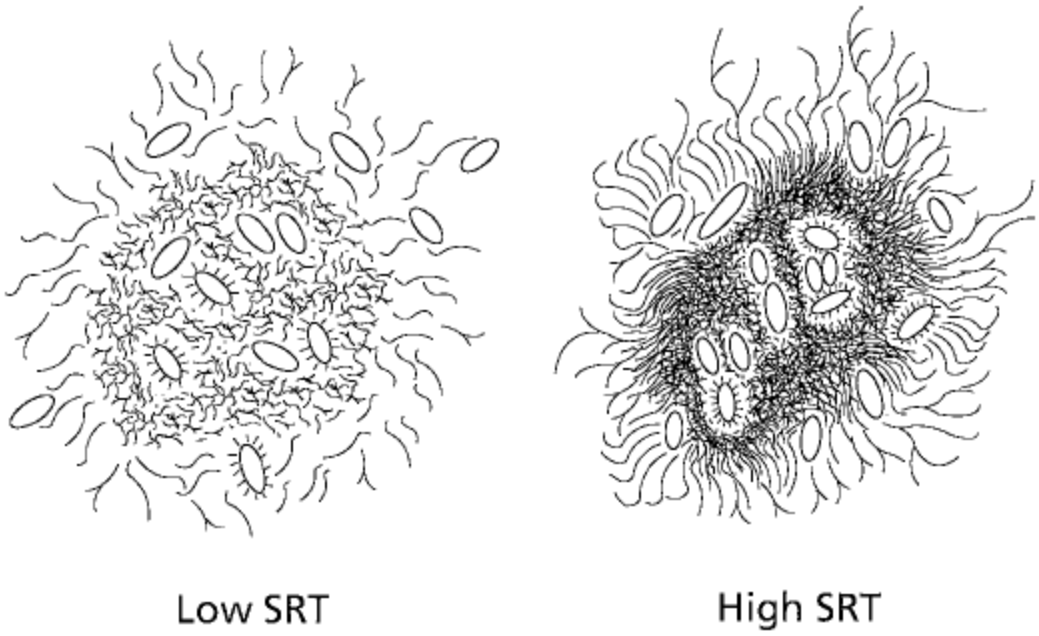

Figure 2.3 A schematic of a two layer sludge floc (Liao et al., 2002)

Bisogni et al. (1971) indicated that by changing the SRT from 0.5 to 12 days, SVI started to decrease from 150 to 20 ml/g and the soluble COD in the effluent dropped from 125 to 52 mg/L. However, based on the total biomass in the effluent, the best total solid removal was observed at an SRT between 4 to 10 days (Bisogni et al., 1971). Eckenfelder (1979) also pointed out that well flocculated organisms are more likely to form in the sludge ages between 2 to 20 days.

2.3 MBBR Systems

In the past decades there has been a renewed interest in biofilm processes for wastewater treatment with new technologies showing improved performance compared to traditional biofilm systems. Traditional systems such as trickling filters are not volume effective; mechanical failure has been a common problem with RBCs; and it is hard to distribute

the load evenly over the entire carrier surface in fixed media submerged biofilters (Rusten et al., 2006).

MBBR systems, developed in Norway in the early 1990s, have been shown to overcome many prior operational problems. MBBR systems, like AS systems, require a clarifier or solid separation unit downstream to the aeration basin, however there is no sludge recycle between the solids separates and the aeration tank for MBBR processes. The name moving bed arises from the fact that 30 to 70% of the aeration basin volume is taken up by plastic carrier material that moves freely within the basin due to diffused bubble aeration and/or mechanical mixing. The carriers are kept inside the reactor by a sieve that is placed at the outlet of the vessel. Figure 2.4 shows the carriers movement in aerobic and anaerobic MBBR treatment systems. The bacterial biofilm that grows attached to the carrier material is the engine for the biodegradation of wastewater constituents. The aeration system also supplies sufficient oxygen so that at least the outer layers of the biofilms are aerobic and thus are capable of proving relatively rapid biodegradation. The biofilms grow and partially eventually detach from the carrier and the detached segments are carried by the liquid into the secondary clarifier for separation. The biologically-produced solid production by this system is 10 times less than that of the AS systems (Åhl et al., 2006).

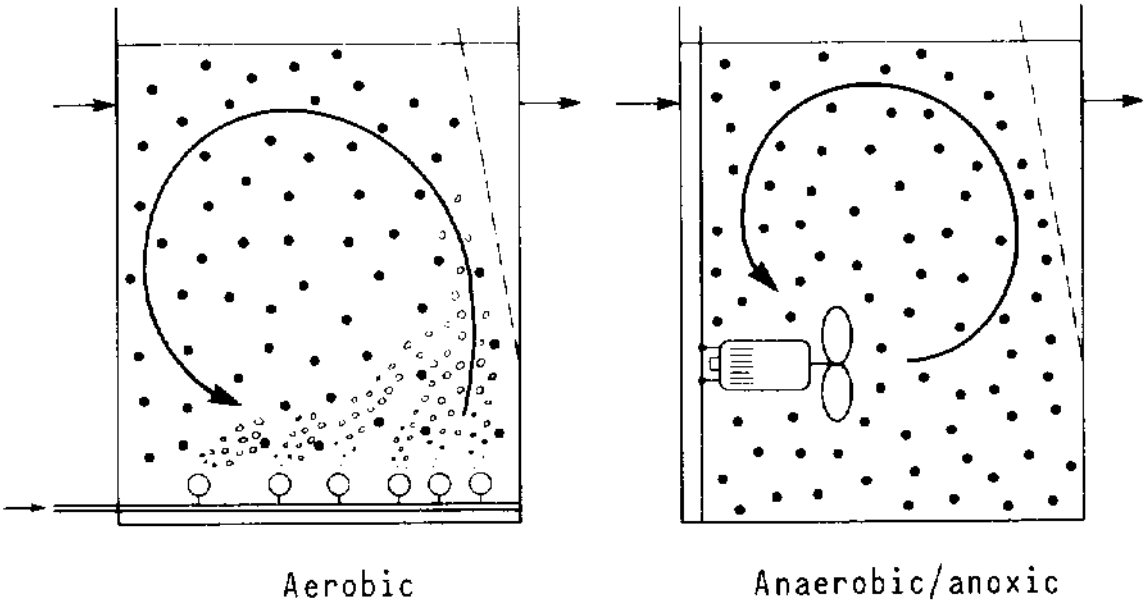

Figure 2.4 Carrier movements in aerobic and anaerobic MBBR (Ødegaard et al., 1994)

The idea behind the MBBR development was to keep advantages of both AS and biofilter processes and eliminate the drawbacks as much as possible. In contrast with other biofilm reactors, the MBBR process uses the whole volume of the tank for treatment as does the AS process and in contrast with AS, MBBR systems do not have sludge recycle. Additional advantages include: lower space requirements than AS plants due to high available surface area for bacterial growth on suspended carriers; lower cost associated with biomass separation due to lower biomass concentration than that of AS systems; the biomass embedded in the biofilms may be utilized in specific applications with greater ease as compared to AS systems because of the lack of sludge return in this system (Ødegaard et al., 1994); these systems are able to maintain nitrifying activity in cold temperatures (Wessman et al., 2006); MBBR systems are able to meet similar objectives to an AS system,; backwashing is not required (Water Environment Federation, 2010).

The MBBR system has been used for many different treatment applications. As the need for nitrogen removal came into focus, Ødegaard and Rusten (1995) gathered data from various small full-scale wastewater treatment plants and the MBBR systems started to develop. However, later, organic matter removal MBBR treatment systems were developed. Currently, MBBR systems are used as stand-alone treatment solutions and in tandem with other treatment processes including AS and membrane bioreactors for high strength organic wastewaters MBBR processes. For instance, Sunner et al. (1999) combined an MBBR system with an AS system to provide high efficiency carbonaceous removal to a high strength wastewater (BOD= 763 mg O_2/L). Ødegaard (2006) describes typical MBBR applications systems in a train sequence to achieve nitrification, nitrogen removal and BOD/COD removal. Figure 2.5 shows common treatment trains for BOD/COD removal that includes MBBR systems.

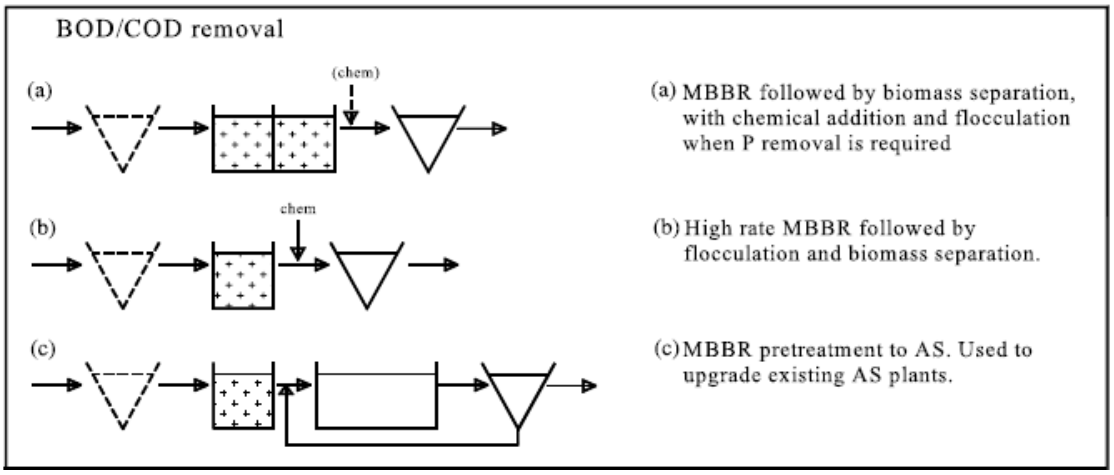

Figure 2.5 Typical moving bed biofilm process flow diagrams for BOD/COD removal (Ødegaard, 2006)

Due to the compactness of the MBBR process, the hydraulic residence time for the process of BOD/COD removal is as low as 30-90 min. The hydraulic residence time change depends on the organic load and the strength of the wastewater. In the process, biodegradable and soluble organic matters will be degraded. Part of particulate matter is trapped in irregularities of the biomass attached to carriers where it is hydrolysed and degraded and the other part will pass through the reactor, more or less unchanged.

Figure 2.6 shows total COD SALR versus obtainable removal rate for two different carriers in MBBR systems. It should be noted that Anoxkaldnes K1 and K2 are different carriers with the same specific surface area (500 m^2/m^3). The line in Figure 2.6 marks the removal rate of COD at 100% biomass separation. It shows that a high removal rate of COD is possible even at high SALRs for MBBR treatment systems if good downstream biomass separation can be achieved (Ødegaard, 2006).

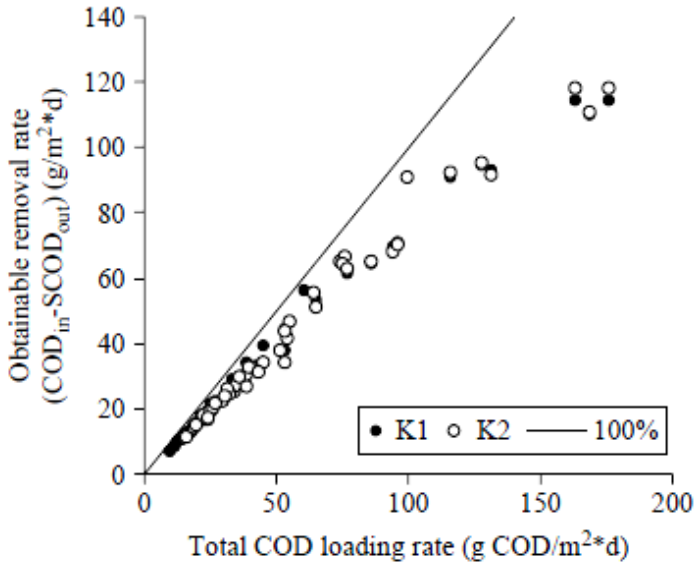

Figure 2.6 Obtainable COD removal rate versus COD loading rate (H. Ødegaard, 2006)

2.3.1 Factors affecting MBBR systems performance

Various parameters can affect the performance of the attached growth MBBR system such as, environmental factors, operational parameters, carrier size and shape and percent fill. Carrier size and shape along with percent will be discussed in the detail in the sections below.

2.3.1.1 Carrier size and shape

Ødegaard et al. (2000) studied the influence of carrier's size and shape on the performance of MBBR systems. They did this study on carriers from different manufacturers. They found the MBBR organic loading rates per carriers surface area (i.e. g COD/m^2·d) plays an important role in the treatment efficiency of MBBR reactors. Higher surface area was shown to significantly improve the performance of these systems. Specifically, the influence of the carrier surface area shows that no difference in removal rates was observed between carriers with different shapes but the same surface area (Ødegaard et al., 2000). Therefore, the performance of the system appears independent of the shape of carriers and totally dependent on the surface area of the carriers. Figure 2.7 shows carrier characteristics of several common MBBR carriers with different size and shapes and their specific surface area. The manufacturer of the carriers listed below is Veolia Inc.

Manufacturer	Name	Bulk Specific Surface Area[1]	Dimensions (Depth; Diameter)	Carrier Photograph
Veolia Inc.	AnoxKaldnes™ K1 or K1 Heavy	500 m^2/m^3	7 mm; 10 mm	
	AnoxKaldnes™ K3	500 m^2/m^3	12 mm; 25 mm	
	AnoxKaldnes™ Biofilm Chip (M)	1,200 m^2/m^3	2 mm; 48 mm	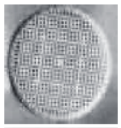
	AnoxKaldnes™ Biofilm Chip (P)	900 m^2/m^3	3 mm; 45 mm	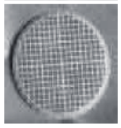
	AnoxKaldnes™ Matrix™ Sol	800 m^2/m^3	4 mm; 25 mm	

Figure 2.7 Carrier characteristics reported by manufacturer (McQuarrie and Boltz, 2011)

2.3.1.2 Effect of percent fill

Wang et al. (2005) investigated the influence of carrier percent fill on the removal rate of contaminants, biomass and biofilm activity in a suspended carrier biofilm reactor. Percent fill is the volume occupied by the carriers based on the empty bed volume. As the carrier percent fill by volume increased from 10% to 75% and the COD removal rate increased from 58.4% to 68.4% (at a fill of 50%) and then decreased to 63.3%; thus the optimum carrier concentration observed was approximately 50%. It also had an indirect relation with the suspended biomass concentration in the reactor, with increasing the carrier concentration the suspended biomass concentration in the reactors started to decrease.

However, the average biomass production on the carriers had a peak value at the 50% concentration of carriers (Wang et al., 2005).

2.3.2 Settling characteristics and particle size distribution of MBBR systems solids

As mentioned, solids concentrations in MBBR systems are lower than that of AS systems and it has been reported that the settleability of particles in MBBR system are poorer than that of the mixed liquor from conventional AS systems (Leiknes and Ødegaard, 2001). However, filters downstream of these processes (MBBR and AS) worked better in the case of MBBR systems because they produce less solids (Sombatsompop el al., 2006). Ivanovic et al. (2008) treated a wastewater with a COD concentration of 242 mg/L using an MBBR reactor with a 4 hours HRT followed by membrane separation to reduce the suspended particles. The particle size distribution showed that the largest volume of the suspended particles is in the range of 5-200 μm. However, the number distribution showed that the most number of particles are submicron particles with a number based average diameter of 0.7 μm.

The particle size distribution, the solids characteristics, turbidity and settling characteristics of the MBBR biologically-produced solids are affected by many factors. These factors include HRT, organic SALR, carrier percent fill and aeration rate. In this literature review, the impact of each is explained in detailed bellow.

2.3.2.1 Impact of HRT

Åhl et al. (2006) found that increasing the HRT caused a shift towards the larger particles in terms of volume percentage of particles and the peak for the particles with the highest percentage volume also shifted to larger sizes. As shown in the Figure 2.8b, they did this

experiment at HRTs of 1 to 4 hours and in terms of number of particles, there was an increase in the smaller particle fraction by increasing HRT, particularly at HRTs of higher than 2 hours (Åhl et al., 2006). It should be noted that SALR was decreased in their study as HRT was increased. They also pointed out that the removal of particles by settling was better in the reactors with higher HRTs and lower SALRs. However, in addition to higher HRT at low SALR loaded reactors, the COD concentration did not change significantly.

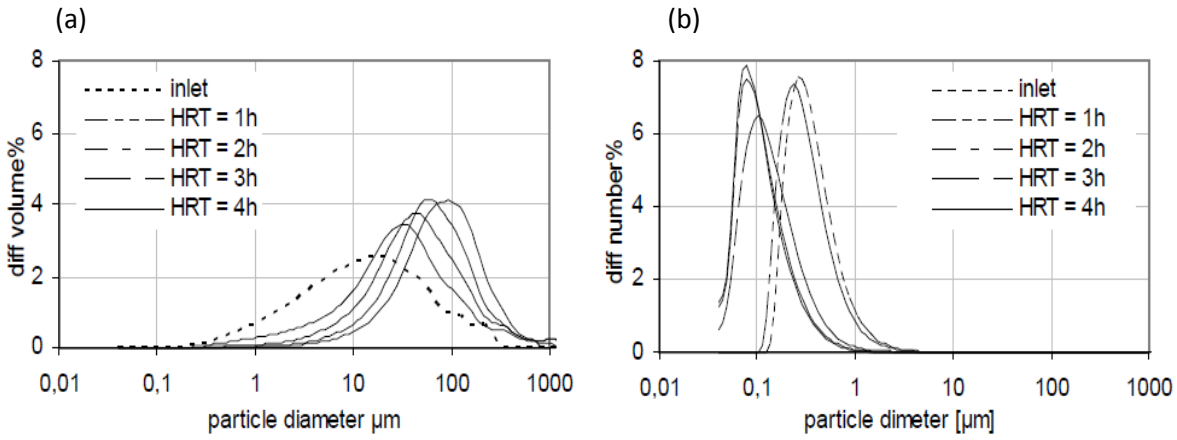

Figure 2.8 Development of particle diameter as a function of HRT: a) based on particle volumes; b) based on particle number (Åhl et al., 2006)

In another study, Melin et al. (2005) changed the HRT in a pilot scale MBBR/membrane processes from 0.45 to 4 hours to investigate the effect of this factor on the fouling of the membrane system. They found that there is a clear shift towards smaller particles when the HRT of the system is shorter. As Figure 2.9 shows the volume percentage for particles <1µm is negligible and a high percentage of solids volumes is for particles with diameters larger than 10µm. There was a significant increase in the particle sizes as the HRT increased from 1 h to 3 h while the SALR decreased.

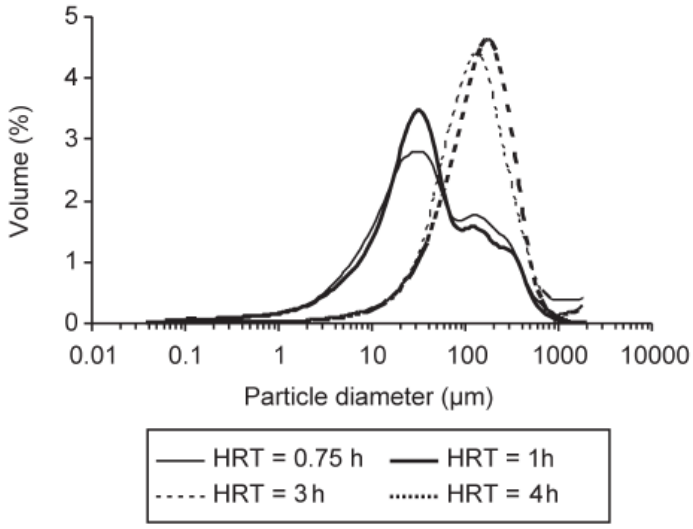

Figure 2.9 Particle size distributions in terms of volume percentage for MBBR reactor effluent (Melin et al., 2005)

2.3.2.2 Impact of SALR

Aygun el al. (2008) found that increasing the organic SALR in MBBR systems from 6 to 96 g COD/m^2·d resulted in a solid production increase from 0.12 to 0.56 kg TSS/kg COD. In addition, Åhl et al. (2006) filtered the effluent of an MBBR reactor by using a membrane filtration system and they found that increasing the MBBR's organic SALR decreased the transmembrane pressure (TMP). That change was caused by higher solid concentration in the effluent of MBBR reactors at higher SALRs. By running a reactor at lower SALRs Åhl et al. (2006) showed that there is a clear effect on the particles size distribution between the influent and effluent of an MBBR reactor (Figure 2.10). In fact aggregation was observed along with an increase in cumulative and differential volume percentage, indicating a shift towards larger particles at an SALR of 7 g O_2/m^2·d and HRT of 3 hours. On the other hand, the differential number analysis (Figure 2.10a)

showed that there was an increase in the number of smaller particles in the effluent so smaller particles was not incorporated into the aggregates. This could be as the result of non-ideal flocculation conditions, particle stability and biomass characteristics. As shown in Figure 2.11, for higher SALRs the transformation of particles is less than that at lower SALRs and the smaller particle profile remained similar to the influent (Åhl et al., 2006). In addition, Ivanovic et al. (2005) found that by increasing the SALR from COD 12.1 g $O_2/m^2 \cdot d$ to 47.9 g $O_2/m^2 \cdot d$, the number of submicron particles, the suspended solid concentration, undesirable flocs structures and number of filaments in the effluent increased (Ivanovic et al., 2005).

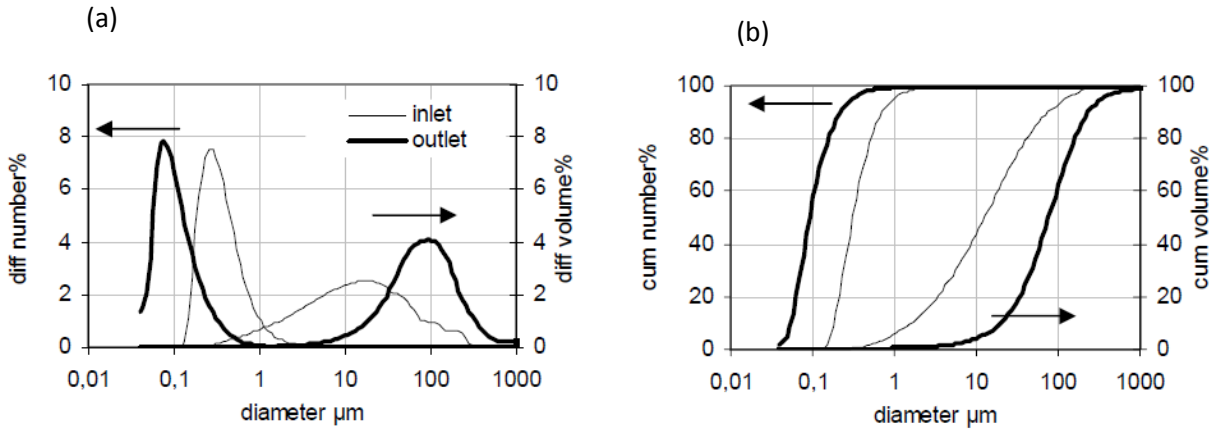

Figure 2.10 MBBR reactors particle size distributions in number and volume percentage –low loading rate COD 7 g $O_2/m^2 \cdot d$; a) differential distribution, b) cumulative distribution (Åhl et al., 2006)

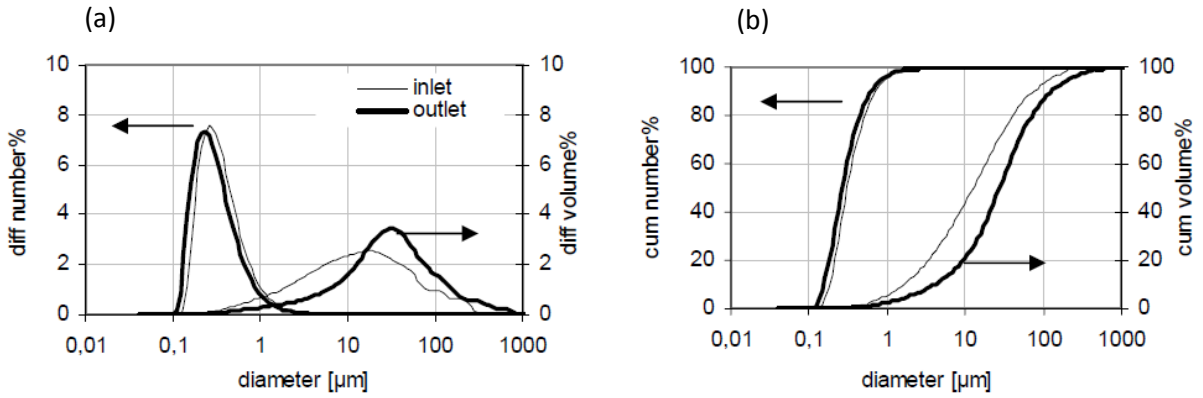

Figure 2.11 MBBR reactors particle size distributions in number and volume percentage –high loading rate COD 24 g $O_2/m^2 \cdot d$; a) differential distribution, b) cumulative distribution (Åhl et al., 2006)

Furthermore, (Ødegaard et al., 2000) showed that the removal of particles by settling is related to the organic SALR of an MBBR reactor and it decreases suddenly by increasing the SALR. Ivanovic and Leiknes (2012) also revealed that at lower organic SALRs (less than 10 g $COD/m^2 \cdot d$), particles tend to settle more easily and produced well-formed and compact flocs. They suggested that the addition of a metal coagulant or cationic polymer would overcome the poor settling characteristics of biologically-produced solids at higher SALRs.

2.3.2.3 Impact of aeration rate

The degree of aeration could affect the particle sizes as intense aeration can cause shearing of larger particles producing smaller ones. According to Åhl et al. (2006) the degree of aeration will break the larger aggregates into smaller ones but they will always remain larger than 20 µm. In another study, Lee et al. (2006) ran an MBBR reactor coupled with a membrane bioreactor and they found that by increasing the air flow rate from 5 to 9 litre per minute (LPM) in a 6 litres reactor, the biological floc sizes decreased

from 61.2 to 37.3 μm. In another study, Rahimi et al. (2010) operated an MBBR system in series with a membrane compartment to find the optimum aeration rate for less clogging of the membrane part after leaving the MBBR reactors and higher removal rates of pollutional matters. They found that in lower aeration rates the filamentous organisms in the flocs will increase but with raising the aeration rate to the higher levels, the filamentous organisms will start to decrease suddenly. On the other hand, increasing the aeration rate causes more floc shearing and the resulting smaller particles have lower settling velocities that produce higher SVI values (Rahimi et al., 2010). However, Rahimi et al. (2010) could not find a clear correlation between SVI and the rate of aeration in their study. They also found a parabolic correlation between the aeration rate and the attached biofilm growth concentration.

2.3.2.4 Impact of percent fill of carriers

Lee et al. (2006) revealed that by increasing the percent fill of carriers from 5% to 20%, microbial floc sizes decreased from 73.5 to 49.6 um. This again could be attributed to collisions between carrier particles as well as the collisions between the carrier particles and the suspended particles (Lee et al., 2006).

2.4 Summary

The information about the biologically-produced solids in AS systems is well defined. There are many articles about SVI, settling velocity, flocculation, sludge density, sedimentation and other settling characteristics for these systems (Forster, 1983; Sears, 2006; Janczukowicz, 2000) In fact, for designing a sedimentation tank or other processes for AS (for particles removal) there are standard design procedures available. However,

when an MBBR is considered for a new wastewater treatment application, there is much less information and a pilot demonstration is often required to design the system. In particular, the MBBR particle characteristics, size distribution and settling characteristics are not well quantified in many applications or studies with the effect of various factors (such as HRT and SALR) remaining not well defined. As a result, an investigation on the impact of MBBR reactor design and operational characteristics on the particle size distribution is needed as it greatly impacts the MBBR process performance and costs.

Chapter 3

Experimental Plan, Materials and Method

3.1 Experimental Plan

The experimental work for this study was divided into three stages. The first stage included the operation of three AS laboratory reactors each with a different SRT and the second stage included operating three laboratory MBBR reactors with three different organic SALRs and the third stage included the operation of these MBBR reactors at three different HRTs. All reactors were run to determine the effect of the operational parameters (SRT, SALR and HRT) on the characteristics of biologically-produced solids. Specially, the study measured the concentration of TSS and volatile suspended solid (VSS), the SVI and decantation index (DI), characterized the particles size distribution and used environmental scanning electron microscopy (ESEM) to characterize the biofilm attached to the carriers in the MBBR reactors. The COD removal rates and percentage was used to verify the steady state conditions for the above reactors during all experimental stages.

3.2 Inoculum Source for AS and MBBR Laboratory Reactors

The inoculum source for all the laboratory reactors was sampled from the Robert O.Pickard Environmental Center (ROPEC) wastewater treatment plant in Ottawa. This center provides secondary treatment (AS process) to approximately 720,000 people in Ottawa (City of Ottawa Website). The inoculum was in fact thickened waste activated sludge (TWAS) with a TSS concentration of 60000 mg/L. The sample was diluted 30

times to a solid concentration of approximately 2000 mg/L TSS prior to being added to the AS and MBBR reactors. In the case of the AS reactors the membrane of the porous pot design (described in detail in Section 3.4) did not allow the biomass to exit the reactor and thus a one-time inoculation of the reactors with the biomass source was adequate for start-up. However, the MBBR reactors were fed with the innoculum source which was the mixed liquor from already seeded AS reactors. The MBBR reactors were fed continually once a day for approximately five days until the biofilm growth was observed on the carriers.

3.3 Synthetic Wastewater

All of the laboratory reactors in this experimental work were fed with the same synthetic wastewater (SWW) recipe. The SWW was prepared by carefully adding three synthetic stocks (carbon constituents, nutrient constituents and trace constituents) to tap water. Table 3.1 shows the composition of the SWW recipe used to make a wastewater with 380 mg/L of COD; the SWW used in this study is a modified version of the Delatolla et al. (2009) synthetic wastewater recipe.

The synthetic wastewater feed was prepared in 30 L batches for the AS reactors and 20 L batches for the MBBR reactors. The feed was prepared every day to avoid microbial growth in the feed stock and kept at room temperature (20°C). The feed solution was prepared by adding the three stock solutions together with each stock solution being stored at 4°C until used. The first stock solution contained the carbon source for the reactors. In this solution, glucose and acetate were added as sources of readily biodegradable organic carbon with peptone being added as a more complex carbon

source that is more difficult to degrade. Peptone is derived from different proteins, animal milk and meat. The COD, nutrient and trace metal concentrations for the various reactors under the various operating conditions were adjusted to meet the loading rate requirements by increasing or reducing the glucose, acetate and peptone concentration of the SWW. The glucose, peptone and sodium acetate ratio was always kept constant when adjusting the COD concentration for the various feed requirements of the study. The second stock solution contained nitrogen (NH_4-Cl), phosphorus ($KH_2PO_4.2H_2O$), $FeCl_3$, ethylenediaminetetraacetic acid (EDTA) as a chelating agent and alkalinity ($NaHCO_3$). As previously mentioned, the nutrient stock solution was stored separately from the carbon stock solution to prevent possible bacterial activity. The third stock solution consisted of trace metal compounds which are required for biological growth as micro nutrients.

As the macro nutrient requirements of microbial growth include nitrogen, phosphorous and iron. The theoretical chemical formula of bacterial cells prepared by Droste (1997) of $C_5H_7NO_2P_{0.074}$ was used to verify adequate nitrogen and phosphorus concentrations at all COD concentrations of the SWW feed. Based on this bacterial cell composition the COD:N:P ratio in the feed wastewater was required to be 100:5:1. The total nitrogen (TN) in the SWW is the sum of nitrogen from NH_4-Cl and EDTA and the only source for phosphorus is $KH_2PO_4.2H_2O$. Therefore, total nitrogen and total phosphorus concentration in the SWW was calculated to be 22 mg/L and 7 mg/L, respectively when the COD was 380 mg/L. In addition, the trace and nutrient constituents solutions also diluted in the same pattern with carbon constituents solution to keep the COD:N:P ratio

always constant. Overall, the COD:N:P ratio in the SWW satisfied the ratio that required for aerobic bacterica reported by Droste (1997).

Table 3.1 Synthetic wastewater recipe-COD = 380 mg/L

Compound	**Concentration (mg/L)**	**Supplier**	**Grade**
Carbon Constituents	----------	----------	----------
$C_6H_{12}O_6$	150.00	Grain Process Enterpriser	ACS
Peptone	150.00	Fisher Scientific	Bacteriological
NaAc	80.00	Fisher Scientific	ACS
Nutrient constituents	----------	----------	----------
NH_4Cl	40.00	MP Biomedicals	ACS
$KH_2PO_4.2H_2O$	44.10	Fisher Scientific	HPLC
EDTA	3.00	Fisher Scientific	Molecular biology
$NaHCO_3$	125.00	Fisher Scientific	ACS
$FeCl_3.6H_2O$	0.45	Acros	ACS
Trace Constituents	----------	Fisher Scientific	----------
$MgSO_4.7H_2O$	20.00	Fisher Scientific	Laboratory use
H_3BO_3	0.05	MP Biomedicals	ACS
$CuSO_4.5H_2O$	0.01	Fisher Scientific	Laboratory use
KI	0.05	Fisher Scientific	ACS
$MnCl_2.4H_2O$	0.04	Fisher Scientific	ACS
$ZnSO_4.7H_2O$	0.04	Acros	ACS
$Na_2MoO_4.2H_2O$	0.10	Fisher Scientific	Laboratory use
$CoCl_2.6H_2O$	0.01	Fisher Scientific	ACS
$CaCl_2$	10.60	Fisher Scientific	ACS

3.4 Activated Sludge Reactors

Porous pot reactors (Bird and Tole Company, Bledlow Ridge, UK) were used in this study to investigate the biological solids produced by conventional treatment systems. Specifically, the porous pot reactors were used to simulate AS systems where these types of laboratory reactors have been shown to produce effluents typical of AS systems (US EPA, 2008). AS systems consist of an influent feed, an aeration basin, a clarifier, a return AS recycle pathway, a waste sludge removal pathway and a final effluent pathway. The porous pot reactors differ in that they do not have a clarifier and the effluent permeates through a porous membrane, which facilitates control of the SRT in the laboratory environment. The membrane eliminates the need for the return recycling AS pathway as the biomass remains in the porous pot reactor all the time.

To investigate the biological solids produced by conventional WWTP; three porous pot reactors were operated at three SRTs of 5, 10 and 15 days. Figure 3.1 shows a schematic of the experimental setup of the three reactors. A 30 L bucket equipped with a mixer was the influent source of the reactors. The mixer operated continuously to keep the influent homogeneous for the whole duration of the experiments. A porous stone diffuser was used to constantly aerate the reactors and was placed at the bottom of each reactor to uniformly distribute the required air, keep the reactors completely mixed and keep the biomass suspended. The influent was pumped into the system using a peristaltic pump (752450, Cole Palmer, Chicago, Illinois) and the effluent exited the reactors by means of gravitational flow.

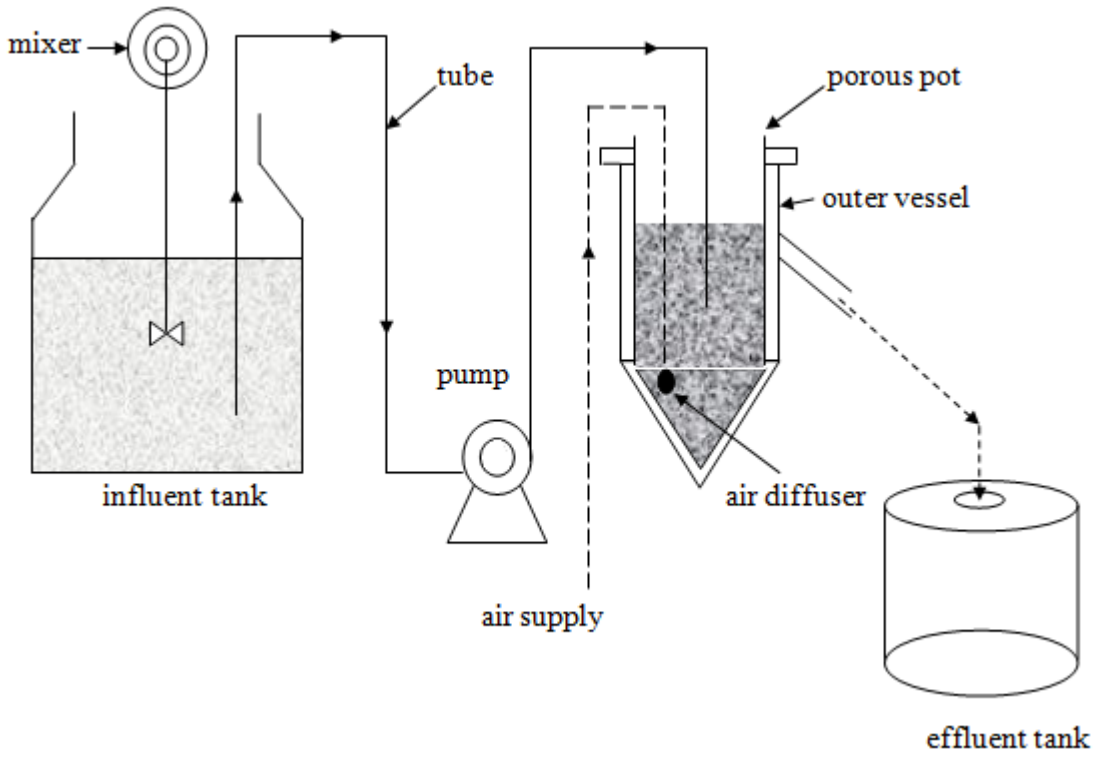

Figure 3.1 Experimental setup of laboratory porous pot reactors

Figure 3.2 shows a detailed schematic of the porous pot reactors. The membrane is made from 2 mm thick porous polythene sheets with a nominal pore size of 96 μm. The membrane is shaped into a 14 cm diameter cylinder with a conical base which has a 45^{o} angle slope. The membrane is housed inside a 15 cm diameter PVC vessel with PVC supporting rings that keep the porous pot a distance of 0.5 cm from the outer vessel. During operation, the space between the porous pot and the vessel wall is filled with effluent which exits via the outer tube located 17.2 cm above the base of the cylinder. This design maintains a 3 L liquid volume within the porous pot reactor at all times.

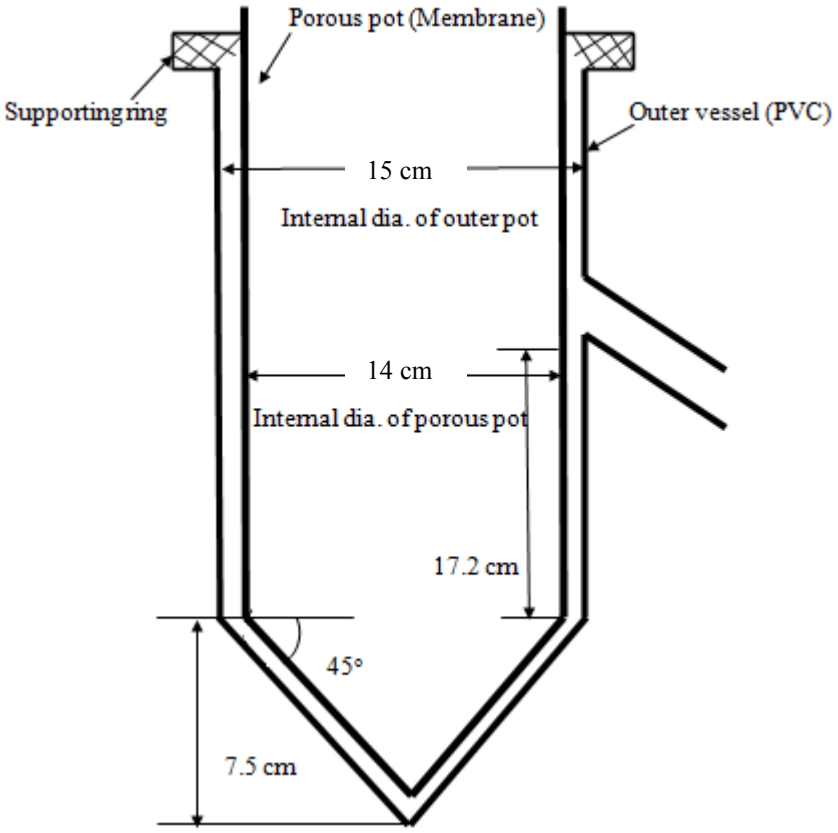

Figure 3.2 Detailed schematic of a laboratory porous pot reactor

Throughout the experimental phase, the three AS reactors were run at three different SRTs, at the same HRT, with the same synthetic feed and at the same temperature (20°C). The summary of the operational conditions are shown in the Table 3.2.

Table 3.2 AS reactors operational conditions

AS Reactors SRT (days)	HRT (hrs)	F/M (kg COD/kgVSS·d)	Loading rate (g COD/L·d)	pH	DO (mg O_2/L)
5	6	0.8	1.6	7.1	4.5
10	6	0.6	1.6	6.8	4.5
15	6	0.5	1.6	6.9	4.4

During start-up it was noticed that the AS reactors did not function well with an HRT of 3 hours, because the biologically-produced solids caused clogging of the porous pot walls, foam formation and an over flow of the reactors. The lowest HRT that eliminated clogging was 4 hours. Hence an HRT of 6 hours was chosen for the three reactors to prevent clogging and simulate a conventional AS system.

The SRT of each reactor was kept constant by removing mixed liquor from the reactors each day; where the mixed liquor is simply the liquid mixture of solids and dissolved constituents within the reactors. The mixed liquor volume that was removed in order to maintain the appropriate SRT was calculated according to the following equation:

$$Q_w = \frac{X_V \cdot V - Q \cdot X_{Ve} \cdot SRT}{X_V \cdot SRT} \qquad \text{Eq. 3.1}$$

where, Q_w = wastage flowrate of mixed liquor to be removed (L/day); X_v = mixed liquor volatile suspended solid (MLVSS) concentration inside the porous pot reactor (mg/L); V = volume of the reactor; X_{ve} = volatile suspended solid (VSS) concentration in the effluent (mg/L); SRT = sludge retention time (day) and Q = influent flowrate (L/day).

Based on the flow rate, the constant volume of the reactors, the known SRT and the data measured from the previous day, the wastage flow rate was calculated each day. The following is an example of the calculation used to keep the SRT at 15 days. For example, the known reactor volume (V = 3 L), flow rate (Q= 11.82 L/day) along with the required SRT of 15 days were used with the previous day measurements of Xv = 3595 mg/L and X_{ve} = 2 mg/L to calculate the required wastage flow rate (Q_w) as shown:

$$Q_w = \frac{3595\ \left(\frac{mg}{L}\right) \cdot 3(L) - 11.82(\frac{L}{day}) \cdot 2(\frac{mg}{L}) \cdot 15(day)}{3595\left(\frac{mg}{L}\right) \cdot 15(day)} = 0.193\ L/day$$

It should be noted that after the mixed liquor was removed from the reactor, the MLVSS concentration (X_v) and the effluent VSS concentration (X_{ve}) increased slightly but did not cause the SRT to change.

During start-up of the reactors, the porous pot reactors clogged every day and were cleaned daily. After a period of acclimatization, the porous pots worked for almost a month without any clogging or fouling problems and were cleaned monthly. The following modified cleaning protocol recommended by the Bird and Tole Company was used:

- Transfer the wastewater inside the porous pot into a new porous pot reactor
- Wash the clogged pot with water
- Submerge the pot into a 13% sodium hypochlorite solution for a duration of 3 days
- Rinse the pot with water to remove all the traces of hypochlorite

3.5 MBBR Reactors

The MBBR reactors were operated throughout the course of study. As shown in Figure 3.3, the MBBR process consists of an influent reservoir, an influent peristaltic pump, an aerated cylindrical reactor and an effluent collection tank. A porous stone diffuser that covers the complete bottom of the reactor was used to distribute the air inside the reactor. Sufficient air was supplied to enable the plastic carriers to circulate inside the reactor.

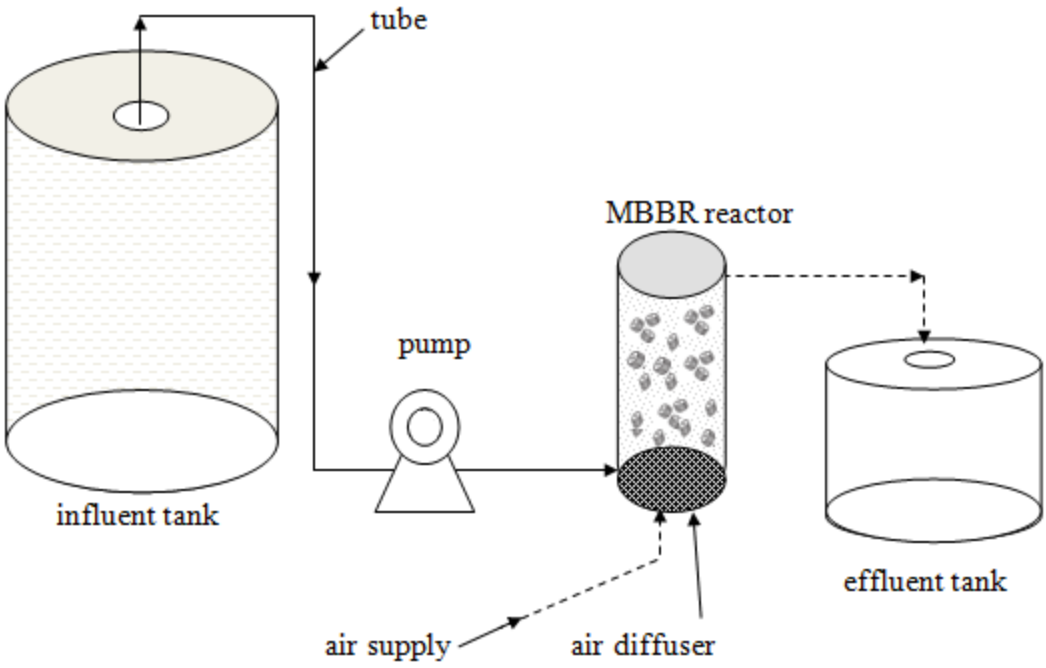

Figure 3.3 Experimental setup of laboratory MBBR reactor

Figure 3.4 shows details of the MBBR reactor design; the base was removable to allow access to the air diffuser at the bottom of the reactor enabling the base to be unscrewed and the air diffuser to be detached for cleaning. The reactor outlet was located so as to keep the volume of the reactor 900 ml with the effluent exiting through a tube that flows to the effluent collection tank by gravity. A sieve in front of the outlet was installed to

keep the carriers from exiting the reactor. All three MBBR reactors were identical and contained 50% by volume of K1 Anoxkaldness carriers. The DO concentration was maintained at 4.2 mg O_2/L in all reactors throughout the study.

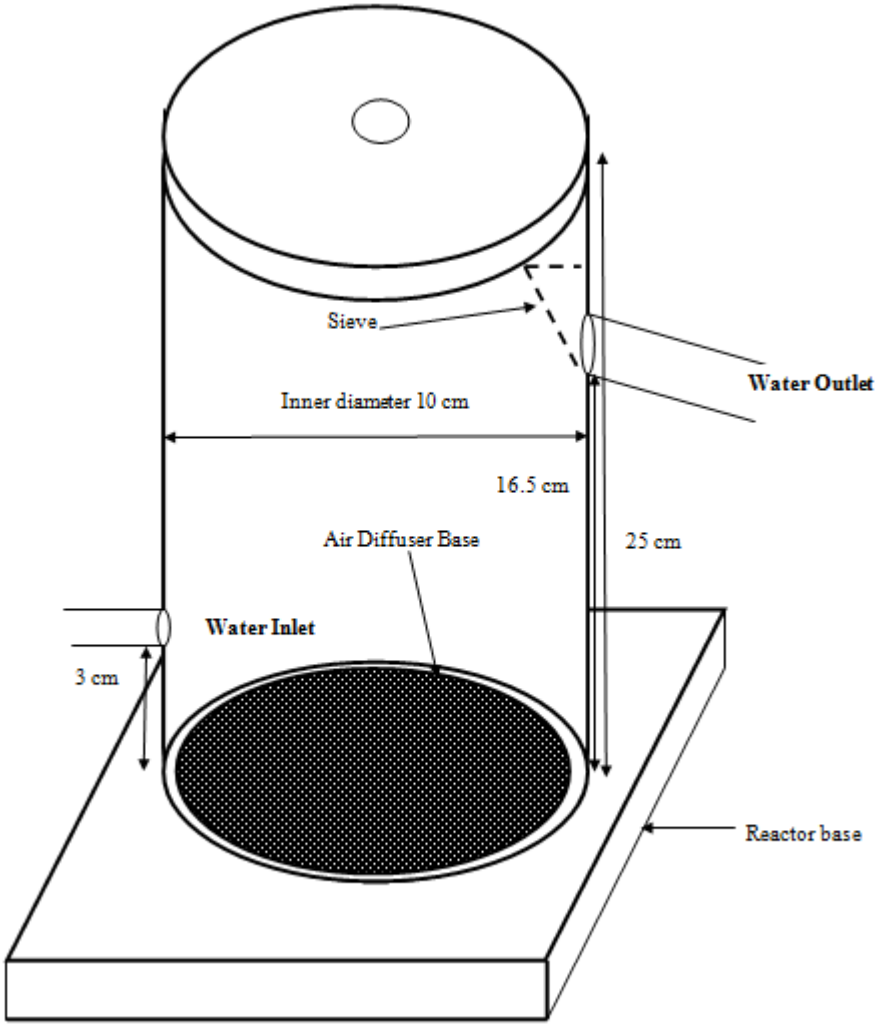

Figure 3.4 Detailed schematic of a laboratory MBBR reactor

The MBBR reactors were operated during two different experimental phases. In the first phase the HRT was the same in the three reactors and the COD SALR differed in each reactor. It should be noted that the HRT in MBBR reactors is calculated based on the empty bed volume of the reactors. The reactors were operated at low, medium and high

COD SALRs. A summary of the operational condition during the first experimental phase is shown in Table 3.3.

Table 3.3 MBBR reactors operational condition - first experimental phase

MBBR Reactors SALR (g COD/m^2·d)	**Flowrate (L/day)**	**HRT (hrs)**	**DO (mg O_2/L)**	**pH**	**COD (mg/L)**
9	20	1	4.2	7.0	97
32	20	1	4.3	7.0	354
64	20	1	4.3	7.0	692

The three MBBR reactors were inoculated with biomass from ROPEC as described in Section 3.2. After inoculation all three reactors were run for three weeks with an HRT of 6 hours to promote attached growth and to reach the steady state condition. However, after this three week period there was no growth on the carriers. In fact, the biomass in all three reactors was suspended and they were operating like a completely mixed aeration tank; as the start-up HRT was too long to promote attachment. By decreasing the HRT to 1 hour, the biofilm started to grow on the inner surface of the carriers. To promote attachment with this low HRT, the biomass was seeded from the already started AS reactors with a volume of 1 ml of mixed liquor being added to each MBBR reactor once a day for a period of 3 days. Three COD SALRs of 9, 32 and 64 g COD/m^2·d was loaded to in the three MBBR reactors during the first phase of experiment by using feed SWW with COD concentrations of 97, 354 and 692 mg/L at a flow rate of 20 L/day. Each reactor was fed from its own reservoir with the capacity to feed for 24 hours, or in other words, for 24 HRTs.

In the second phase of the MBBR experiments, the SALR was kept constant at 32 g COD/m^2·d in all reactors and the HRT was varied from 1 (low) to 1.5 (medium) and 2 (high) hours. The HRT of two of the three reactors were increased gradually to reach medium and high HRTs for the second MBBR experimental phase. To keep the COD SALR the same at different HRTs, the COD concentration was also changed. The summary of the operational conditions in the second MBBR experimental phase is shown in Table 3.4.

Table 3.4 MBBR reactors operational condition - second experimental phase

MBBR Reactors HRT (hours)	**Flowrate (L/day)**	**SALR (g COD/m^2·d)**	**DO (mg O_2/L)**	**pH**	**COD (mg/L)**
1	20	32	4.1	7.0	354
1.5	13	32	4.2	7.0	477
2	10	32	4.1	7.0	692

Cleaning the MBBR reactors was very critical in this study as the MBBR reactors were used to evaluate the biological solids produced by biomass attached to the carriers and not from detachment from other surfaces such as side walls and the aeration tube. Thus, the inside wall of the reactors and the aeration tube were washed twice a week with 13% sodium hypochlorite and water to remove any attached biomass and to remove any biomass settled at the bottom of the reactor.

3.6 Analytical Methods

All of the samples that were extracted from the system were as small as possible to minimize the effects on the operation of the reactors. DO and pH were measured and

controlled every day. Total COD, VSS and TSS were measured twice a week until the reactors reached steady state conditions and were measured in triplicate every second day after steady state was reached. The analytical techniques used are described below.

The pH was measured using Accumet-Excel Dual Channel pH/Ion meter-XL25 while a Thermo Orion-810 probe was used to measure the DO concentrations. The pH and DO measurements followed standard methods 4500-H^+ B and 4500OG, respectively. TN was measured using a Combustion Analyzer-Apollo 9000 according to standard method 5310-B and the P concentration was measured using standard method 4500-PD. The COD was monitoring using the HACH-DR 5000 method based on Jirka and Carter (1975) with specific vials for COD measurements (TNT 822 COD vial). Standard method 2540-D was used to analyze total and volatile suspended solids. Well-mixed samples were filtered through glass-fiber filters by filtration apparatus. The glass-fiber filters that were used in these measurements were Millipore glass-fiber filters, AP series, circles 4.7 cm diameter.

3.7 Settleability and Particle Characteristic Methods

The settling characteristics of the biological solids produced by the laboratory AS reactors and the MBBR reactors were evaluated using DI and SVI assays. These two assays were performed twice a week in triplicate during the steady state conditions of all the reactors.

The SVI was measured using standard method 2710-D. The SVI parameter used to characterize the settling ability of a sample and was determined by pouring 1 litre of mixed liquor from the reactors into a 1 litre graduated cylinder. After 30 minutes, the

settled sludge volume was measured by observation of solid water interface and the SVI was calculated by dividing this volume by the average TSS concentration of the sample. Specifically the SVI was calculated by the following formula:

$$SVI = \frac{V_{Settled}}{TSS} \times 1000 \qquad \text{Eq. 3.2}$$

where, SVI = sludge volume index (ml/g); $V_{Settled}$ = settled sludge volume after 30 minutes (ml/L); TSS = total suspended solid concentration (mg/L). In addition, the SVI value depends on the MLSS concentration of the sample. For example, if a sample with a MLSS concentration of 10000 mg/L settles very little, the calculated SVI value will be approximately 100 ml/g (which is considered as a good SVI value) due its high TSS value (Davis, 2010).

A second parameter used to determine the settling ability of biologically-produced solids is the DI. Equation 3.3 shows the formula used to calculate the DI of a sample.

$$DI = \frac{TSS_0 - TSS_{30\ min.}}{TSS_0} \times 100 \qquad \text{Eq. 3.3}$$

where, DI = decantation index (%); TSS_0 = TSS at time of sampling (mg/L); $TSS_{30\ min.}$ = TSS of clarified liquid after 30 minutes of settling (mg/L). A 1 litre sample is allowed to settle inside a conical glass as shown in Figure 3.5 in order to perform the DI assay. The TSS_{30min} sample is taken from the top of the cone glass after the settling period is complete. Overall, DI is used in industry as an index of the settling ability of produced particles. The higher the DI percentage the greater settling has occurred in the sample.

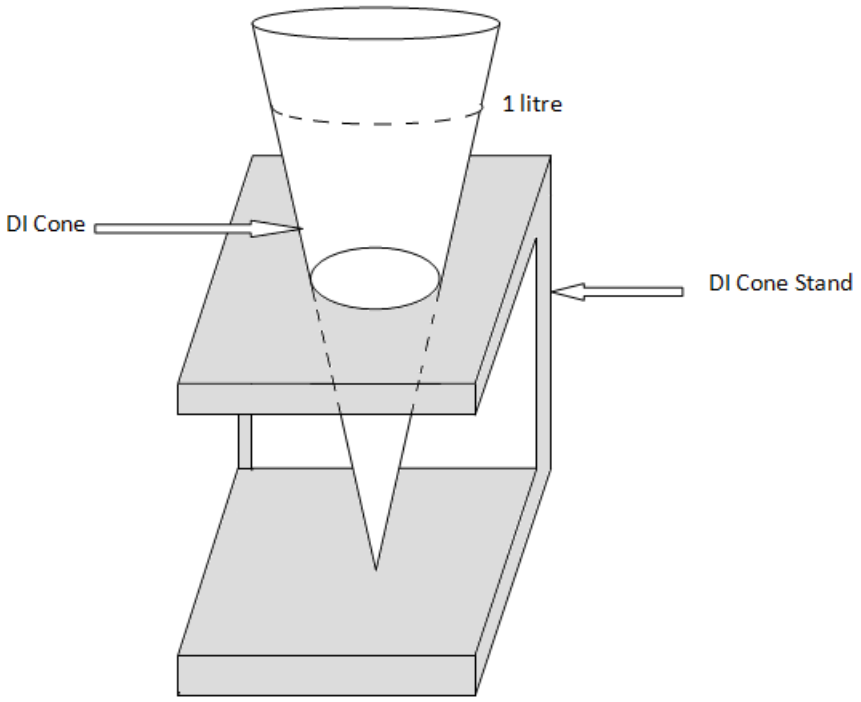

Figure 3.5 Schematic of DI apparatus setup

3.8 Particle Size Distribution Analysis

The particle size distribution of the biologically-produced solids was measured using a Brightwell Digital Particle Analyzer (DPA) Model 4100. The DPA results based on the volume of particles versus particle size diameter for the reactor effluent before settling and after 30 minutes of settling are presented in chapters 4, 5 and 6 of this work for each of the experimental phases. 1000 ml of the MBBR samples were filtered using a 400 μm mesh filter prior to analysis. 10 ml of the AS samples were diluted to 1000 ml prior to filtration with a 400 μm mesh filter and DPA analysis. A magnetic stirrer operated at a low speed kept all of the solids suspended (in 1 litre beaker) prior to being delivered to the DPA flow cell via a peristaltic pump. It should be mentioned that stirring the samples

even at low speeds may leads to collision of particles together that can make bigger or smaller particles and also delivering the sample through the tubing may change the particle sizes as well. The whole analysis was completed within 1 hour. The low-magnitude adjustment was utilized for the current study as it can detect particles in the range of 2-400 μm. Due to the detection range, the 400 μm mesh was used for filtration of particles larger than 400 μm prior to the analysis. The DPA system utilized micro flow imaging (MFI) technology, shown in Figure 3.6, to analyze the population of particles in the flow.

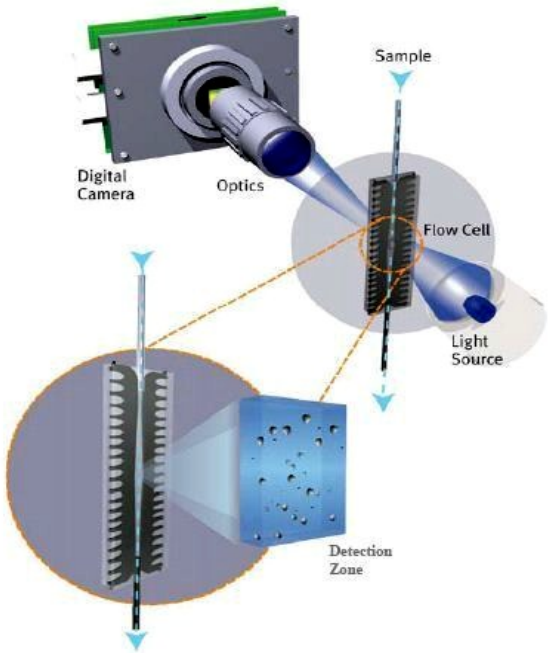

Figure 3.6 Brightwell MFI (Brightwell Technologies Website)

Based on the instrumental setting used in this study, the DPA system operated with the following parameters: optical magnification of 4.88x, display resolution of 0.25 μm, field of view of 1.75 mm x 1.4 mm and pixel resolution of 1280 x 1024. The peristaltic pump

used to deliver the sample to the flow cell which was mounted in front of a digital camera. The camera captures images of the sample as it pass through the flow cell with the images being analyzed by the internal software of the instrumentation to determine the particle size, particle count/concentration and morphology of the solids (Brightwell Technologies Incorporation, Ottawa, Ontario).

To ensure that the flow cell was properly reading the size and particle distribution, two standard solutions with 5.00 and 10.00 μm mean particle diameters were utilized to calibrate the system before each analysis. Table 3.5 shows the results of 5 calibration runs with 95% confidence interval (C.I.).

Table 3.5 Calibration results

Standard solution (μm)	**Measured mean particle size±95% C.I. (μm)**
5.00	5.00±0.75
10.00	10.00±0.87

The particle orientation during the analysis could affect the final results of the DPA. This is due to the fact that most of the particles are not symmetrical and the size detected by the system is dependent on the orientation of the particles, as shown in Figure 3.7 (Abbas, 2004). Moreover, the DPA software reports sizing of the particles based on the assumption that all the particles are spheres and thus it calculates an equivalent circular diameter (ECD) which is the maximum diameter of the projected image. It should be noted that other researchers have also used the same assumption as the DPA software. Wu et al. (2008) analysed the produced particles in AS effluents using a Malvern

Mastersizer system. In this study, the researchers assumed that all of the particles were spherical for sample analysis.

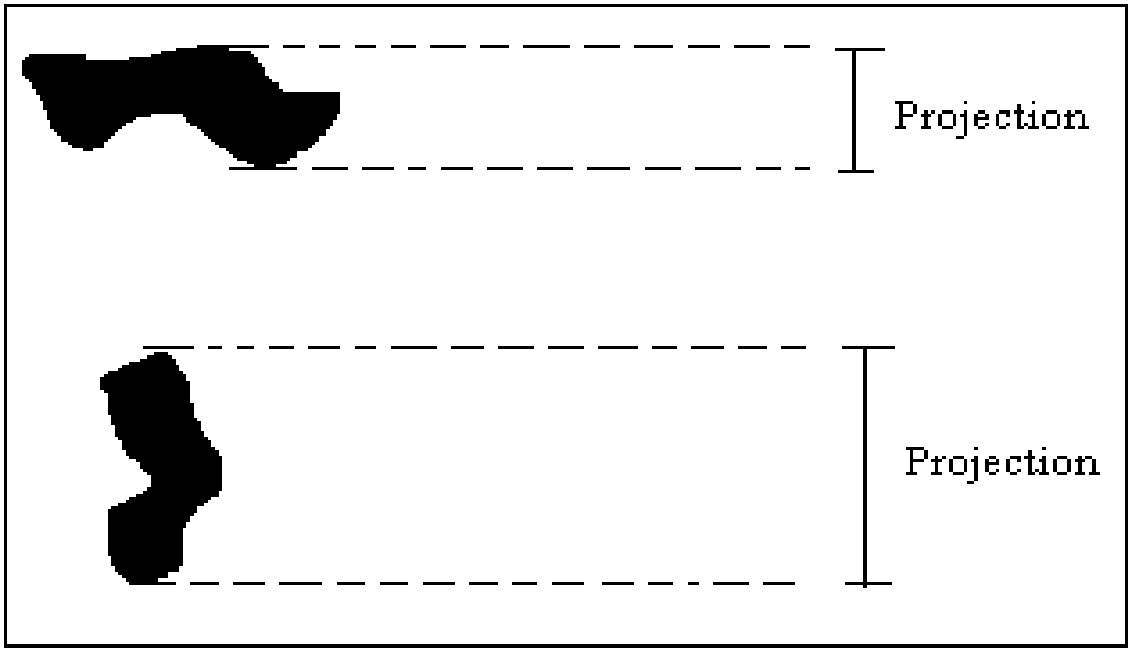

Figure 3.7 Size projection of HIACROYCO 9064 light-blocking particle counter (Abbas, 2004)

The DPA system produces hundreds of pictures for each sample which are divided into two categories, grayscale and binary (black and white) images. In binary mode, an automatic threshold is applied by the software to differentiate between the particles and the background. Figures 3.8a and Figure 3.8b show acquired DPA images of a sample where, the black portion of Figure 3.8b identifies a counted particle while the thinner string shaped objects are not taken into account by the instrumentation. However, thicker string shaped objects shown in Figure 3.8c are considered as particles as is illustrated in Figure 3.8d where the filamentous shapes are thicker. As such, it is concluded that the DPA instrument can underestimate the number and the volume of particles of samples.

This underestimation cannot be adjusted using our DPA instrument and as such the DPA values acquired were compared to traditional solids measurements of TSS to quantify the potential underestimation.

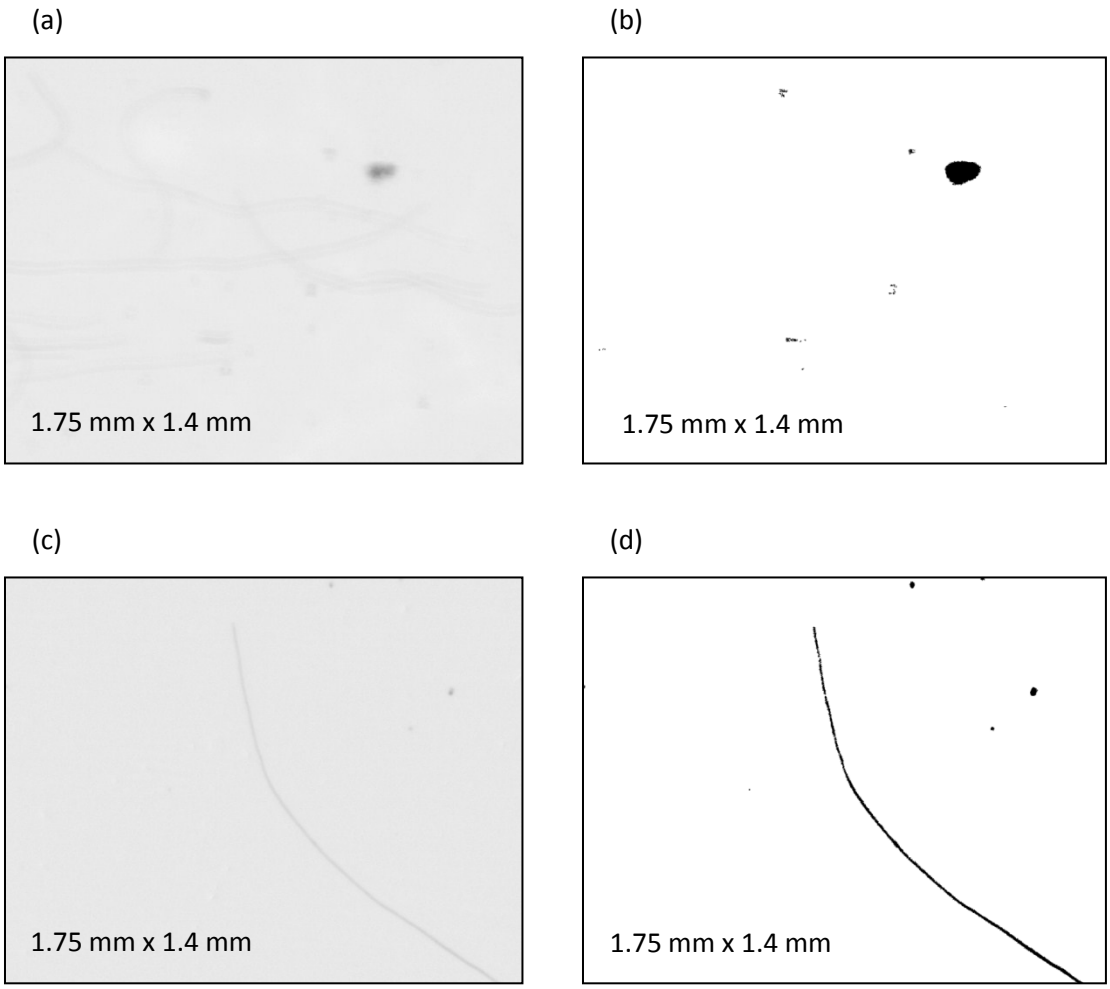

Figure 3.8 DPA images of particles showing sensitivity to string shaped particles (a) and (c) grayscale picture, (b) and (d) binary scale picture

In addition to calculating the ECD of the particles, the DPA instrument also determines the circularity coefficient (circumference of an equivalent area circle/perimeter of actual particle) of the particle which varies between 0-1 for each particle. When this parameter is one, the shape of the two-dimensional object in the image is exactly a circle. This

parameter was used in this study to better estimate the volume of each particle. Because the circularity versus #particles/ml output of the DPA instruments was normally distributed for all samples, the average circularity coefficient (CC) was used in the following formula to calculate the volume of each particle in this study:

$$V = \frac{4}{3} \cdot \pi r^3 \cdot \frac{1}{C} \quad \text{Eq. 3.4}$$

where, r = equivalent circular diameter (μm); C = average circularity coefficient and V= volume of a particle (μm^3). The volume for the particles >400 μm that were filtered before analysis were calculated using the following formula:

$$V_{>400} = Mass_{>400} \cdot \frac{1}{\rho} \quad \text{Eq. 3.5}$$

where, $V_{>400}$ = volume of the particles larger than 400 μm (ml); $Mass_{>400}$ = mass of particles larger than 400 μm (mg); and ρ = density of the solids- (mg/ml).

The following equation can be generated based on the known value of TSS. In addition, with the mass of the produced particles known from the filtration of particles >400 μm, the following equation can be rearranged for calculation of the unknown density:

$$TSS = \frac{V_{<400} + (Mass_{>400} \cdot \frac{1}{\rho})}{V_{TL}} \cdot \rho \quad \text{Eq. 3.6}$$

where, TSS= total suspended solids (mg/L); $V_{<400}$ = total volume of the solids less than 400 μm (ml); V_{TL}= total volume of the liquid (L); and ρ= density of the solids (mg/ml). Therefore, the density of the produced particles can be calculated by the following equation:

$$\rho = \frac{TSS \cdot V_{TL} - (Mass_{>400})}{V_{<400}} \quad \text{Eq. 3.7}$$

After calculating the density of the particles for each sample, an error calculation was performed in order to determine the density that best relates the experimental TSS to the TSS calculated by the DPA analysis. Based on the limited variation observed in the density of the various samples, one constant density was assumed for each system (AS and MBBR reactors); this calculated density was in turn used to express the particles >400 μm in terms of volume rather than mass and subsequently compare them to the DPA results.

3.9 ESEM Analysis

Scanning electron microscopy (SEM) is a high magnification form of microscopy which bombards the sample with a beam of electrons. This electron beam is very narrow and as such can resolve very high magnifications (up to 1,000,000x). The electron beam emitted by the instrument is directed at the surface of the object and it's interaction with the sample's atoms emits signals used to produce digital images of the sample. Therefore, electrons that scatter back reveal a surface image of the object (Carleton University SEM Lab. Website). SEM systems work in two different modes described as secondary electron detection and backscattered electron detection. The SEM analysis in this study is been done with secondary electron mode. Modified versions of an SEM called an ESEM was utilized by Delatolla et al. (2009) to acquire images of biofilm without the need for sample preparation. As such an ESEM was used in this study. A variable pressure chamber which ranges between 13.3 and 2666.4 Pascal replaces the high pressure chamber of a traditional SEM in an ESEM and this chamber enables acquisition of high magnification images of wet samples such as bacterial biofilms without sample preparation (Little et al., 1991; Delatolla et al., 2009). The ESEM analyses of the study

was performed using the *Tescan Vega-II XMU VPSEM*, Tescan USA Inc., Cranberry Twp., PA, USA at the Carleton University SEM laboratory, Ottawa, Ontario, Canada. Magnifications of 15, 50 and 1000x were used to show the thickness and morphology of biofim attached to the MBBR carriers.

Chapter 4

Effect of SRT on AS Biologically-Produced Solids

This chapter studies the settling characteristics and particle size distribution of biological solids produced by AS systems using three porous pot reactors operated at different SRTs. The AS reactor results presented herein are used as a baseline, conventional treatment system, comparison to the MBBR reactors results of Chapters 5 and 6.

COD was used to monitor the performance of the AS reactors and to validate that steady state conditions were achieved. In addition, the biologically-produced solids were characterized by measuring the MLSS and MLVSS concentrations, the SVI and the DI, while the DPA system was used to characterize the particle size distribution.

4.1 Operational Conditions of AS Reactors

After approximately 60 days of operation, the AS reactors reached steady state conditions; where sixty days of operation equate to 12, 6 and 4 SRTs, respectively, for the reactors operating at SRTs of 5, 10 and 15 days. Thus each reactor was operated longer than the three SRTs rule of thumb to achieve steady state conditions. Once at steady state, the reactors were operated for an additional 68 days. The COD concentration was maintained constant in the feed while the COD concentration remained approximately unchanged in the reactors throughout the steady state period. The pH of the influent remained neutral at 7.0±0.1 and the DO concentration was maintained between 4 and 4.5 mg/L.

Table 4.1 shows the average influent and effluent COD concentrations, the average values for loading rate, F/M and COD removal percentage at the three SRTs. The ± values in this table (as well as those in subsequent tables and the error bars in the subsequent graphs) are the ± 95% C.I. values from triplicate measurements. The AS reactors operated with SRTs of 5, 10 and 15 days exhibited COD removals of 94±2, 93±2 and 94±2%, respectively which implies that the COD removal rate is independent of the SRT for the synthetic wastewater that was fed to the reactors. These removal values are within the typical range for the AS process (Metcalf and Eddy, 2003). Figure A-1 to A-3 of Appendix A show the influent and effluent COD concentrations for each reactor plotted with respect to time. The influent and effluent COD concentrations of the reactors deviated only slightly about the average COD concentrations, their 95% C.I.'s were only 6±1 mg/L and 5±0 mg/L, respectively.

Table 4.1 AS steady state operating conditions

AS Reactors SRT (days)	**Loading Rate (g COD/L·d)**	**F/M (kg COD/kg VSS·d)**	**Average Influent COD± 95% C.I. (mg/L)**	**Average Effluent COD± 95% C.I. (mg/L)**	**Average COD removal ± 95% C.I. (%)**
5	1.6±0.02	0.8±0.08	413±7	24±5	94±2
10	1.6±0.02	0.6±0.03	417±6	27±5	93±2
15	1.6±0.02	0.5±0.03	413±6	24±5	94±2

Table 4.1 shows that increasing the SRT from 5 days to 15 days does not change the effluent COD concentrations and COD removal rates at the 95% confidence level. These results are similar to those of Eckenfelder (1979), who found that an AS system with an SRT greater than 7 days provide similar BOD removal efficiencies up to an SRT of 40

days. In addition, Barr et al. (1996) monitored AS systems to study the effect of HRT and SRT on the performance of the system by varying the SRT between 5 to 15 days, and they found that there was no improvement in COD removal rates for SRTs longer than 5 days. It should also be noted that the synthetic carbon source of the synthetic wastewater may have been too readily degradable to show removal efficiency shifts as a function of SRT.

4.2 MLSS and MLVSS of AS Reactors

The MLSS and MLVSS concentrations were monitored for the three reactors with the MLSS concentrations plotted with respect to time shown in Figure B-1 in Appendix B. Figure 4.1 show that the average MLSS and MLVSS concentrations of the three AS reactors increased with increasing SRT. The MLSS concentration increased from 1879±91 mg/L to 3586±150 mg/L when SRT increased from 5 to 15 days. For all three of the reactors, the calculated deviations in MLSS and MLVSS were low during steady state conditions and thus confirm that the reactors were at steady state.

These results are in agreement with those obtained by Bisogni et al. (1971), who demonstrated that by increasing the SRT from 0.25 to 12 days in a bench scale AS system with an HRT of 6 hours, the MLSS concentration increased from 81 mg/L to 2294 mg/L.

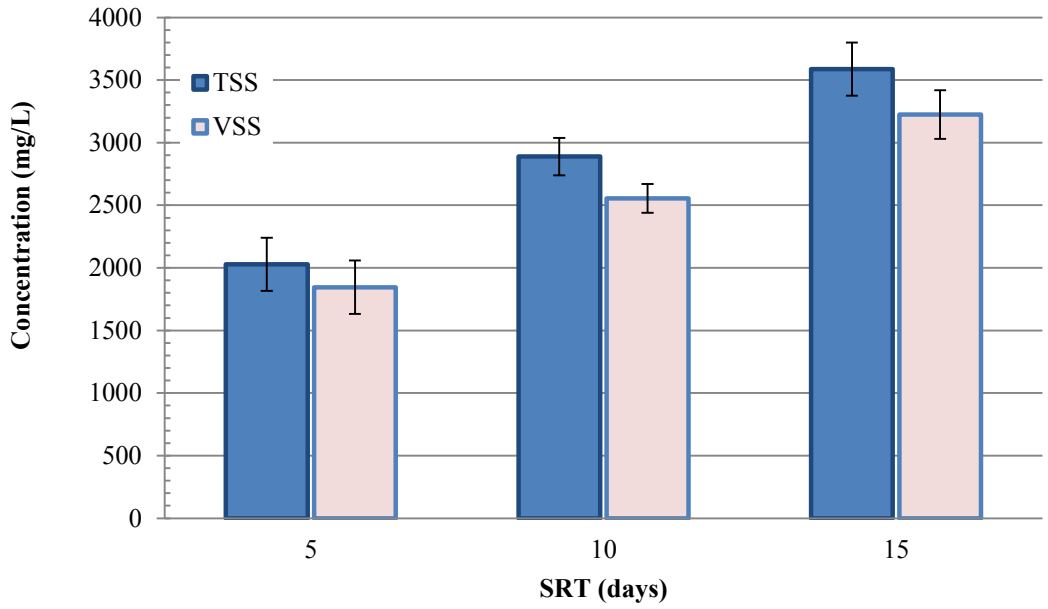

Figure 4.1 MLSS and MLVSS concentrations in the AS reactors operated at different SRTs

Table 4.2 shows the average MLVSS/MLSS ratio for all three reactors. The MLVSS/MLSS ratios are statistically similar at the various SRTs. The MLVSS values at SRTs of 5, 10 and 15 are 10±0.02, 11±0.03 and 10±0.02% lower than the MLSS concentrations, respectively. As noted above the similarity in MLSS/MLVSS ratios and observed biomass yields at the different SRTs may be due to the synthetic wastewater that was fed to all three reactors.

Table 4.2 MLVSS/MLSS for the AS reactors operated at various SRTs

AS Reactors SRT (days)	MLVSS/MLSS± 95% C.I.
5	0.90±0.02
10	0.89±0.03
15	0.90±0.02

Based on the design equations for an AS system, the MLVSS concentration is directly related to the SRT, as shown in Equation 4.1 (Metcalf and Eddy, 2003). All the reactors were operated with the same HRT and the influent and effluent COD concentration were similar at the three SRTs. Two other factors that are remained unknown ("b" and "Y") can be calculated by linear regression which is done below.

$$MLVSS = \frac{SRT}{HRT} \cdot \frac{Y \cdot (COD_{in} - COD_{out})}{(1 + b \cdot SRT)} \qquad \text{Eq. 4.1}$$

where, all the concentrations units are mg/L in the equation and both SRT and HRT unit is day and b = decay coefficient (1/day) and Y = biomass yield (g VSS formed / g COD consumed).

To find b and Y values, a linear regression, shown in Figure 4.2, is implemented based on Eq. 4.2. This equation is generated from Eq. 4.1 to plot a line for finding b and Y.

$$\frac{1}{SRT} = \frac{Y \cdot (COD_{in} - COD_{out})}{MLVSS \cdot HRT} - b \qquad \text{Eq. 4.2}$$

Therefore, by plotting the terms that are multiplied to "Y" (which is called "T") versus "1/SRT", a line is produced where the intercept is b and the slope is Y. Figure 4.2 shows this plot for average values of reactors with three SRTs. Figure 4.2 shows that the decay coefficient is approximately 0.121 and the average biomass yield is approximately 0.376.

It should be noted that both of these values are within the typical ranges reported by Metcalf and Eddy (2003).

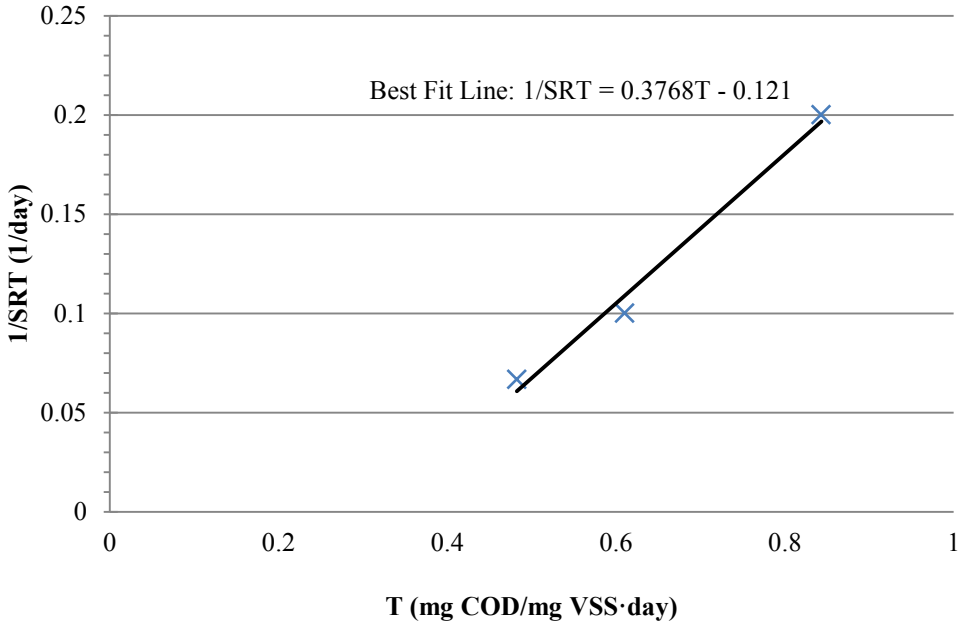

Figure 4.2 Linear regression for finding b and Y of AS reactors at three SRTs

Moreover, since the feed solution of the AS reactors did not contain any solids, the MLVSS can be assumed to be simply the concentration of the biomass and cell debris while the MLSS consisted of the MLVSS plus the fixed suspended solids (FSS) from the mineralized cell debris. This is shown in Equations 4.3 and 4.4 (Metcalf and Eddy 2003).

$$MLVSS = biomass + cell\ debris + nbVSS \quad \text{Eq. 4.3}$$

$$MLSS = biomass + cell\ debris + nbVSS + FSS \quad \text{Eq. 4.4}$$

where, all the concentrations units are mg/L in the equation and nbVSS = non biodegradable volatile suspended solid concentration (mg/L) and FSS = fixed suspended solids concentration (mg/L). Given that the influent was void of nbVSS and FSS, based

on equations 4.1, 4.3, 4.4 and Figure 4.2, it is expected that under the laboratory operating conditions the MLSS and MLVSS be in fact directly related to the SRT of the reactors; thus the observed increases in the MLSS and MLVSS values at higher SRTs observed in this study is described well by the equations above.

4.3 Sludge Volume Index

The SVI values for the reactors with SRTs of 5, 10 and 15 days are shown in Figure 4.3. This figure shows that SVI values decrease from 247±11 to 54±1 ml/g with increasing SRT from 5 to 15 days. Therefore, these indicate that increasing the SRT values of the systems had a positive impact on the settling characteristics of biologically-produced solids. Eckenfelder (1979) also found that poorly-formed flocs with high SVI values is more likely to occur when the SRT is between 2 and 9 days and well-formed flocs start to appear as SRT increases. Well flocculated organisms with low SVI values are more likely to occur in SRTs between 13-18 days for AS reactors (Eckenfelder, 1979).

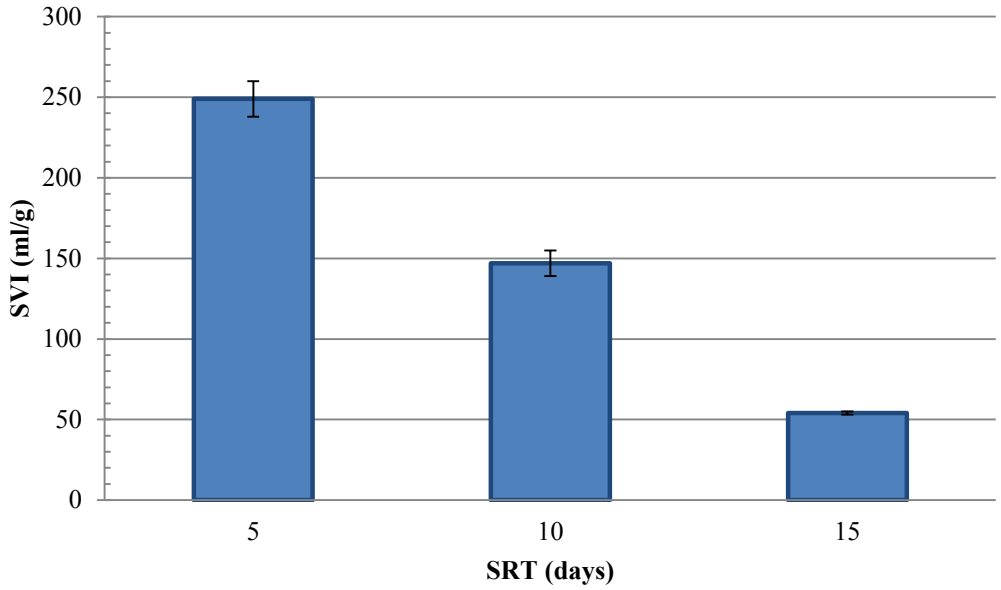

Figure 4.3 SVI values for the AS reactors operated at various SRTs

A positive impact on the settling characteristics with increasing SRT could be due to the production of more compact flocs toward an ideal quality for floc formation and a reduction in excess of EPS formation that is the main reason for viscous bulking (Wanner, 1994). Jin et al. (2003) showed that poor settling could be related to morphological properties (size distribution, structure, density and filaments), microbial population (bacteria, filament and protozoa), physical properties (flocculating ability, surface properties, and stability) and the chemical constituents (polymers, inorganic salts, extractable EPS). Growth of filamentous organisms could also be a possible explanation for occurrence of higher SVI values at lower SRTs. This growth is often considered the most important reason for bulking in AS systems (Metcalf and Eddy, 2003) since it may result in severe bulking (Pipes, 1997). Influent and process conditions such as HRT, SRT, DO, temperature and pH can also affect the settling properties. However, all three of the reactors in this study had the same values of these parameters other than the SRT. From

this data, it is evident that the best settling ability was observed for the reactor with the SRT of 15 days.

4.4 Decantation Index

The DI analysis was used in addition to SVI measurements to quantify the settleability of particles. Although DI is not used as frequently as SVI, DI is used quite regularly in the wastewater treatment industry. Figure 4.4 shows the relationship between the measured DI values and SRTs. The figure shows that as SRT increases in AS reactors, the DI also increases. Additionally from SRT 10 days to SRT 15 days, the DI increased significantly which shows that settling ability of the AS biologically-produced solids improved significantly in that range.

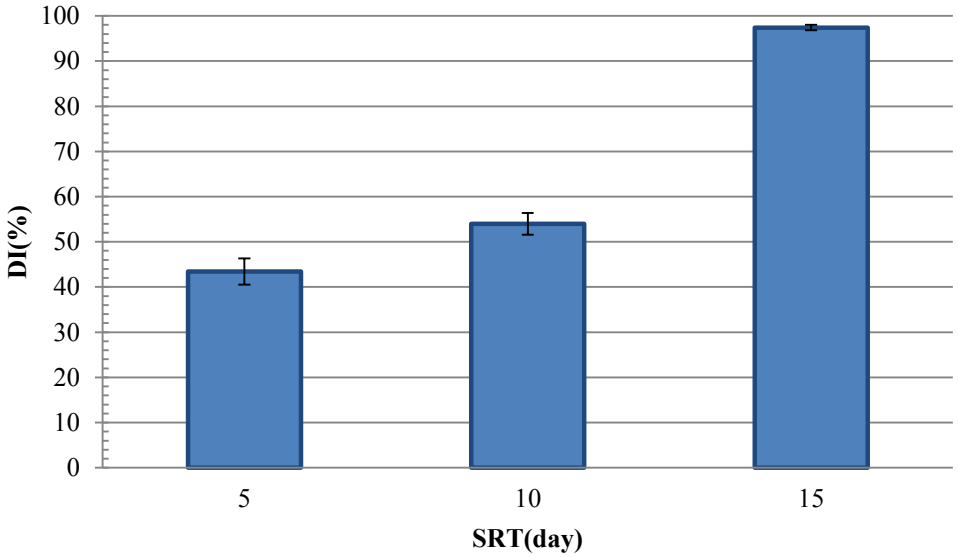

Figure 4.4 DI values for the AS reactors operated at various SRTs

The current section showed that in higher SRTs, higher DI values are observed that is an indicator of higher settling ability. Additionally, based on the discussion in Section 4.3, excess filamentous growth may be the main reason for poor settling in low SRTs.

Results in Section 4.3 showed that higher SRTs had lower SVI values which indicate better settling characteristics for solids. Therefore, the DI results support the SVI findings and conclusion presented in Section 4.3.

The fact that the laboratory scale AS reactors operated with SRTs of 5 and 10 days produced poorly settling mixed liquor was not expected. In fact, there are a large number of full-scale AS systems operating in this SRT range without settling problems. Thus, the poor settling seems to be associated with the wastewater characteristics and possibly due to the large fraction of readily biodegradable organics. Wastewaters from many sources have different characteristics and some wastewaters behave like the synthetic wastewater used in this study. Furthermore, even if the synthetic wastewater is not fully representative of a typical wastewater this research is still valuable as the main objective is a direct comparison of the settling characteristics of the solids produced by AS and MBBR systems.

4.5 Particle Distribution Analysis

The particle size distribution analysis was completed using a MFI technology, specifically the Brightwell DPA, to analyze the biologically-produced solids. Figure 4.5 shows three DPA images for AS samples from reactors with different SRTs. Each image was analyzed using the software that accompanies the instrument. Figure 4.5a shows an image of a mixed liquor sample from the 5 day SRT reactor, it is clear that there are many string-shaped objects that could be considered filamentous bacteria and the number of these objects decreases for the 10 day SRT reactor image (Figure 4.5b). Moreover, based

on the MFI images there is no evidence of existence of string shape objects in the reactor with SRT of 15 days as Figure 4.4c shows.

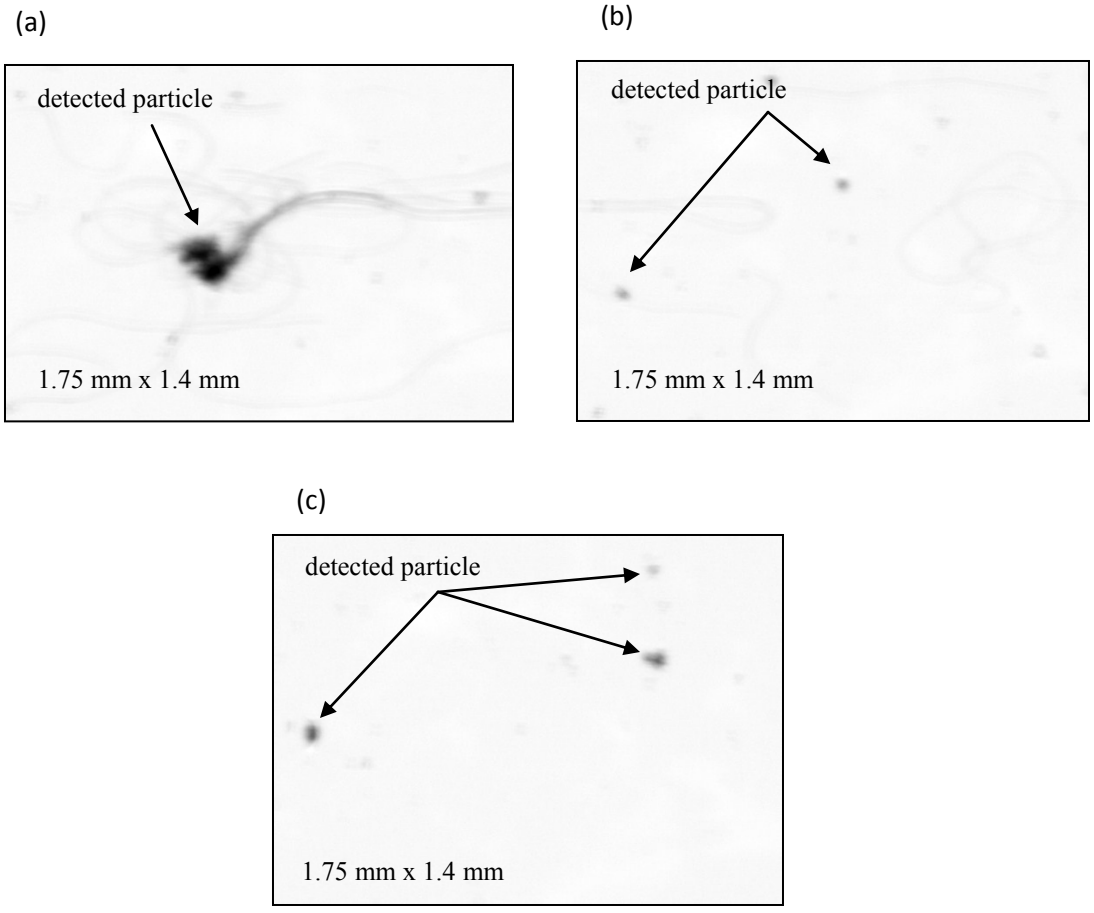

Figure 4.5 DPA grayscale images of the AS reactors operated at different SRTs (a) SRT = 5 days, (b) SRT = 10 days and (c) SRT = 15 days

Table 4.3 shows the mean CC values for all the reactors. It is clear that CC did not change significantly by increasing the SRT as it remained approximately 0.35±0.03. The inverse of the CC values at each SRT was used to calculate the volume of the solids detected by DPA analysis as described in Section 3.9.

Table 4.3 Mean CC of the AS reactors operated at various SRTs

AS Reactors SRT (days)	Mean CC±95% C.I. (mg/L)
5	0.34±0.03
10	0.37±0.03
15	0.35±0.01

The contribution of the >400 μm particles to the total particle volume was calculated by measuring the mass of particles captured by filtration through a 400 μm mesh and dividing the mass by an estimated density. This enabled the volume of solids between 2-400 μm, measured using DPA, to be comparable to the solids >400 μm that were filtered and weighed. The average density of the solids was estimated by an error calculation between the experimental TSS values measured using standard methods and the TSS values approximated from the DPA. The percentage errors for these two sets of data are shown in Table D-1 Appendix D, where a density of 1150 mg/ml had the lowest percentage error value. This density value is slightly lower than the one value of 1250 mg/ml reported in Metcalf and Eddy (2003), and this lower density possibly leads to poorer settling.

DPA analysis was conducted for two types of samples: (i) mixed liquor samples (referred to as unsettled or before settling); and (ii) the supernatant of the mixed liquor after 30 minutes of settling (referred to as after settling). “Before settling” samples were immediately injected into the DPA upon sampling, while “after settling” samples were allowed to settle under undisturbed, quiescent conditions, for 30 minutes and

subsequently decanted, the decanted liquid was injected into the DPA. A settling time of 30 minutes is based upon the chosen quiescent time used in the DI analysis.

The results for percent volume distributions of particles in the mixed liquor (before settling) at the three SRTs are shown in Figure 4.6. It should be noted that the values plotted in the figures of this section are the average for 6 measurements (duplicate at three measurements). The right side of Figure 4.6 shows that the percent volume contributions of particles in the range of 2-400 μm at SRTs of 5, 10 and 15 days are 42±3, 45±3 and 56±5%, respectively. At an SRT of 5 days, a high volume percentage of particles (19±1%) between 2-400 μm are located are in the range of 300-400 μm, but otherwise the particle volume is fairly evenly distributed. In contrast, the volume percentage of particles between 2-400 μm at an SRT of 15 days in the range of 300-400 μm is only 7±2%, with 21±2% of the particles being attributed to the range of 60-100 μm and the percent volume gradually decreases as the particle sizes increase. The particle size distribution of the particles between 2-400 μm based on percent volume for the biologically-produced solids at an SRT of 10 days shows characteristics that are comparable to those from the 5 and 15 day SRTs reactors in that it has a peak in the small particle range (particles between 2-100 μm comprise 14±2% of the total volume) and at the large particle range (particles between 240-340 μm comprising 19±1% of the volume). Therefore, at SRT 5 days the particles volume are more distributed in the larger ranges, while at SRT 15 days, most of the particles volume are located in the smaller range and the volume of particles at intermediate SRT (10 days) is distributed at both the beginning and end of the particle size ranges with less volume attributed to the middle ranges. This trend of decreasing particle size with increased SRT is again demonstrated

for particles >400 µm (Figure 4.6), where the volume percentages for particles >400 µm increased from 58±2 to 55±3 and 44±6% as the SRT increased from 5 to 10 and 15 days, respectively.

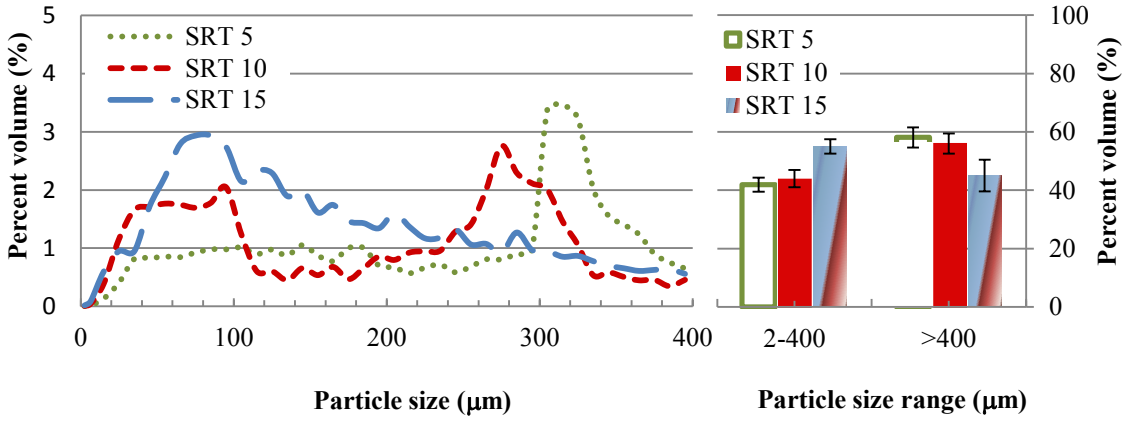

Figure 4.6 Volume based particle size distributions of particles between 2-400 µm and > 400 µm for AS reactors operating at three different SRTs for mixed liquor samples (before settling)

Figure 4.7 shows the percent volume distribution for particles between 2 and 400 µm along with the overall percentage of particles in the range of 2-400 µm and >400 µm for both "before settling" and "after settling" samples from the three different SRT AS systems. Figure 4.8 shows the percentage removal for the various particle size fractions based on the "before settling" and "after settling" (i.e. supernatant) data. The values of the after settling samples shown in Figure 4.7 are based on the total volume of the sample in the unsettled mixed liquor and because of this the percentages of the 2-400 and >400 µm fractions do not add up to 100%. Figure 4.7a shows that at an SRT of 5 days the difference between the unsettled and the settled percentage are 32±2 and 53±2% in the size ranges of 2-400 and >400 µm . This is again shown on the right side of Figure 4.8. Based on these two values and fraction of the particle volumes in both of these ranges

one can calculate that the overall volume percentage removal at an SRT of 5 days is 44±3%. In addition, the left side of Figure 4.7a shows that for the particles smaller than 400 μm, the removal percentage at an SRT of 5 days is poor throughout the entire particle size range as the difference between prior and after settling are minimal with no definite pattern.

The right side of Figure 4.8 shows that for the mixed liquor of the 10 day SRT reactor, 30 minutes of settlement removed 23±1 and 80±2% of particles in the 2-400 and >400 μm size ranges, respectively. Moreover, the left side of Figure 4.7b shows poor settling at an SRT of 10 days throughout the particle size distribution with a slightly improved removal between small particle range and in the 240-340 μm size range. Figure 4.8 shows that the volume removal percentage varies through the particle size distribution. The overall removal percentage for total volume of particles at an SRT of 10 days is 54±4%.

Based on the difference between the unsettled and the settled percentage of the 2-400 and >400 μm particle groups the right side of Figure 4.7c demonstrates that at an SRT of 15 days, settling removed 95±1 and 100±0% of the particles in these groups. The total volume percentage particle removal for the 15 day SRT activated sludge reactor was calculated to be 97±1%. From the left side of Figure 4.7c it can be seen that while particles >30 μm settled well, there is a significant reduction in the volume percent removal of particles in the range of 2-30 μm.

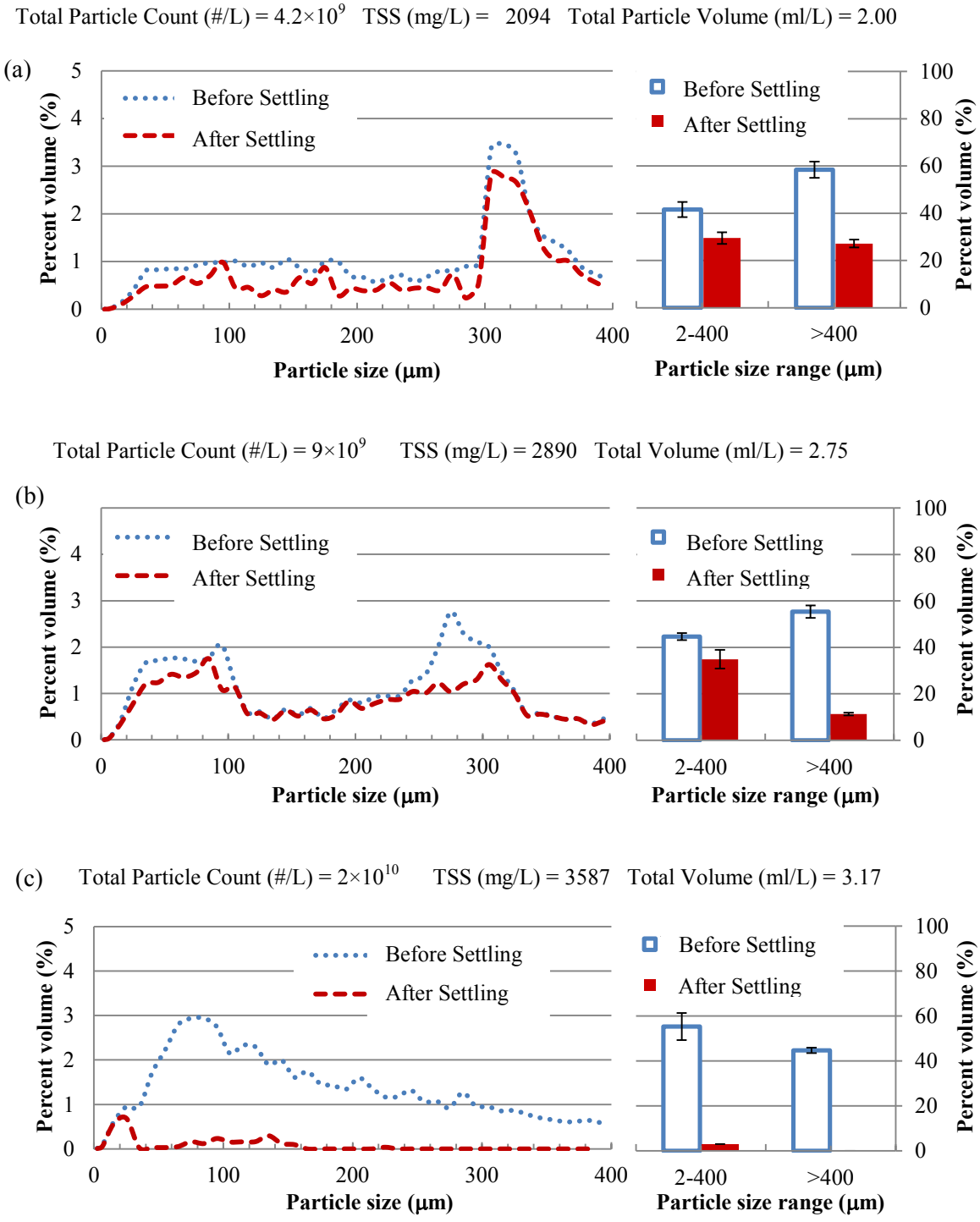

Figure 4.7 Percent volume distribution of particles between 2-400 μm and > 400 μm before settling and after settling for the AS systems operating with SRTs of (a) 5 days, (b) 10 days, and (c) 15 days

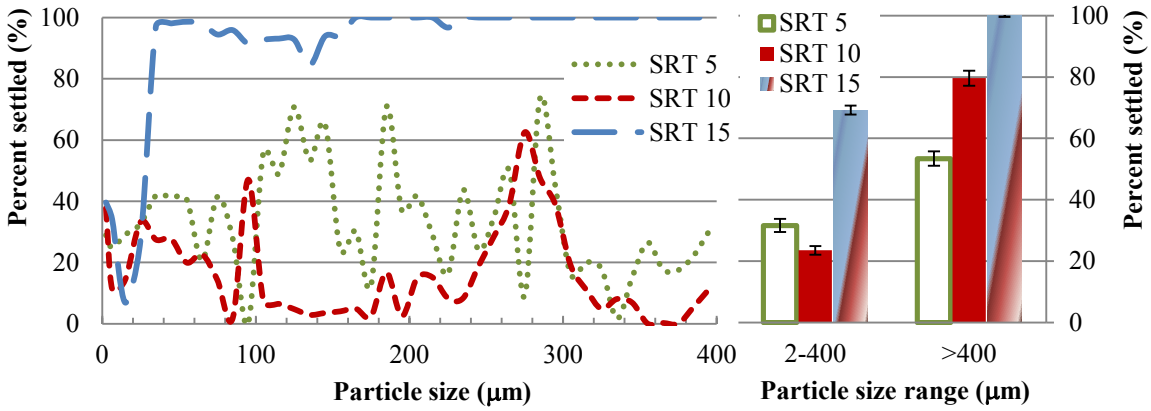

Figure 4.8 Volume percentage removals of particles between 2-400 µm and > 400 µm for AS reactors operating at three different SRTs

Table 4.4 summarizes the particle size distribution analysis results for "before settling" and "after settling" mixed liquor for all three AS reactors. It shows that by decreasing the SRT from 15 to 5 days, the total number of particles prior to settling as well as the total volume of particles following settling decreased. Another significant observation is the decrease in the mean particle diameter as the SRT decreased, in the samples prior to settling and following settling. As shown in Figure 4.8, improved particle removal was achieved with increasing SRT yet Table 4.4 shows that the mixed liquor's average particle size decreased with increasing SRT; thus it appears that settling is impacted more by the SRT-related differences in particle characteristics than the changes in particle size.

Table 4.4 Particle size distribution characteristics of AS reactors at different SRTs

AS Reactors SRT (days)	Total Number of Particles (#/ml)		Total Concentration of Particles (ml/L)		Mean Particle Diameter (μm)	
	Before Settling	After Settling	Before Settling	After Settling	Before Settling	After Settling
5	$(42.0\pm3)\times10^{5}$	$(29.0\pm2)\times10^{5}$	$(20.0\pm1)\times10^{-1}$	$(11.2\pm1)\times10^{-1}$	15.0±2	13.0±2
10	$(95.0\pm7)\times10^{5}$	$(70.0\pm5)\times10^{5}$	$(27.5\pm2)\times10^{-1}$	$(12.6\pm1)\times10^{-1}$	14.0±1	6.0±1
15	$(160.0\pm9)\times10^{5}$	$(66.0\pm4)\times10^{5}$	$(31.7\pm2)\times10^{-1}$	$(1.0\pm1)\times10^{-1}$	8.0±1	4.0±1

Table 4.5 summarizes the percent number of particles in different particle size ranges at three SRTs, this is in contrast to the percent particle volumes discussed up to now. As shown in the shaded column in Table 4.5, the percent number at various ranges shows that particles between 2-20 μm in size, were responsible for 77, 80 and 92% of the number-based percentage at SRTs of 5, 10 and 15 days, respectively. The volume percentage for this range was really negligible at all three SRTs as most of the volume percentages were originated from particles >50 μm. Li and Ganczarczyk (1991) analyzed flocs from conventional activated sludge plants and they found that particles >50 μm were the major source of particle volume and the smaller size ranges comprised a very low percentage of the volume. They also pointed out that in terms of number percentages the contribution of particles <16 μm is high (17-70%) while the volume percentage for this range is negligible. Similar results were obtained in this study, indicating that the produced flocs have similar properties to those present in other conventional AS reactors.

Table 4.5 Percent number of particles in different ranges for AS reactors

AS Reactors SRT (days)		**Number Percentage (%)**							
-------	Range (μm)	2-3	3-10	10-20	2-20*	20-30	30-40	40-100	100-400
5	-----	48.0±4	18.0±1	11.0±1	77.0±6	9.0±0	6.0±0	7.0±0	1.0±0
10	-----	46.0±2	21.0±1	13.0±1	80.0±4	9.5±0	5.3±0	4.8±0	0.4±0
15	-----	66.0±5	17.0±2	9.1±1	92.1±8	3.3±0	0.8±0	3.3±0	0.5±0

* Summation of the previous three columns

Table 4.6 summarizes the SVI, DI and percent volume removal and percent number removal for AS reactors at three SRTs. This table shows that for each SRT the percent volume removal was always greater than number percentage removal. Therefore, it is apparent that the particles removed at each SRT were the larger particles that have larger volumes. From the SVI, DI and percent volume removal all confirmed poor particle removal by settling for the mixed liquor of the 5 day SRT reactor. In contrast, the AS reactor with the longest SRT (15 days) showed the best particle removal with only poor settling at the small particle ranges. This means that, the reactor with the SRT of 15 days produced larger and more effectively settling particles than the other two reactors. In addition, the DI values measured using standard filtration methods at all SRTs was very close to the percent volume settled values calculated from the DPA results and as such serves as a validation of the DPA results.

Table 4.6 SVI, DI, percent volume and percent number removed that measured by DPA for AS reactors at different SRTs

AS Reactors SRT (days)	SVI ± 95% C.I. (ml/g)	DI ±95% C.I. (%)	Settled Effluent TSS (mg/L)	Percent Volume Removal ± 95% C.I. (%)	Percent Number Removal ± 95% C.I. (%)
5	247±11	43±3	1075±96	44±3	30±4
10	147±8	51±3	1416±118	54±4	26±3
15	54±1	97±1	108±7	97±2	40±2

Chapter 5

Effect of SALR on MBBR Biologically-Produced Solids

As explained in Section 3.5, three identical laboratory MBBR reactors were operated with different SALRs for a period of 55 days. This experimental phase was used to investigate the biologically-produced solids in MBBR reactors.

COD measurements were monitored to evaluate the performance of the MBBR reactors and to validate steady state conditions. TSS, VSS, SVI, DI and DPA measurements were used to characterize the biologically-produced solids and to evaluate their settling characteristics. Finally, ESEM was used to acquire images of the MBBR carriers to investigate the effects of different SALRs on the morphology and thickness of the produced biofilm.

5.1 Operational Conditions of the MBBR Reactors

Three MBBR reactors were operated with an intermediate SALR (32 g COD/m^2·d) for two weeks to allow for biofilm growth to develop on the carriers. Following this, the SALRs were changed to 9 g COD/ m^2·d, 32 g COD/ m^2·d and 64 g COD/ m^2·d to investigate the relationship between SALR and the biologically-produced and detached solids. The feed COD concentration was maintained constant while the COD concentration inside the reactors remained approximately unchanged throughout the experimental phase. The pH remained neutral at value of 7.0±0.1 and the DO concentration of the reactors was maintained at 4.2±0.2 mg/L. After 12 days of running the three MBBR reactors, the variations in the percent COD removal and the SALR were

less than 3% and 0.4 g COD/m^2·d, respectively, and thus the steady state conditions were deemed to be achieved. Once at steady state the reactors were operated for an additional 43 days. COD concentrations as a function of time at the three different SALRs are presented in Appendix A, Figures A-4 to A-6.

Table 5.1 summarizes the influent COD, effluent COD and average percent removal for the three MBBR reactors. The ± values in this table (as well as those in subsequent tables and the error bars in the graphs) are the ±95% C.I. values from triplicate measurements. The MBBR reactors with organic SALRs of 9, 32 and 64 g COD/m^2·d showed 75±2, 74±3 and 65±2 % removal of influent COD, respectively. The COD removal at SALR of 32 g COD/m^2·d was very close to the removal achieved by the first reactor (9 g COD/m^2·d) despite the higher SALR and the COD removal percentage in the reactor with the highest SALR was approximately 10% lower than the other two reactors. It is expected to have lower removal efficiency with increasing loading. Furthermore, it should be noted that 64 g COD/m^2·d is a very high loading for a municipal wastewater treatment system, and it actually approaches loadings applied to roughing MBBRs used as pre-treatment for a second biological treatment process.

Table 5.1 MBBR steady state operating conditions

MBBR Reactors SALR (g COD/m^2·d)	**Average Influent COD±95% C.I. (mg/L)**	**Average Effluent COD±95% C.I. (mg/L)**	**Average Removal Percentage±95% C.I. (%)**
9	92±2	23±2	75±2
32	348±10	86±4	74±3
64	683±15	232±8	65±2

Other than the first reactor which had an effluent COD concentration of 23±2 mg/L, the effluent concentrations observed for the other two reactors were fairly high. The intermediate reactor had an effluent COD concentration of 86±4 mg/L while the reactor with the highest loading rate had an effluent COD concentration of 232±8 mg /L. Based on the COD effluent concentrations further treatment prior to discharge would normally be required for the effluent of the highest loading MBBR and also possibly for that of the intermediate loading MBBR.

As mentioned above, the moderate efficiency of the MBBR reactors is likely due to their short (one hour) HRT. Currently, in industries with high strength organic wastewaters MBBR processes are used in series to other MBBR units or as roughing units in tandem with other treatment processes including AS and lagoons. Leiknes and Ødegaard (2001) combined an MBBR reactor with a membrane bioreactor (MBR) to build a pilot plant for treatment of wastewaters with high SALRs (100-150 g COD/m^2·d) and HRTs of 20-30 minutes in order to investigate the COD removal rate within the system. Their pilot-scale study concluded that 85 to 90% of the COD can be removed by the MBBR-MBR system. Sunner et al. (1999) also followed MBBR treatment by another biotreatment process (an AS reactor) as for the treatment of a high strength wastewater (BOD = up to 763 mg/L and ammonia = 37.8 mg as N/L). Overall, the two stage process achieved over 90% ammonia removal as well as providing full treatment to meet carbonaceous BOD standards.

Table 5.2 shows the SRT and the volumetric loading rate of the MBBR reactors. It should be noted that SRT and volumetric loading rate are not commonly used to describe the operation of biofilm or MBBR systems. However, for comparison to the AS data

presented in Chapter 4 these parameters were calculated for this study. Equation 5.1 which is extracted from the fundamental SRT definition of an AS system, was adapted for MBBR systems as follows:

$$SRT = \frac{(No.\,of\ carriers) \cdot (M_{VSS})}{Q \cdot (VSS_{eff})} \qquad \text{Eq. 5.1}$$

where, No. of carriers = the number of bio carriers in the reactor; M_{VSS} = the VSS of the biofilm attached to a carrier (mg); Q = the reactor flowrate (L/day); VSS_{eff} = the VSS concentration of the effluent (mg/L). The SRT was thus estimated by the detachment rate of particles from the suspended carriers. In addition, because volumetric loading rate as a parameter does not take the percent fill and the specific surface area of carriers into account, it does not incorporate the quantity of biofilm in the system in its calculation. As it is shown in Table 5.2, both SRT and volumetric loading rate are increasing as SALR increases.

Table 5.2 SRT and volumetric loading rate of MBBR reactors operated at various SALRs

MBBR Reactors SALR (g COD/m^2·d)	**SRT (days)**	**Loading Rate (g COD/L·d)**
9	0.9±0.1	2.04±0.04
32	0.9±0.1	7.8±0.2
64	3.8±0.3	15.2±0.3

Section 4.1 showed that the COD removal rate for AS reactors was always higher than 90% while the MBBR reactors in the study were operated to achieve lower COD removal with lower than 70% COD removal at the higher SALRs. The operation of the

MBBR laboratory reactors at lower COD removal percentages was an outcome of operating the MBBRs under low HRTs to maintain optimal attached growth in all the reactors being fed with SWW.

5.2 Effluent TSS and VSS of the MBBR Reactors

The history of the effluent TSS and VSS concentrations of the three MBBR reactors operating with different SALRs are reported in Appendix B and Figure B-2. Figure 5.1 illustrates the average effluent TSS and VSS concentrations at three SALRs. Note that as this study used a soluble wastewater as the feed, it does not contain any influent TSS or VSS. Accordingly one cannot calculate VSS and TSS removals, in fact the effluent VSS and FSS (i.e. the non-VSS portion of TSS) in this study is derived from the biofilm and biomass or simply detached biofilm. As shown in Figure 5.1, the average TSS of the MBBR reactors increased from 21.7±3 to 145±11 mg/L as the SALR increased from 9 to 64 g COD/m^2·d. For all three of the reactors, the calculated 95% C.I.s were small, thus confirming the steady performance of the MBBR reactors.

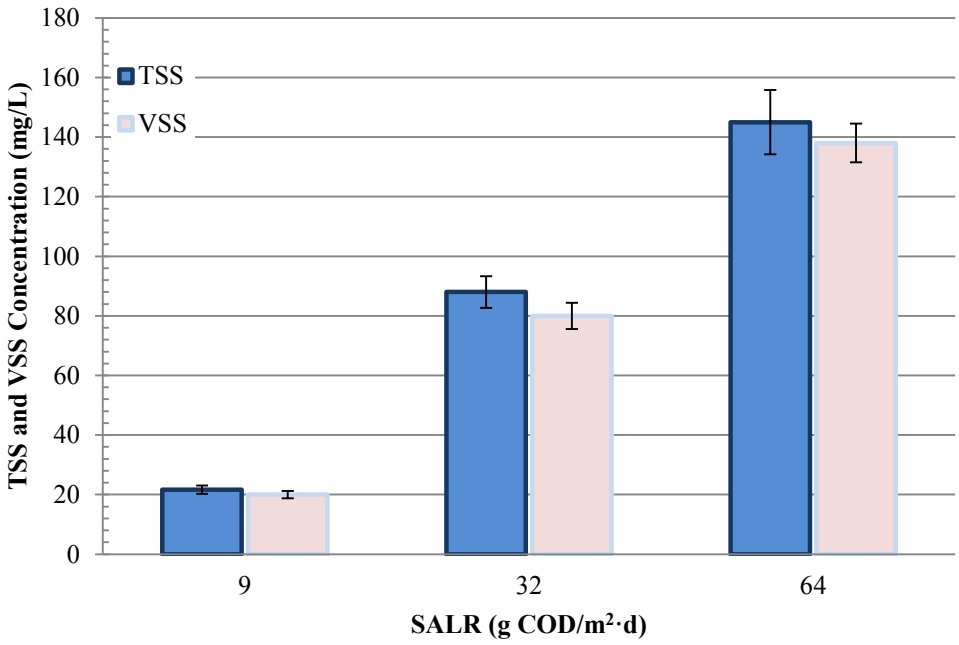

Figure 5.1 TSS and VSS concentrations in the MBBR reactors operated at various SALRs

This study validates the works of Hosseiny and Borghei (2002) who found that by increasing the influent COD concentration from 225 to 4361 mg/L the VSS concentration (which showed a linear relationship with TSS) increased from 380 to 1470 mg/L. It should be noted that VSS showed a linear relationship with TSS. In the current study, the TSS concentration increased from 21.7±3 to 145±11 mg/L with as the effluent COD concentration increased from 92 to 692 mg/L.

The SALR and the resulting VSS/TSS ratios for the three reactors are summarized in Table 5.3. From here, it is evident that the VSS concentration is similar to the TSS concentration. Overall, approximately 94% of the effluent TSS is volatile with less than 7% being fixed. This is not surprising as the effluent TSS is expected to be primarily

detached biofilm and biomass with the FSS likely being primarily mineralized biologically derived materials.

Table 5.3 VSS/TSS ratio for MBBR reactors operated at various SALRs

MBBR Reactors SALR (g COD/m^2·d)	**VSS/TSS± 95% C.I.**
9	0.95±0.04
32	0.94±0.02
64	0.94±0.03

Section 4.2, which presented the results from the MLSS and MLVSS analyses of AS reactors shows that the MLSS concentration ranges between 1879±91 mg/L and 3586±150 mg/L for SRTs of 5 and 15 days, respectively. On the other hand, the effluent TSS concentration for the MBBR reactors at SALRs between 9 to 64 g COD/m^2·d varies in the range of 21.7±3 to 145±11 mg/L. As expected the AS reactors show significantly higher concentration of suspended solids than the MBBR reactors. Åhl et al. (2006) also stated that the solids produced by attached growth systems are expected to be at least 10 times less than suspended growth systems.

The MLVSS/MLSS ratio for AS discussed in Section 4.3 and the values were approximately 0.90 for all three reactors. In addition, as discussed in the current section, the VSS/TSS ratio for all MBBR reactors were approximately 0.94 that is slightly higher than that of AS reactors. It should be noted that since the feed solution does not contain any solids, the MLVSS concentration is the sum of concentrations of the biomass and cell debris. The slightly higher VSS/TSS ratio for MBBR reactors may be due to

experimental error or can be related to the lower removal efficiency of the MBBR reactors that will result in less mineralized final products.

5.3 Sludge Volume Index

The SVI values for the MBBR reactors at different SALRs are shown in Figure 5.2. As this figure shows, the SVI value increased as the MBBR reactor SALR increased that may suggest a lower capability to settle. As a result, observation of low settling potential of the biologically-produced solids is expected to be due to the negative impact of SALR on the settling characteristics of the solids.

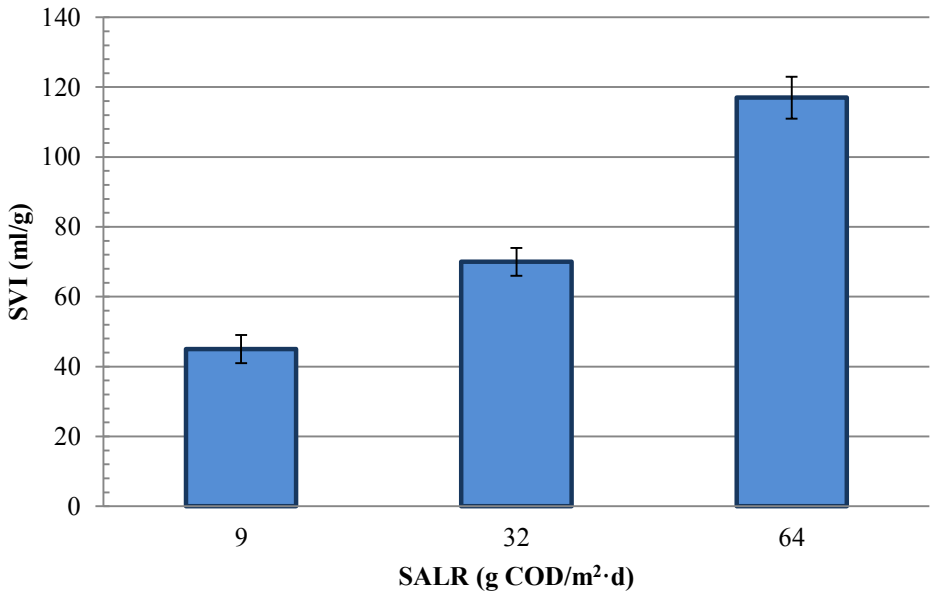

Figure 5.2 SVI values for MBBR reactors operated at various SALRs

Ivanovic and Leiknes (2012) conducted a study on solid separation in MBBR systems using different techniques (i.e. sedimentation, filtration and membrane separation) and they also found similar results. They pointed out that higher organic SALR in MBBR systems has a negative effect on sedimentation of biologically-produced solids.

Furthermore, they recommended that in order to overcome the poor settling potential of particles in high SALR MBBR systems the addition of a metallic coagulant or cationic polymer would be beneficial.

Section 4.3, which presented the effects of SRT on SVI in AS reactors, showed that SVI decreased from 247±118 to 54±1 ml/g as the SRT increased from 5 to 15 days. Conversely, the SVI of the MBBR reactors varies between 45±4 ml/g and 117±6 ml/g at SALRs of 9 and 64 g COD/m^2·d, respectively. Generally, the overall lower average SVI values for MBBR reactors show better settling characteristics than the mixed liquor from the AS reactors. The lower settling rates of the AS mixed liquor may be related to the higher TSS concentration and the fact that in general solids settling velocities decrease with increasing concentration. This restricts any direct comparison with respect to settling ability of the particles in the two systems.

5.4 Decantation Index

The DI analysis was used in addition to SVI measurements to quantify the settling characteristics of the particles. Figure 5.3 shows the average DI value for the effluent of the MBBR reactors operating at different SALRs. The average DI for the reactors showed that as the SALR increased from 9 to 64 g COD/m^2·d, DI values decreased from 77±4 to 63±4%. Thus, the DI results showed that higher SALRs in MBBR reactors lead to lower removal of biologically-produced solids by settling. The DI results thus support the SVI findings and conclusion presented in Section 5.3.

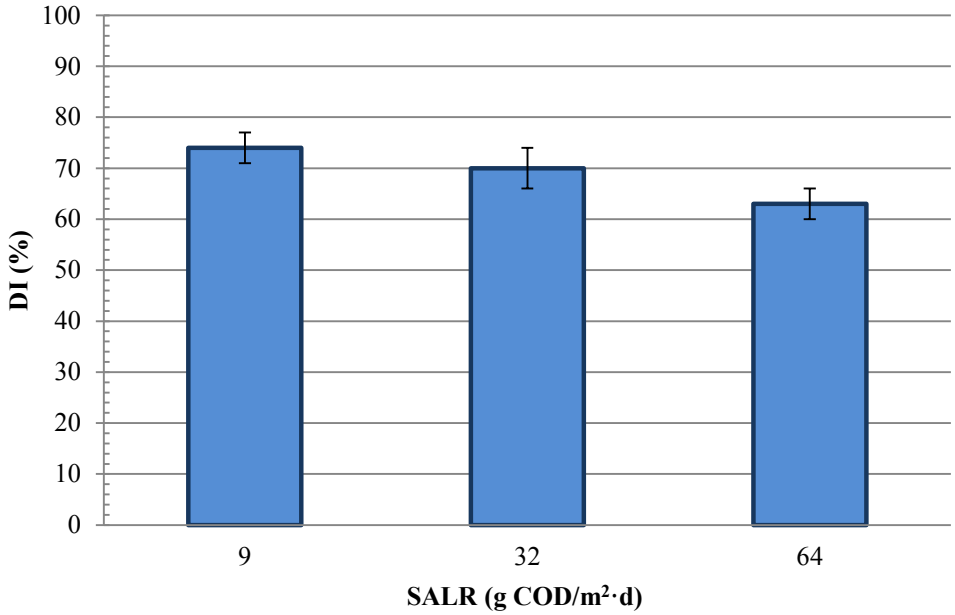

Figure 5.3 DI values for MBBR reactors operated at various SALRs

As discussed in Section 4.4, as the AS SRTs increased from 5 to 15 days the DI increased from 51±4% to 97±1%, respectively. The DI values decreased from 77±4% to 63±4% for the MBBR reactors as the SALRs increased from 9 to 64 g COD/m^2·d. Therefore, the DI results indicate that settling characteristics of AS biologically-produced solids varied from poor to excellent with increasing SRT values, while the settling characteristics of the MBBR biologically-produced solids varied between good and moderate depending on SALR values. However, once again it is important to mention that the significantly higher concentration of particles in the AS effluent do not allow for a fair comparison to the more dilute MBBR effluent.

5.5 Particle Distribution Analysis

As previously mentioned, the DPA system was used to capture hundreds of particle images of each sample by MFI to analyze the biologically-produced solids in the process.

Each image was analyzed using the software that accompanies the instrument. Figure 5.4 shows typical DPA images for of the MBBR reactors at different SALRs. Specifically, Figure 5.4a,b,c shows sample DPA images of the reactor effluent for the MBBRs operated with SALRs of 9, 32 and 64 g COD/m^2·d, respectively. The images show that the number of particles (and thus the concentration of particles) increases with increasing SALR.

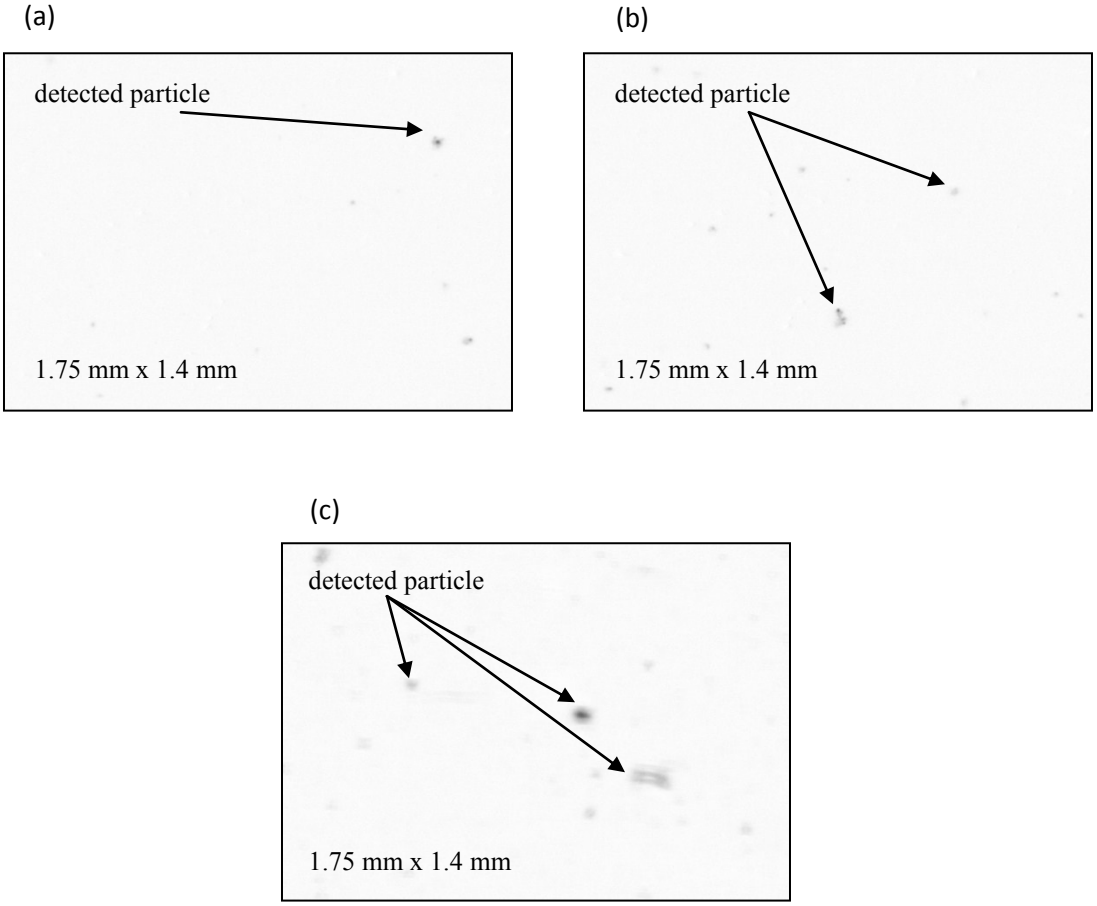

Figure 5.4 DPA grayscale images of MBBR reactors operated at different SALRs (a) 9 g COD/m^2·d, (b) 32 g COD/m^2·d and (c) 64 g COD/m^2·d

Table 5.4 shows the mean CC and 95% C.I. of the MBBR's biologically-produced solids at different MBBR SALRs. The CC values decreased from 0.75±0.03 to 0.53±0.02 as the SALR increased from 9 to 64 g COD/m^2·d. The inverse of the CC values of each SALR

was used to calculate the volume of the solids detected by DPA analysis as described in Section 3.9.

Table 5.4 Mean CC of MBBR reactors operated at various SALRs

MBBR Reactors SALR (g COD/m^2·d)	**Mean CC±95% C.I.**
9	0.75±0.03
32	0.60±0.04
64	0.53±0.02

The volume of the particles >400 μm has calculated by filtering the sample with a 400 μm filter, measuring the mass of solids captured and dividing it by an estimated solid density. This enabled the comparison of the volume of solids >400 μm with those in the 2-400 μm size range, measured using DPA. The average density of the solids was approximated by calculation of error percentage between the experimental TSS values measured using standard methods and the TSS values calculated from the DPA data. As shown in Appendix-D Table D-2, an approximate solids density of 1100 mg/ml showed the lowest percentage error and thus was used to approximate the volume of solids >400 μm.

DPA analysis is implemented for two kinds of samples: (i) MBBR reactors effluents (referred to as unsettled or before settling), and (ii) the supernatant of the effluent after 30 minutes of settling (referred to as "after settling" or "settled"). As described in Section 3.8, the "before settling" samples were immediately injected into the DPA upon sampling, while the "after settling" samples were allowed to settle under undisturbed,

quiescent conditions for 30 minutes with the decanted liquid was injected into the DPA. A settling time of 30 minutes was chosen based upon the quiescent time used in the DI analysis.

As discussed in Section 4.5, the approximated density for AS reactors was calculated to be 1150 mg/ml while the value for the MBBR reactors was 1100 mg/ml. Therefore, higher DI values at high SRTs for AS reactors could be due to higher average density of solids in mixed liquor. However, even higher densities could not improve settling characteristics in lower SRTs for AS reactors which could be due to high filamentous growth.

The percent volume distributions of the biologically-produced solids at three different SALRs for "before settling" samples are shown in Figure 5.5. The first three bars in Figure 5.5 show that 94±2, 86±3 and 80±3% of the total volume of particles are located in the range of 2-400 μm at SALRs of 9, 32 and 64 gCOD/m^2·d, respectively. A significant quantity of the particles between 2-400 μm are located in the range of 120-180 μm at 9 gCOD/m^2·d; this peak in quantity shifts to the range of 140-220 μm at 32 gCOD/m^2·d and to 180-260 μm at 64 gCOD/m^2·d. However, the three distributions are similar in that they show a large peak in the 100 to 260 μm range. This trend of increasing particle size with increased SALR is again demonstrated for particles >400 μm, where the volume percentages increased from 6±1 to, 13±2 and 20±2% as the SALR increased from 9 to 32 and 64 gCOD/m^2·d, respectively as shown in the last three bars in Figure 5.5.

As discussed in Section 4.5, the volume percentage of AS biologically-produced particles varies significantly by changing SRT with a clear trend towards larger particles at lower SRTs. In addition, Table 4.4 shows that increasing SRT led to a decrease in the mean particle diameter. On the other hand, the particle size distribution of the MBBR reactors followed a pattern with a shift towards larger particles at higher SALRs.

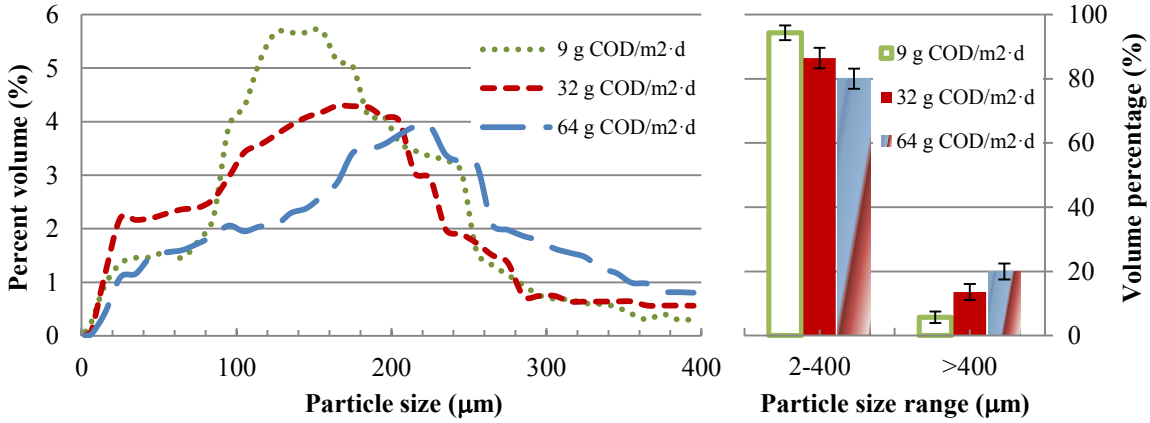

Figure 5.5 Volume based particle size distributions of particles between 2-400 µm and > 400 µm for MBBR reactors operating at three different SALRs for effluent samples (before settling)

Figure 5.6 shows percent volume distribution graphs for samples prior to and following settling and the overall percent volume of particles in the ranges 2-400 µm and >400 µm at the three SALRs. Figure 5.7 shows the percent volume removal by settling at the three SALRs based on the effluent and "after settling" data. The right side of Figure 5.6a shows the percentages of the 2-400 and >400 µm particle ranges for the SALR of 9 gCOD/m^2·d, the values for the settled samples are based on the total volume of sample in the unsettled effluent and because of this the percentages of the settled 2-400 and >400 µm particles do not add up to 100%. From the difference between the unsettled and the settled percentage it can be observed that among the biologically particles produced in the 9 gCOD/m^2·d

MBBR 72±2 and 100±0% of the particles between 2 and 400 and >400 μm were removed during the settling period, respectively. This can also be seen in the right side of Figure 5.7. Moreover, the left hand side of Figure 5.6a and the blue line in Figure 5.7 illustrate that for the particles between 2-400 μm (of the 9 gCOD/m^2·d MBBR effluent) significant settling occurs throughout the particle size distribution, with a slightly lower removal percentage observed for particles between 10-30 μm and 180-300 μm. Overall, 74±5% of the total volume of particles >2 μm were removed by 30 minutes of settlement at SALR of 9 gCOD/m^2·d.

The right side of Figure 5.7 shows that for the effluent of the 32 gCOD/m^2·d MBBR reactor, 62±3 and 100±0% of the particles between 2 and 400 and >400 μm were removed by settling, respectively. Overall, 70±3% of the total volume of particles >2 μm were removed by the settling period. This indicates a slight increase in the percentage of unsettled particles at an SALR of 32 gCOD/m^2·d as compared to 9 gCOD/m^2·d. Figure 5.6b and Figure 5.7 show that the percent volume settled is moderate throughout the particles size distribution at an SALR of 32 gCOD/m^2·d; with a decrease in the settlement characteristics observed in the 20-40 μm and 260-320 μm for particle ranges.

Based on the difference between the unsettled and the settled percentage of the 2-400 and >400 μm particle groups the right side of Figure 5.7 demonstrates for the 64 gCOD/m^2·d MBBR effluent 62±2 and 100±0% of the particles, respectively, settled. Overall, the total volume percentage removal for particles >2 μm at 64 gCOD/m^2·d after the settling period was 63±2% as there are many more 2-400 μm particles than >400 μm particles. Figure 5.6c and Figure 5.7 show moderate percent volume settling for particles between 2 and

400 μm at an SALR of 64 gCOD/m^2·d throughout the particle size distribution with a sudden drop in settling efficiency in the 20-60 μm and 260-320 μm size ranges.

Figure 4.7 and Figure 4.8 in Section 4.5 presented the percent volume removal of biologically-produced solids in AS systems operating at different SRTs. These figures showed that the settled percentage varied through the particles size range with considerably lower percent removals in the particle range >300 μm at the two lower SRTs while almost all the solids were completely settled out of solution at the 15 days SRT. On the other hand, the MBBR reactors demonstrated that better overall settling was observed for the more dilute MBBR effluents and that all the particles >400 μm were completely settled out of solution at all the SALRs. Furthermore, the MBBR reactors at various SALRs demonstrated two distinct ranges of poorer settling of 10-60 μm and 260-380 μm and percent removals were fairly uniform for all three MBBR reactors. In addition, as discussed in Section 3, the solids produced in these two systems cannot be differently compared. However, this comparison is been done as AS reactors are being used as a baseline in this study.

Total Particle Count (#/L) = 4.6×10^{8} TSS (mg/L) = 22 Total Particle Volume (ml/L) =0.020

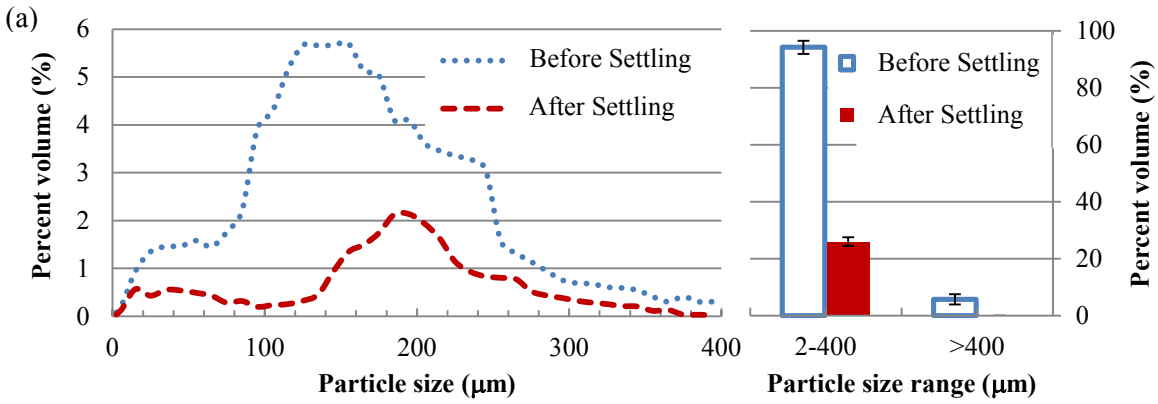

Total Particle Count (#/L) = 1.4×10^{9} TSS (mg/L) = 88 Total Particle Volume (ml/L) =0.073

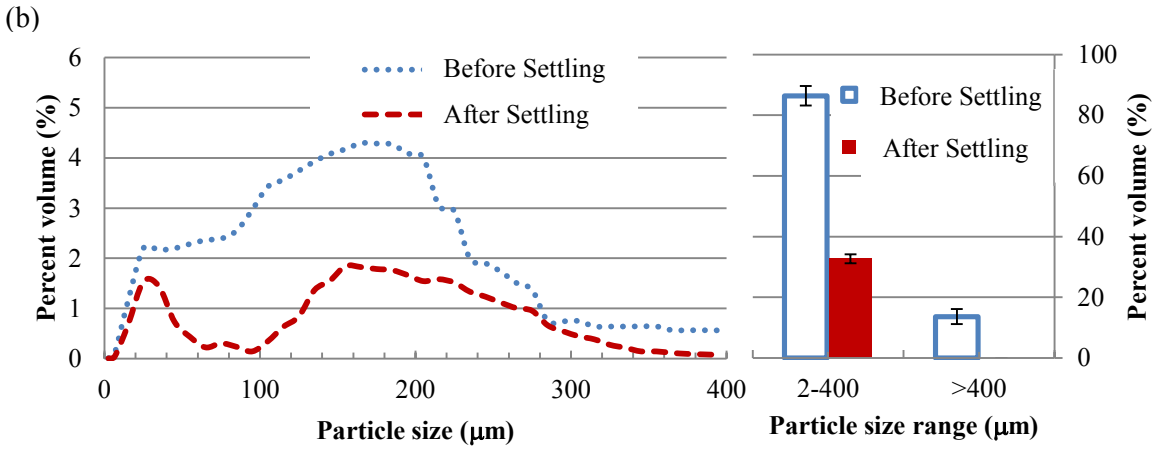

Total Particle Count (#/L) = 3.9×10^{9} TSS (mg/L) = 145 Total Particle Volume (ml/L) =0.140

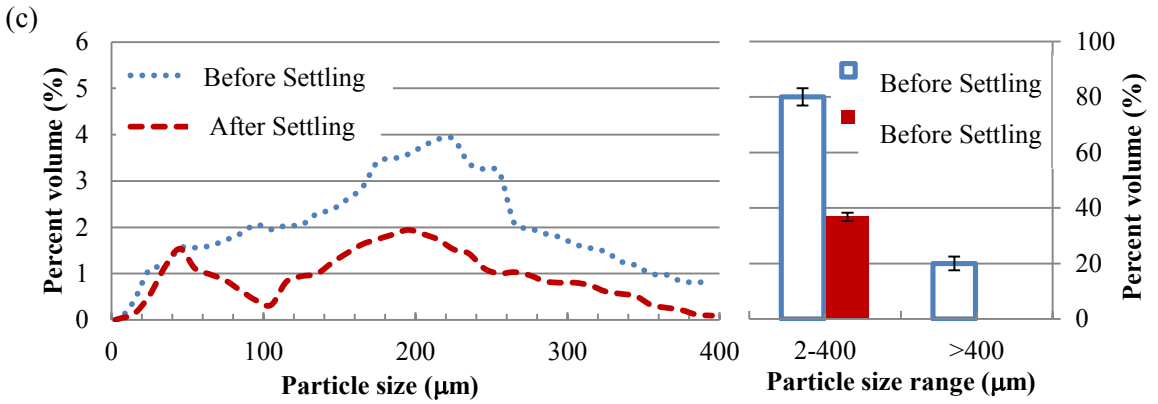

Figure 5.6 Percent volume distribution of particles between 2-400 µm and and > 400 µm before settling and after settling at (a) 9 gCOD/m^2·d, (b) 32 gCOD/m^2·d and (c) 64 gCOD/m^2·d SALRs

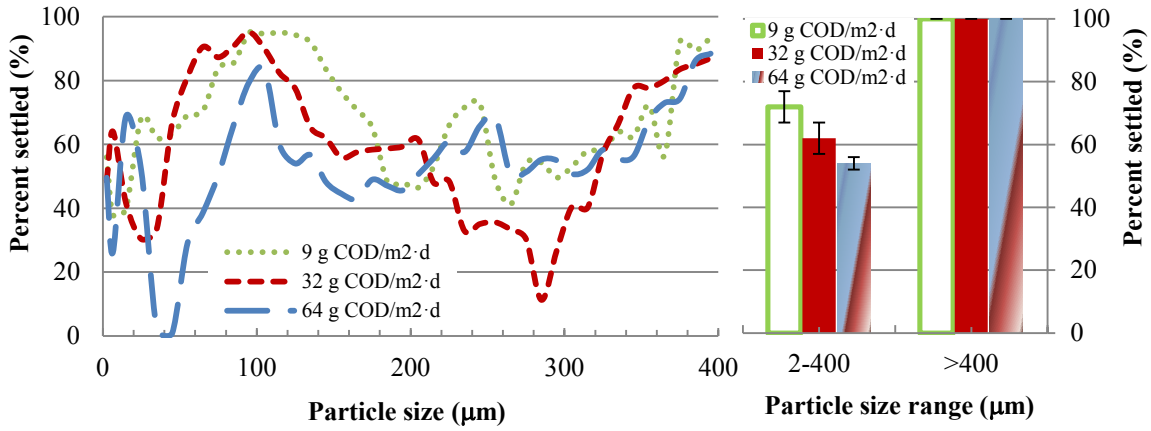

Figure 5.7 Volume percentage removals of particles between 2-400 µm and > 400 µm for MBBR reactors operating at three different SALRs

Table 5.5 summarizes the total number of particles, the total volume of particles as well as the mean particle diameter by number for the "before settling" and the "after settling" effluents of the biologically-produced solids at the three SALRs. The total number and volume of particles in both the prior and after settling effluents increased significantly as the SALR increased. The mean particle diameter prior to settling increased as SALR increased, however following settling the mean particle diameters at all three SALRs were very close. The observed increase in the "before settling" mean particle size diameter with increasing SALR may be associated with a higher detachment rate due to higher influent carbon concentrations in the reactors with increased SALRs. The higher concentration of solids produced in these systems, may lead to more collisions between particles and subsequent particle adhesion that may hence enhance and ultimately result in the formation of larger particles at higher SALRs. Åhl et al. (2006) also found that particle sizes increased with increases in SALR, while low SALR wastewaters had higher concentrations of submicron particles. As Figure 5.7 shows, larger particle removal was achieved by settling at lower SALRs, conversely, the mean particle diameter increased as

SALR increased, thus implicated that settling is influenced more by the differences in particles characteristics as SALR changes than the changes in particle sizes.

Table 5.5 Particle size distribution characteristics of MBBR reactors at various SALRs

MBBR Reactors SALR (g COD/m^2·d)	**Total Number of Particles (#/ml)**		**Total Volume of Particles (ml/L)**		**Mean Particle Diameter (μm)**	
	Before Settling	After Settling	Before Settling	After Settling	Before Settling	After Settling
9	$(4.6\pm1)\times10^{5}$	$(1.3\pm1)\times10^{5}$	$(20.0\pm2)\times10^{-3}$	$(5.0\pm1)\times10^{-3}$	5±1	4±1
32	$(14.0\pm1)\times10^{5}$	$(4.3\pm1)\times10^{5}$	$(73.0\pm6)\times10^{-3}$	$(24.0\pm2)\times10^{-3}$	12±1	6±1
64	$(38.0\pm3)\times10^{5}$	$(15\pm1)\times10^{5}$	$(140.0\pm11)\times10^{-3}$	$(50.0\pm4)\times10^{-3}$	17±2	6±1

Table 4.4 in Section 4.5 shows the total volume of particles, number of particles and mean particle diameter for biologically-produced solids before and after settling in AS systems operating at different SRTs. The total number of particles, total volume of particles and mean particle size diameters all increased as SRT increased. In MBBR reactors this trend is again observed as all the above named values increased as the SALR of the reactors increased. Thus, both an increase in SRT and SALR for AS and MBBR reactors, respectively, result in an increase of the number and volume of biologically-produced particles in addition to an increase in the mean particle size diameter.

Table 5.5 tabulates the SVI, the DI, the percent particle volume removal and the percent particle number removal due to 30 minutes of settling for all three reactors. Overall, the number percentage of particles removed during settling for each SALR was constantly

less than the volume removal percentage at all SALRs. This is an indication that the number of small particles that were removed during the settling period for each SALR was considerably lower than the number of large particles that settled. This is consistent with before and after settling mean particle diameter data in Table 5.4. Furthermore, although the number of particles removed due to settling increased with an increase in SALR, the volume of particles removed by settling significantly decreased as the SALR increased. The reason for this observed inverse trend is that the higher SALR reactor has a higher mean particle size.

Table 5.6 also illustrates that by increasing the SALR, the SVI also increases and the DI decreases thus indicating that the settling potential of the particles decreases. Hence, demonstrating that the sedimentation characteristics of the high SALR MBBRs is significantly less than low SALR MBBRs. Liao et al. (2003) had a similar finding for the relationship between the removal of particles by settling and the organic SALR of a system. Similarly, Åhl et al. (2006) showed that by increasing the SALR, a non-ideal flocculation condition could occur and the concentration of small particles (<5 μm) increased the settling ability. Ivanovic and Leiknes (2012) also pointed out that sedimentation is only efficient for MBBR systems with low SALRs and the reason for an observed lower settling ability at higher SALRs could be due to the production of poorly aggregated particles. Finally, it should be noted that the DI values quantified based on standard filtration methods correlates very well with the percent volume removal values calculated based on the DPA measurements and as such validates the DPA findings.

Table 5.6 SVI, DI, percent volume and percent number removal for MBBR reactors at various SALRs

MBBR Reactors SALR (g COD/m^2·d)	SVI± 95% C.I. (ml/g)	DI± 95% C.I. (%)	Settled Effluent TSS (mg/L)	Percent Volume Removal ± 95% C.I. (%)	Percent Number Removal ± 95% C.I. (%)
9	45±4	77±4	5±1	74±5	44±3
32	70±4	70±3	26±3	67±5	53±3
64	117±6	63±4	54±4	63±2	61±2

5.6 ESEM of MBBR Carriers

ESEM images of the Anoxkaldness K1 carriers were acquired at three magnifications: 15x, 50x and 1000x. Figure 5.8 shows ESEM images which highlight the thickness of the different biofilms at 50x magnification, while measurements of biofilm thicknesses are shown in Figure 5.9 in images acquired at 50x magnification. The morphology of the attached biofilm on the carriers is shown in Figure 5.10 at a magnification of 1000x.

The average coverage of the biofilm thicknesses (based on twenty measurements) for media from the 9, 32 and 64 g COD/ m^2·d MBBRs were 673±58, 527±34 and 743±70 μm, respectively. The thickness and the structure of the biofilm depend on the following factors: hydrodynamics of the system, nutrient loading, DO concentration and SALR (Cunningham et al., 2001). Biofilm grown under laminar flow conditions has been shown to be thicker and less dense than those grown under turbulent flow conditions and high nutrient concentrations have been shown to produce biofilms that are thicker and denser than biofilms grown under low nutrient conditions (Cunningham et al., 2001).

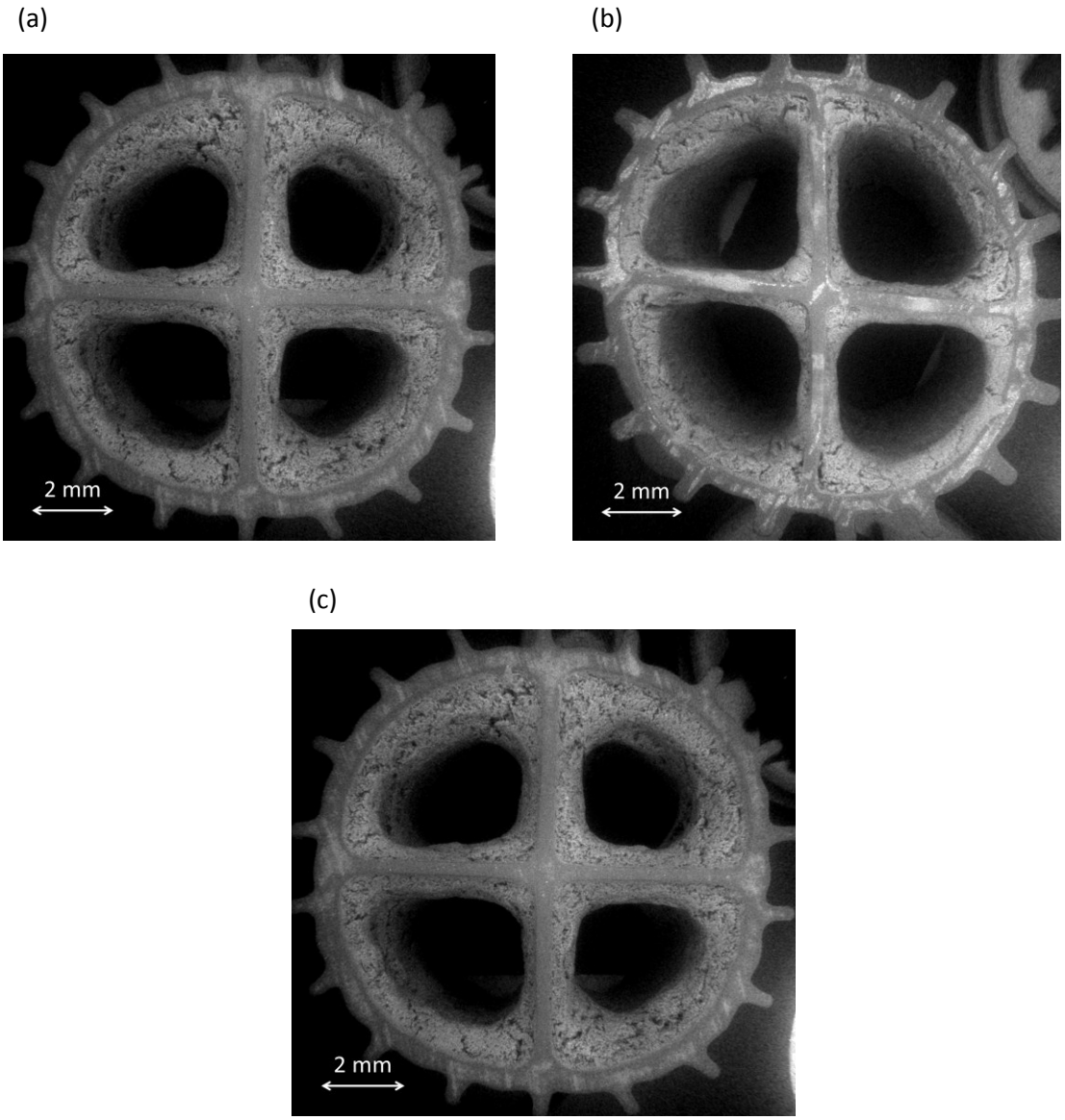

Figure 5.8 ESEM of MBBR reactors at various SALRs acquired at- 15x (a) 9 gCOD/m^2·d (b) 32 gCOD/m^2·d and (c) 64 gCOD/m^2·d

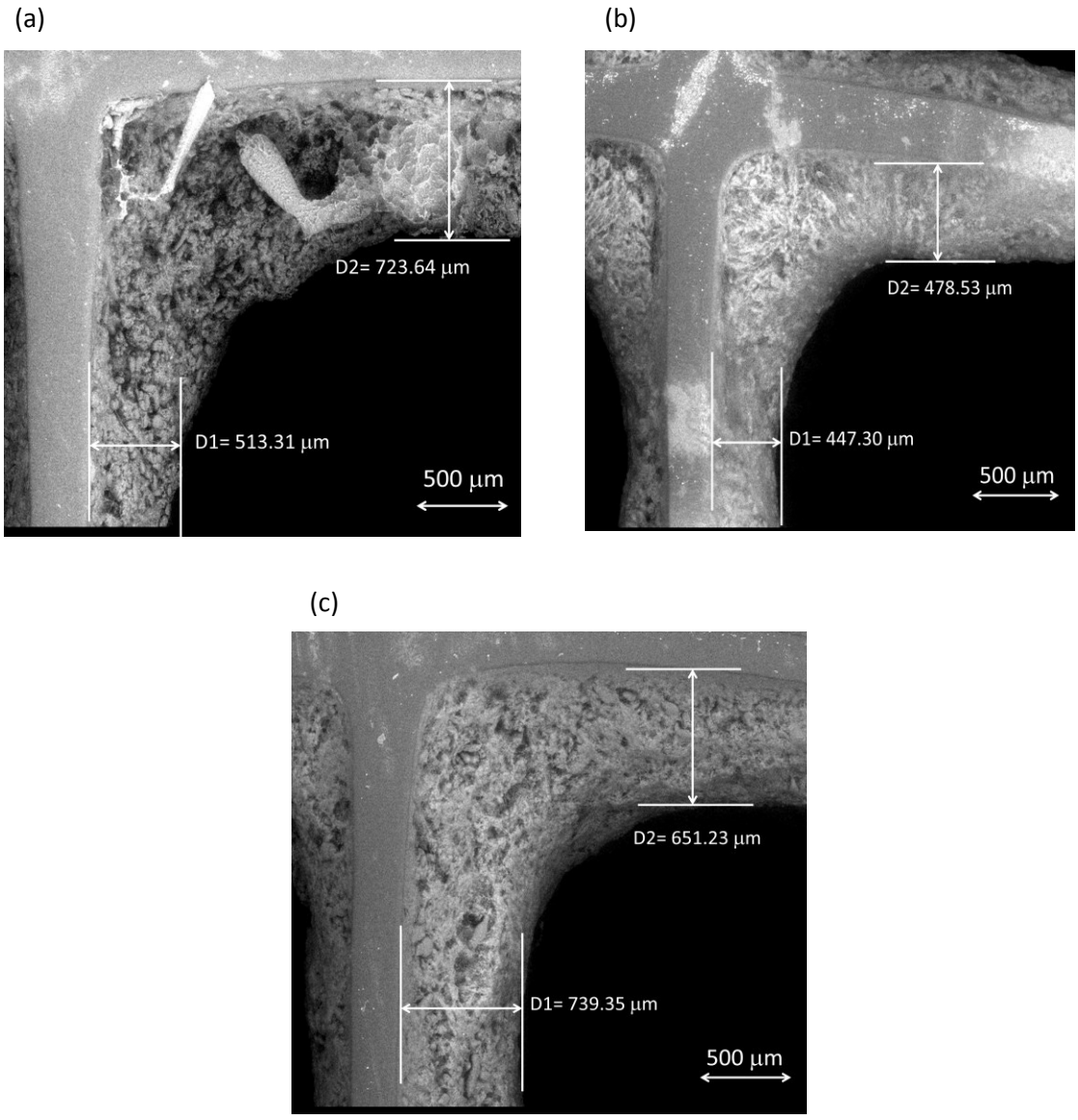

Figure 5.9 ESEM of MBBR reactors at various SALRs acquired at- 50x (a) 9 gCOD/m^2·d (b) 32 gCOD/m^2·d and (c) 64 gCOD/m^2·d

Since fluid flow and aeration rates within the MBBR reactors of this study were similar throughout the experimental phase, the only factors that could have affected the biofilm structure would be the nutrient and organic SALRs. Figure 5.10 shows the SALR impact on the morphology of the attached biofilm. At the lowest SALR the predominately mushroom-shaped biofilm with fewer but larger pores are observed. A mushroom-shaped biofilm is often associated with glucose-grown *P. Aeruginosa* bacteria, which is

dependent on the carbon source and can be found in numerous wastewaters (Klausen et al., 2003). In contrast, at an intermediate SALR string-like biofilms with significantly smaller pores are observed. This biofilm appears denser than the biofilm seen at the lower SALR. The reactor with the highest SALR showed biofilm that demonstrated a combination of mushroom and string like morphologies.

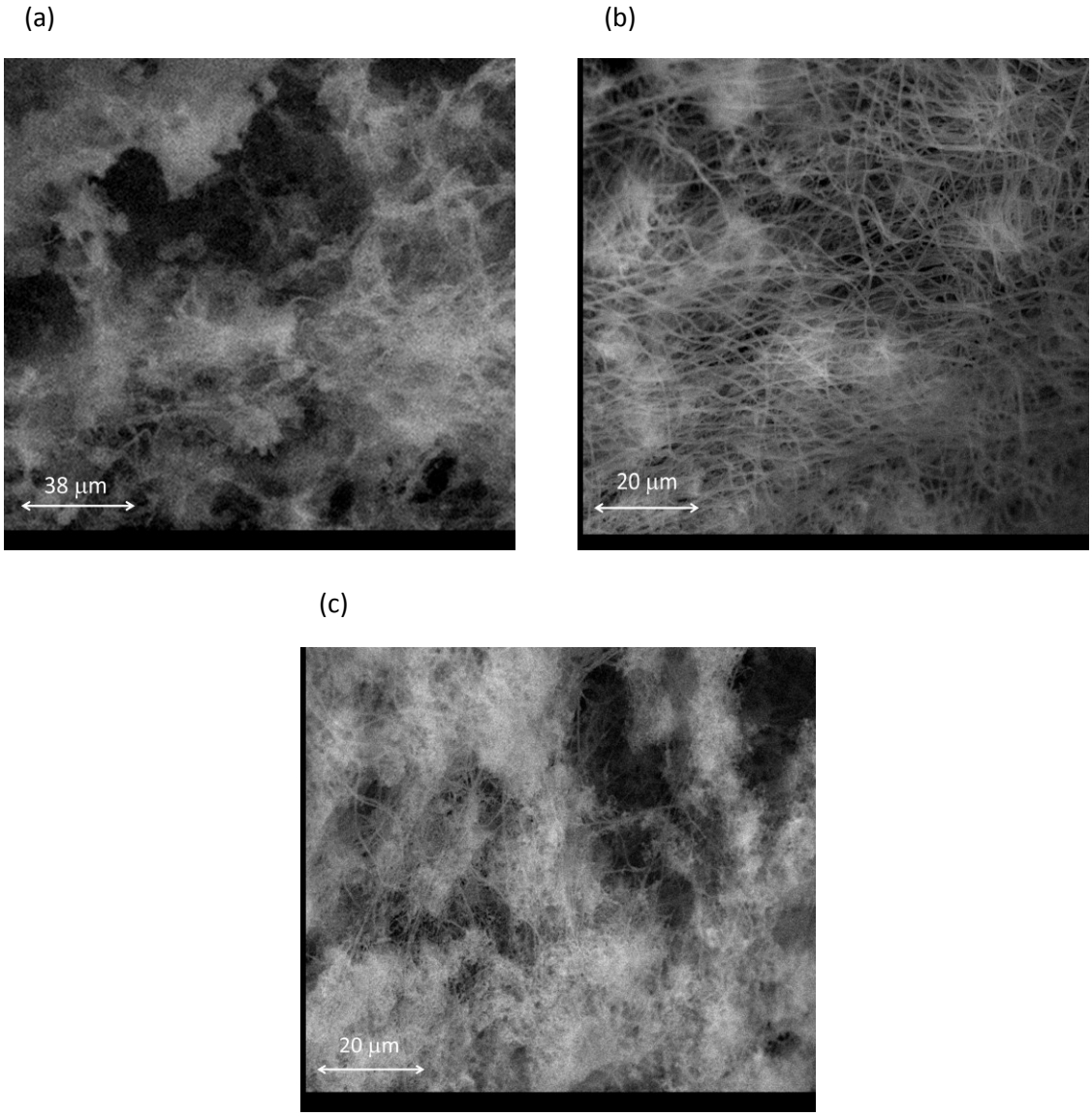

Figure 5.10 ESEM of MBBR reactors at various SALRs acquired at- 1000x (a) 9 gCOD/m^2·d (b) 32 gCOD/m^2·d and (c) 64 gCOD/m^2·d

5.7 MBBR and AS Biomass Yield and Solid Production Comparison

The produced solids and biomass yield in the AS reactors at different SRTs and in the MBBR reactors at different SALRs are shown in Table 5.7. As the values show, the produced solids of the MBBR reactors is at least 8 times lower than the AS reactors under

all conditions. The true biomass yield for the AS reactors is estimated by linear regression for all three reactors with different SRTs and the net biomass yield for MBBR reactors was calculated using Equation 5.2, which is shown below.

$$Y_{net,MBBR} = \frac{Q \cdot VSS_{eff}}{Q \cdot (COD_{in} - COD_{out})} \quad \text{Eq. 5.2}$$

where Q = influent flowrate (L/day); VSS_{eff} = the VSS concentration of effluent (mg/L); COD_{in} = influent COD concentration (mg/L); COD_{out} = effluent COD concentration (mg/L) concentrations are also in (mg/L). To convert the $Y_{net,MBBR}$ to $Y_{true,MBBR}$, Equation 5.3 was applied as follows:

$$Y_{true,MBBR} = Y_{net,MBBR} \cdot (1 + b \cdot SRT) \quad \text{Eq. 5.3}$$

where, b= the decay coefficient (1/day) calculated for AS reactors in Chapter 4 and SRT (day) is been calculated in Section 5.1.

Table 5.7 Solid production and biomass yield of MBBR and AS reactors

Reactor Conditions	**Solid Production (mg TSS/day)**	**Biomass Yield (g VSS/g COD)**
AS, SRT 5 days	23983±2000	0.376±0.03
AS SRT 10 days	34148±2100	0.376±0.03
AS, SRT 15 days	42399±2800	0.376±0.03
MBBR, SALR 9 gCOD/m^2·d	434±20	0.400±0.03
MBBR, SALR 32 gCOD/m^2·d	1760±80	0.330±0.02
MBBR, SALR 64 gCOD/m^2·d	2900±250	0.330±0.03

Chapter 6

Effect of HRT on MBBR Biologically-Produced Solids

As described in Section 3.5 the second experimental phase of MBBR reactors investigates the biologically-produced solids by identical laboratory MBBR reactors functioning at HRTs of 1, 1.5 and 2 hrs for a period of 50 days. An HRT of 4 hrs was also evaluated in a preliminary study, but the biomass did not attach well to the media.

The purpose of measuring the COD concentrations in this chapter was to monitor the performance of the MBBR reactors at different HRTs and to establish that steady state conditions were achieved. TSS, VSS, SVI, DI and DPA analyses were performed to characterize the biologically-produced solids and to evaluate their settling characteristics. Moreover, ESEM images were taken to investigate changes in morphology and thickness of the biofilm on the MBBR carriers in reactors operating at different HRTs.

6.1 Operational Conditions of MBBR Reactors

During this phase of the experiments, the reactors were operated with HRTs of 1, 1.5 and 2hrs using an SALR of 32 g COD/ $m^2 \cdot d$. The pH during steady state operation remained constant at 7.0±0.1 and the DO concentration was maintained at 4.2±0.2 mg/L., One of the reactors from the previous experimental phase (HRT of 1 hour) was already operating under steady state conditions and thus the other two reactors were subjected to a gradual HRT changes from 1 hour to 1.5 and 2 hours. After increasing the HRT slowly over the period of 10 days, these two reactors were operated for 14 consecutive days in which time they achieved steady state conditions. Once at steady state, the reactors were

operated for an additional 40 days. The changes in influent and effluent COD concentrations for the three reactors during the acclimatization phase are shown in Appendix A, Figure A-7 to Figure A-9.

Table 6.1 shows the COD influent and effluent concentration for the three MBBR reactors along with COD removal percentage during steady state conditions. The ± values in this table as well as those in subsequent tables and the error bars in the graphs are the ±95% C.I. values from triplicate measurements. Despite of significant increases in the feed COD concentration necessary to maintain the SALR at 32 g COD/m^2·d while increasing of HRT from 1 to 2 hrs, this only led to a slight increase in the effluent COD concentration and also there was an increase in the COD removals percentage.

Table 6.1 MBBR steady state operating condition

MBBR Reactors HRT (hours)	**Average Influent COD±95% C.I. (mg/L)**	**Average Effluent COD±95% C.I. (mg/L)**	**Average Removal Percentage±95% C.I. (%)**
1	356±8	77±6	78±2
1.5	472±8	81±5	81±3
2	691±11	104±5	85±3

The increasing COD removal pattern with increasing HRT is consistent with results of Borghei and Hosseini (2002) and Melin et al. (2005). In a similar study, Borghei and Hosseini (2002) studied the performance of a set of 22 L MBBR reactors in the treatment of a wastewater that contained different concentrations of phenol. The HRT ranged from 8 hours to 24 hours and the COD removal percentage significantly increased from approximately 75% to 90% as the HRT increased, thus agreeing with the trend observed

in the current study. In a similar study, Melin et al. (2005) operated MBBR systems at varying HRTs (0.75-1 to 3-4 hours) and the COD removal efficiency increased from 83% to 87% as the HRT increased.

Table 6.2 shows the SRT and the volumetric loading rate of the MBBR reactors. As it discussed in Section 5.1, these two parameters are not commonly applied to MBBR reactors. As shown in Table 6.2, by increasing the HRT, the SRT of the reactors is decreased and the volumetric loading rate first decreases as the HRT increased from 1 to 1.5 hours and then it increases as the HRT increased from 1.5 to 2 hours.

Table 6.2 SRT and volumetric loading rate of MBBR reactors operated at various HRTs

MBBR Reactors HRT (hours)	**SRT (days)**	**Loading Rate (g COD/L·d)**
1	0.90±0.1	7.8±0.2
1.5	0.60±0.1	6.8±0.2
2	0.44±0.1	7.6±0.2

6.2 Effluent TSS and VSS of the MBBR Reactors

The effluent TSS and the VSS for the three reactors with varying HRT were monitored immediately after the wastewater exited the system. Figure 6.1 shows the average TSS and VSS concentrations at three MBBR reactors operating at different HRTs. The TSS values were plotted with respect to time in Figure B-3 Appendix B. Note that as this study used a soluble wastewater as the feed, it does not contain any influent TSS or VSS.

Therefore, this study does not investigate VSS and TSS removal or the interaction of detached solids and influent solids; in fact due to the lack of influent solids the effluent VSS and FSS (i.e., the non-VSS portion of TSS) in this study was presumed to be derived from the biofilm and biomass contained in the reactors. Overall, the measurements indicated that by increasing the HRT from 1 hour to 2 hours the TSS concentration also significantly increased and the increases seems to be more significant as the HRT increases from 1 to 1.5 hr as compared to increases from 1.5 to 2 hrs.

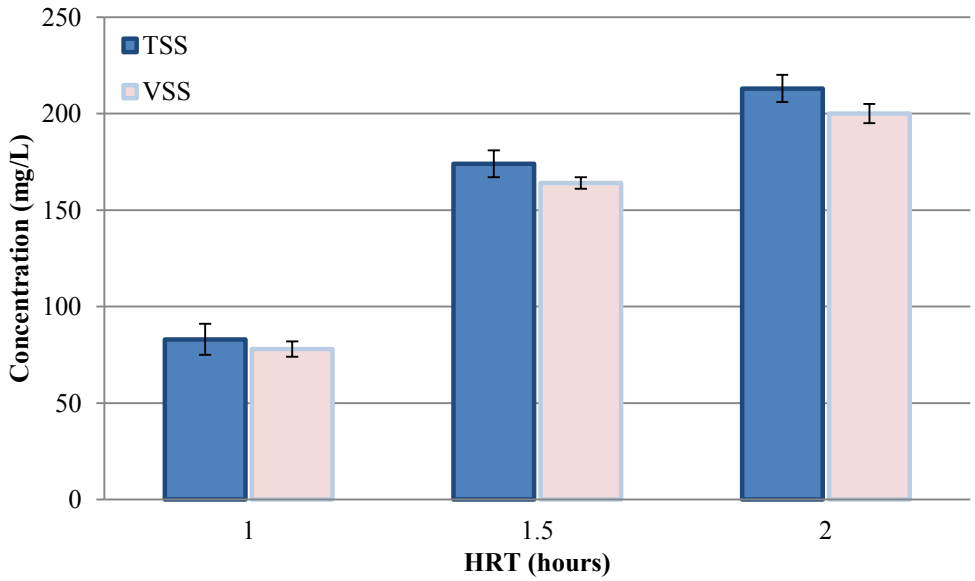

Figure 6.1 TSS and VSS concentrations in the MBBR reactors operated at different HRTs

These results are consistent with those of Åhl et al. (2006) and Ivanovic and Leiknes (2012). Åhl et al. (2006) ran 65 L MBBR reactors housing K1 Anoxkaldness carriers which showed that by increasing the HRT from 45 minutes to 3 hours, the average TSS concentration in the reactors increased from 88 to 126 mg/L. Additionally Ivanovic and Leiknes (2012) suggested that at longer HRTs more biomass will detach from the

suspended carriers in the system and cause higher concentrations of effluent suspended solids.

Table 6.3 shows that the VSS/TSS ratios in the three MBBR reactors were always greater than 90%. These results indicate that the inert portion of suspended solids inside the reactors is consistently less than 10% and that most of the TSS is comprised of volatile material. Considering the VSS/TSS results observed at various SALRs, shown in Table 5.2, the VSS/TSS ratio of the biologically-produced solids were similar at various SALRs and HRTs. This is likely due to the fact that all the reactors in this study were fed with a soluble SWW.

Table 6.3 VSS/TSS ratio for MBBR reactors operated at various HRTs

MBBR Reactors HRT (hours)	**VSS/TSS±95% C.I.**
1	0.93 ± 0.03
1.5	0.91 ± 0.02
2	0.90 ± 0.03

6.3 Sludge Volume Index

Figure 6.2 showed that increasing the HRT of MBBR reactors results in statistically significant increases in the SVI values. This study demonstrates a significant increase in SVI with increasing the HRT from 1 to 2 hours, thus indicating that the settling ability of the produced particles decreases as the HRT was increased. Furthermore, even with very small difference in HRTs (0.5 hours), the SVI showed a substantial increase. Specifically, the reactor with the shortest HRT (1 hour) had an average SVI of 68±4 ml/g which would

be considered as good settling characteristics (based on the good settling empirical rule of thumb for AS systems, i.e. SVI<100) and good separation should be achieved by settling using a clarifier. However, it is difficult to predict the performance of full-scale downstream separation units since the current study does not consider interactions between influent solids and biologically-produced solids. The mean SVI value at an HRT of 1.5 hours was 91±3 ml/g and as such the settling ability at this HRT was less than that of the reactor with the HRT of 1 hour; however it should be mentioned that the higher SVI is still an acceptable value for clarifier design. Finally, the highest SVI was measured at the longest HRT (2 hours), this value of 117±4 ml/g indicates a moderate settling ability.

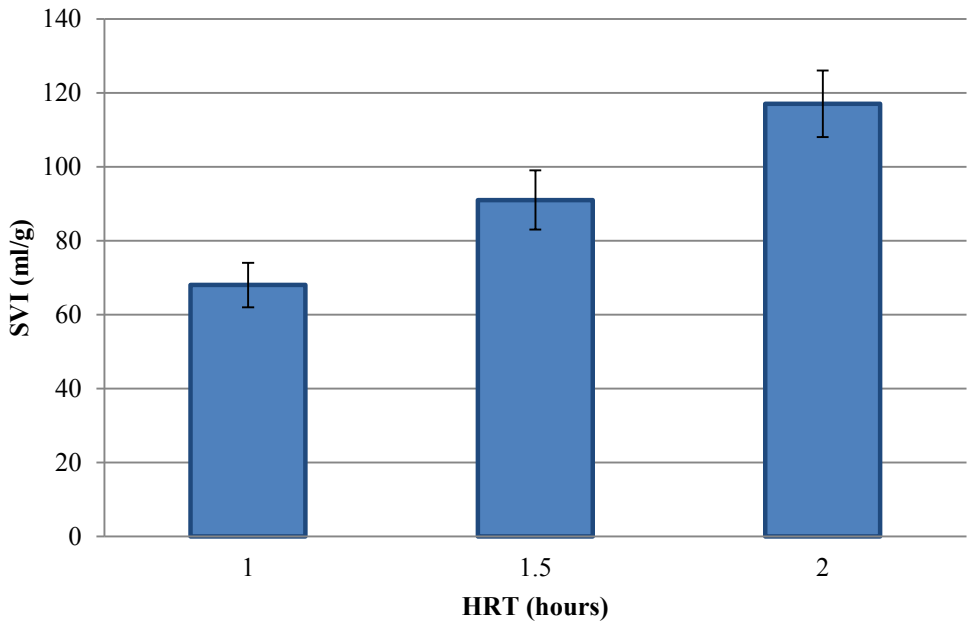

Figure 6.2 SVI values for MBBR reactors operated at various HRTs

As discussed earlier based on the differences of the MBBR and AS produced solids, comparison of their SVI values may not be entirely appropriate, however this chapter still used SVI in order to compare the results of these MBBRs with those in chapter 5. Based

on discussions in Section 5.3 and the current section, increases in both the SALR (section 5.3) and HRT have a negative impact on the settling characteristics of the MBBR biologically-produced solids. However, further information (such as DPA and DI) is required to find out which of these two parameters has more impact on settling characteristics of biologically-produced solids.

6.4 Decantation Index

Figure 6.3 shows that the average DI value of the MBBRs decreased with increasing HRT. All of these DI values show that these solids do not separate well by gravity and that they are consistent with the SVI results.

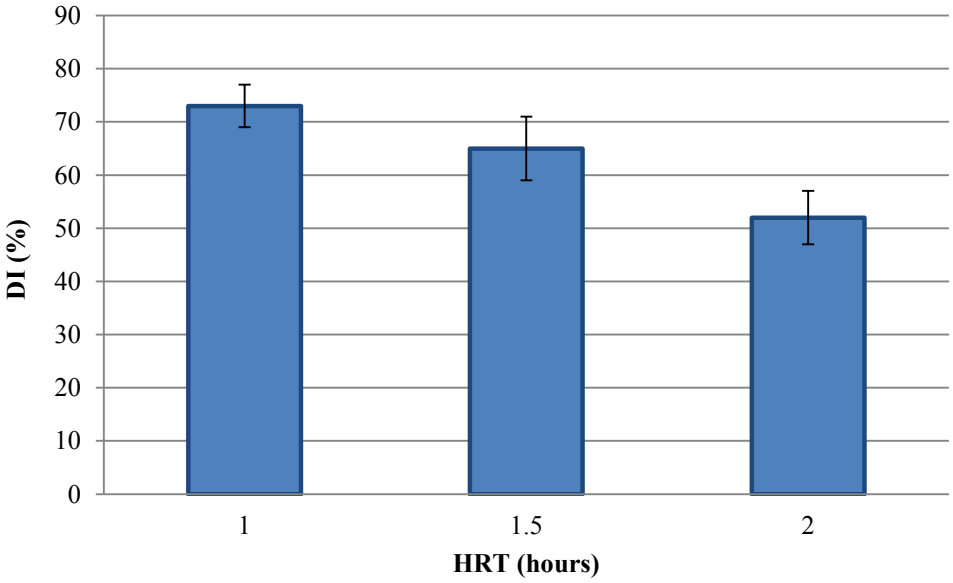

Figure 6.3 DI values for MBBR reactors operated at various HRTs

Section 5.4 discussed the DI values decreased from 77±4% to 63±4% as SALR increased from 9 to 64 g COD/m^2·d. As observed in Figure 6.3, the DI decreased from 73±3 to 52±4% as HRT increased from 1 to 2 hours. Therefore, this shows that the seven-fold

increase in the SALR had a lower impact on the settling characteristics of the biologically-produced solids than a two-fold increase in the HRT.

6.5 Particle Distribution Analysis

As previously mentioned, the DPA system was used to capture hundreds of particle images of each sample by MFI to analyze the particles produced in the MBBR units. Figure 6.4 shows typical DPA images which reflect the difference in particle size caused by altering the HRT. The images show that there is a change in number and size of the particles as the HRT is increased.

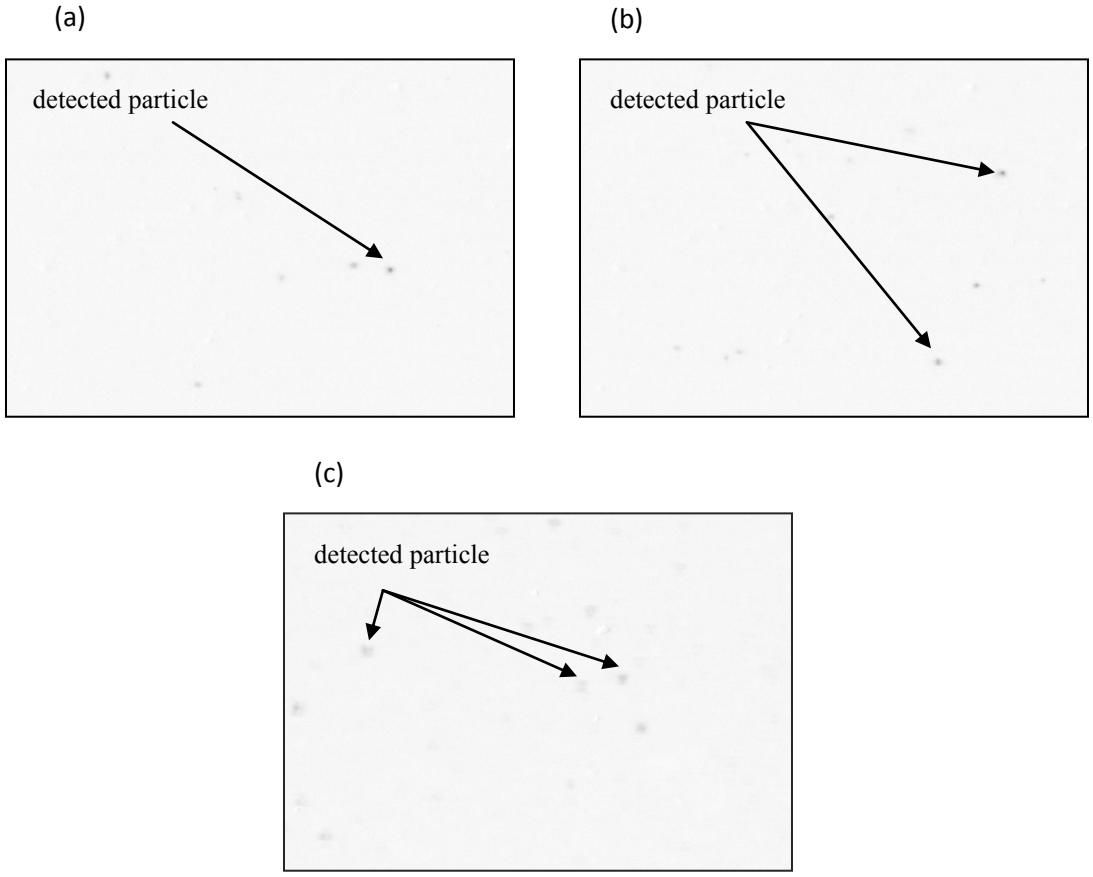

Figure 6.4 DPA grayscale images of MBBR reactors at different HRTs (a) HRT= 1 hour, (b) HRT =1.5 hours and (c) HRT= 2 hours

Table 6.4 summarizes the mean CC values and 95% C.I. for each HRT. From this data, it is evident that the particles had CC values despite the HRT changes. This similarity in spite of the two-fold change in HRT is in contrast to the significant CC change observed with the 7-fold increase in SALR. The inverse of the CC values at each HRT was used to calculate the volume of the solids detected by DPA analysis as described in Section 3.9.

Table 6.4 Mean CC for MBBR reactors operated at different HRTs

MBBR Reactor HRT (hours)	**Mean CC±95% C.I.**
1	0.54±0.02
1.5	0.48±0.04
2	0.49±0.01

As mentioned in Section 5.5, the volume of the particles >400 μm was calculated by filtration of the sample with a 400 μm filter, measuring the mass of solids captured and dividing it by an estimated solids density. This enabled the comparison of the volume of solids >400 μm with those in the 2-400 μm size range, measured using DPA. Appendix-D Table D-3 compares the experimental TSS values measured using standard methods and the TSS values calculated from the DPA data based on an estimated solids density. Minimizing the error between the TSS values resulted in an estimated solids density of 1100 mg/ml.

DPA analysis is performed for two types of samples: (i) MBBR reactors effluents (referred to as unsettled or before settling), and (ii) the supernatant of the effluent after 30 minutes settling period (referred to as “after settling” or “settled”). As described in

Section 3.8, the "before settling" samples were immediately injected into the DPA after they were exited the reactors, while the "after settling" samples were allowed to settle under undisturbed, quiescent conditions, for 30 minutes with the decanted liquid being injected into the DPA system.

The percent volume distributions of the biologically-produced solids in MBBR effluents at the three different HRTs are shown in Figure 6.5. Figure 6.5 shows fairly similar patterns in that a large percentage of the total volumes of the particles are in the range of 2-400 μm at the three HRTs investigated. The total volume of the particles in the range of 2-400 μm is obtained by integrating the area under the curves shown on the left in Figure 6.5 and is presented as the first set of columns in the bar graph portion of the figure (i.e. the right side). The first three bars in Figure 6.5 show that 86±3, 84±4 and 76±4% of total particle volume are attributed to particles in the 2-400 μm range at 1, 1.5 and 2 hours HRTs, respectively. Therefore, the particles >400 μm comprise only 14±2, 16±1 and 24±2% of total volume at 1, 1.5 and 2 hours HRTs, respectively. The size distribution range of 140-220 μm contains the largest percentage volume of particles between the range of 2-400 μm at an HRT of 1 hour; at an HRT of 1.5 hours the largest percentage volume of particles within the 2-400 μm range shifts to 190-250 μm; while at an HRT of 2 hours shifts towards larger particles, i.e. the 200–260 μm range. Moreover, at the three investigated HRTs the particles >300 μm are only responsible for a small percentage of the total volume of particles in the 2-400 μm range: 6±1, 5±1 and 7±1% for HRTs of 1, 1.5 and 2 hours, respectively (Figure 6.5).

Section 5.5 showed the percent volume of biologically-produced solids shifted towards larger particles as SALR increased from 9 to 64 g COD/m^2·d. The increase in HRT from 1 to 2 h shows a similar trend.

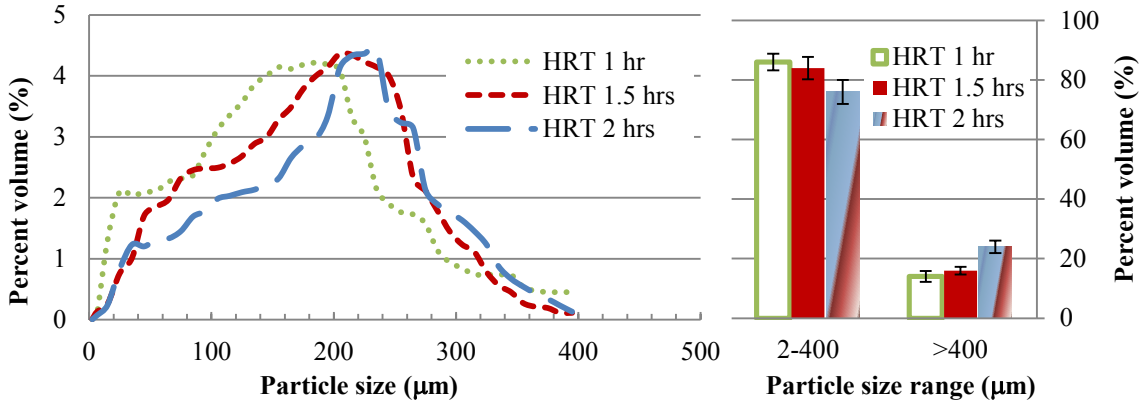

Figure 6.5 Volume based particle size distributions of particles between 2-400 µm and > 400 µm for MBBR reactors operating at three different HRTs for effluent samples (before settling)

Figure 6.6 presents the same particle volume information for samples prior to settling and "after selling" along with the overall percent volume of particles in the ranges 2-400 µm and >400 µm at the three different HRTs. In addition, Figure 6.7 shows the volume removal percentage for the three investigated HRTs based on the effluent and "after settling" data.

The right side of Figure 6.6a shows the percentages of the 2-400 and >400 µm particle ranges at HRT of 1 hour. Again, the values for the settled samples are based on the total volume of sample in the unsettled effluent and because of this the percentages of the settled 2-400 and >400 µm particles do not add up to 100%. From the difference between the unsettled and settled samples it can be concluded that 65±4 and 100±0% settlement is observed in the ranges of 2-400 and >400 µm at an HRT of 1 hour, respectively which

can also be seen in the right side of Figure 6.7. Overall, the total volume of particles >2 μm removed due to 30 minutes of settling at an HRT of 1 hour is 70±4%. Moreover, the left hand side of Figure 6.6a and the blue line in Figure 6.7 show moderate removal by settlement for most particles sizes in the range 2-400 μm at an HRT of 1 hour with the lowest removal occurring in the ranges of 10-40 μm and 260-320 μm and relatively >60% removal for particles in the range 70-220 μm.

The right side of Figure 6.7 shows that 52±3 and 100±0% removal is observed for the 2-400 and >400 μm particle ranges, respectively, at an HRT of 1.5 hours. Overall, the total particle volume removal percentage of particles >2 μm at an HRT of 1.5 hours was 60±3%, which reflects the fact that most particles are in the 2 to 400 μm range. Furthermore, the left hand side of Figure 6.6b and the red line in Figure 6.7 show that fairly low (with average removal lower than 60%) removal is observed throughout the particle size distribution between 2-400 μm with the lowest settleability occurring in the ranges of 30-60 μm and 320-380.

For the 2 h HRT MBBR, the right side of Figure 6.7 (which is based on the difference between the unsettled and the settled percentage in Figure 6.6c) demonstrates that 65±4 and 100±0% removal is of the 2-400 and >400 μm range particles, respectively, at an HRT of 2 hours, respectively. Overall, 54±2% of total volume of particles >2 μm were removed in settling period at an HRT of 2 hours, again. In addition, as Figure 6.7 shows low particle removals (with average removal lower than 50%) occur at most of the particle sizes in the range 2-400 μm at an HRT of 2 hours with the worst removal observed in the ranges of 20-50 μm and 280-340 μm.

Figure 5.6 and Figure 5.7 in Section 5.5 discussed the percent volume removal of biologically-produced solids in MBBR reactors operated at various SALRs. The results showed that the particle size ranges of poor settling were generally found to be between 10-60 μm and between 260-380 μm. Similarly, as discussed in the current section, the biologically-produced particles at different HRTs also showed a lower settling ability in two discrete ranges; 10-60 μm and 260-380 μm.

Total Particle Count: (#/L) = 1.3×10^9 TSS (mg/L) = 82 Total Particle Volume (ml/L) =0.075

(a)

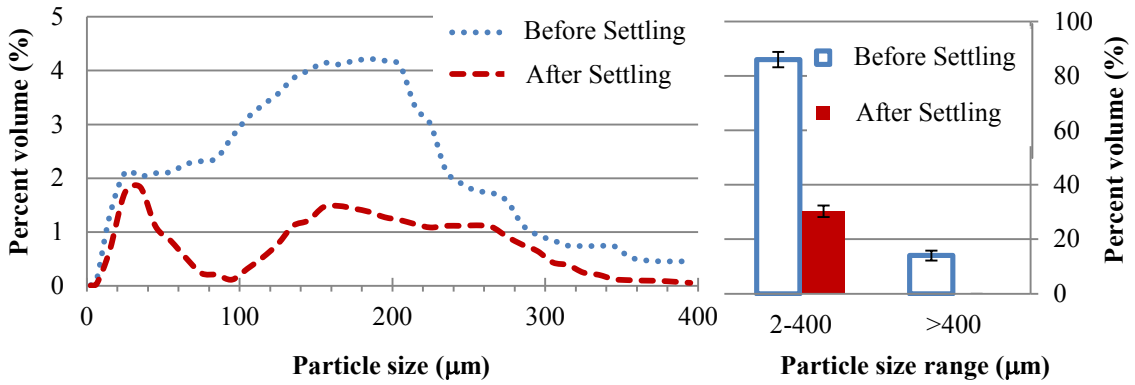

Total Particle Count (#/L) = 2.9×10^9 TSS (mg/L) = 174 Total Particle Volume (ml/L) =0.140

(b)

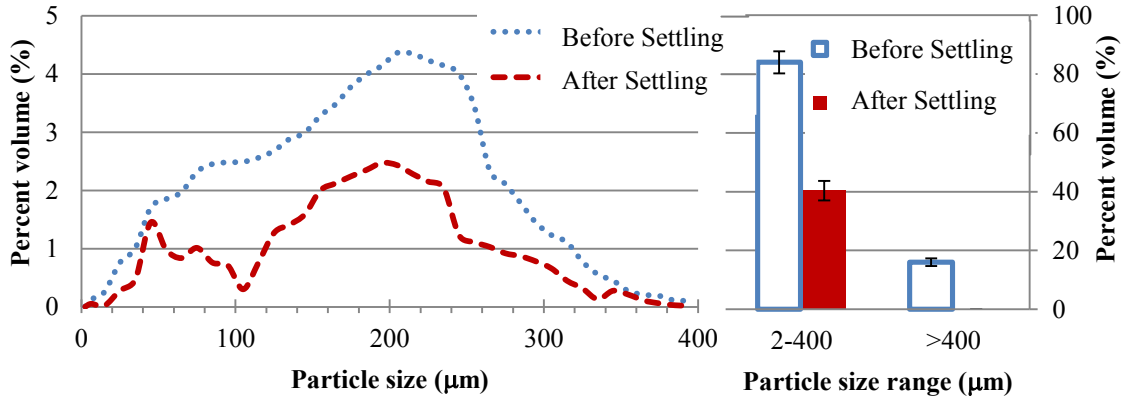

Total Particle Count (#/L) = 5.6×10^9 TSS (mg/L) = 213 Total Particle Volume (ml/L) =0.200

(c)

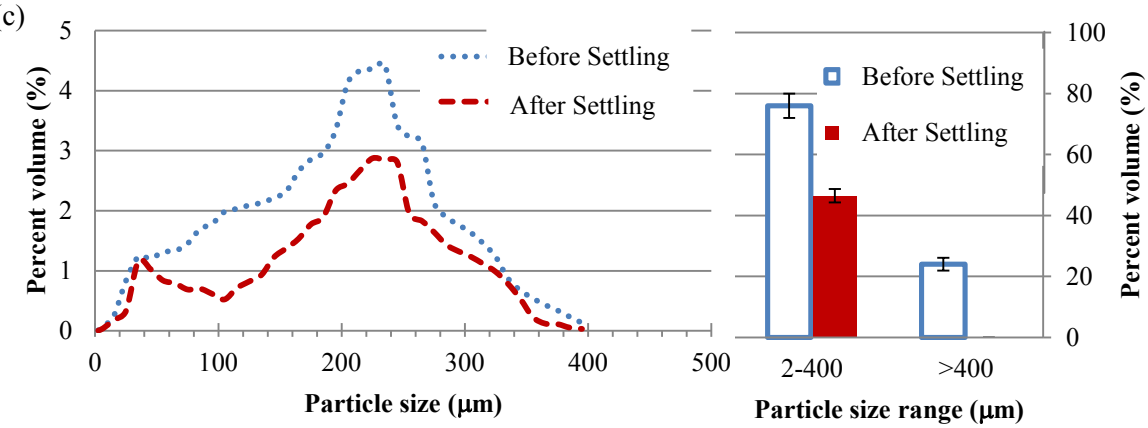

Figure 6.6 Percent volume distribution of particles between 2-400 µm and > 400 µm for before settling and after settling the MBBR reactors operated at (a) 1 hour, (b) 1.5 hours and (c) 2 hours HRT

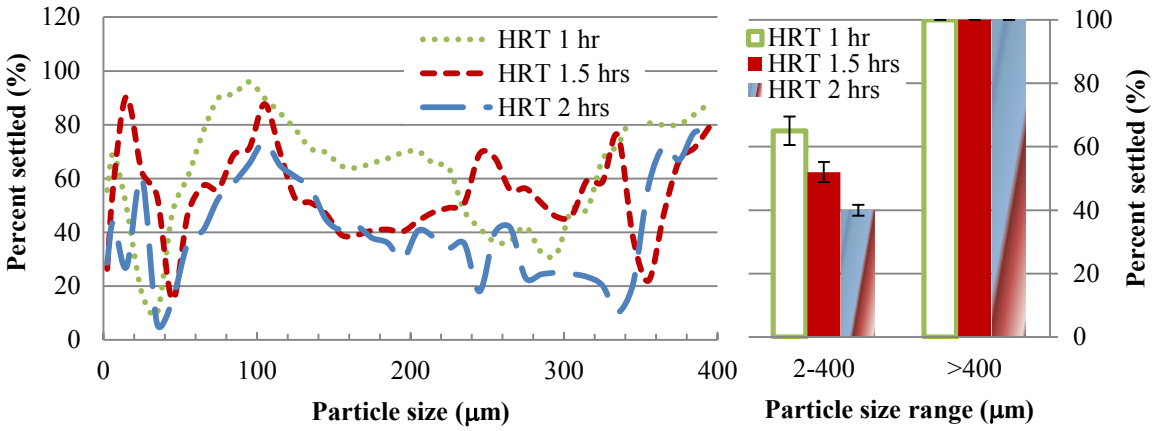

Figure 6.7 Volume percentage removals of particles between 2-400 µm and > 400 µm for MBBR reactors operating at three different HRTs

From Figure 6.5 it can be seen that an HRT of 2 hours shows the higher percentage by volume of particles >400 µm as compared to HRTs of 1 and 1.5 hours. However, Figure 6.6 clearly demonstrates that particles >400 µm are all removed by 30 minutes of settling and thus the potential formation of particles >400 µm at longer HRTs is not responsible for the poor settling characteristics of the biologically-produced solids. From Figures 6.5 and 6.6 it can be seen that particles in the range of 2-400 µm comprise a significant portion of the particles at all HRTs and thus this range of particles do not settle well. In general, the MBBR particles in the 10-60 µm and 260-380 µm size ranges are the worst settling group of particles.

Table 6.5 summarizes the total number of particles, the total volume of particles and the mean particle diameter for the "before settling" and the "after settling" effluents of the biologically-produced solids at the three HRTs. As the HRT increased, the total number and the total volume of particles increased. An increase in HRT has been shown to promote flocs and suspended growth possibly at expense of attached growth on the carriers and this can promote higher quantities of biological solids to remain in

suspension. The number based mean particle diameter of the reactors for "before settling" and "after settling" effluents increased as HRT increased from 1 to 2 hours. As Figure 6.7 shows, larger particle removal by settling is observed at lower HRTs, in contrast, an increase in HRT resulted in larger mean particle diameter, thus implying that settling is impacted more by the differences in particles characteristics as HRT changes than the changes in particle sizes.

Table 6.5 Particle size distribution characteristics of MBBR reactors operated at various HRTs

MBBR Reactors HRT (hours)	**Total Number of Particles (#/ml)**		**Total Volume of Particles (ml/L)**		**Mean Particle Diameter (μm)**	
	Before Settling	After Settling	Before Settling	After Settling	Before Settling	After Settling
1	$(13\pm2)\times10^{5}$	$(3.5\pm1)\times10^{5}$	$(75\pm8)\times10^{-3}$	$(22\pm1)\times10^{-3}$	11±1	6±1
1.5	$(29\pm3)\times10^{5}$	$(11\pm1)\times10^{5}$	$(140\pm11)\times10^{-3}$	$(56\pm6)\times10^{-3}$	13±1	6±1
2	$(55\pm6)\times10^{5}$	$(28\pm2)\times10^{5}$	$(200\pm17)\times10^{-3}$	$(91\pm8)\times10^{-3}$	14±2	8±1

Table 6.6 shows that the SVI, DI, settled effluent TSS, settling percent particle volume removal and settling percent particle number removal decreased with increasing HRT. Overall, the number percentage removal for produced particles at each HRT was always less than the volume percentage removal, indicating that the number of large particles that settled at each HRT was considerably greater than the number of small particles. This is also consistent with before and after settling mean particle diameter data tabulated in

Table 6.5. Moreover, Table 6.6 shows that the DI values are similar to the percent volume removal values measured using the DPA system, therefore validating the DPA results obtained in this study.

Table 6.6 SVI, DI, percent volume and percent number removal measured by DPA for MBBR reactors operated at various HRTs

MBBR Reactors HRT (hours)	SVI ± 95% C.I. (ml/g)	DI ± 95% C.I. (%)	Settled Effluent TSS (mg/L)	Percent Volume Removal ± 95% C.I. (%)	Percent Number Removal ± 95% C.I. (%)
1	68±4	73±3	22±2	70±4	63±1
1.5	91±3	65±4	61±5	60±3	39±3
2	117±4	52±4	102±7	54±2	35±3

Åhl et al. (2006) conducted a previous study investigating detached particles from MBBR carriers at various HRTs and SALRs and the authors found similar results to the DPA analysis in the current study. Åhl et al. found that when the HRT was increased from 45 minutes to 3 hours, the particle size shifted towards larger particles. Moreover, they revealed that by increasing the HRT the number of micron and submicron particles increased at HRTs longer than 2 hours. In a similar study, Melin et al. (2005) altered the HRT in a pilot scale MBBR/membrane process from 0.45 to 4 hours to investigate the effect of HRT on fouling of the membrane system. They also concluded that there is a clear shift towards smaller particles when the HRT of the system is shorter again confirming the results of the current study. Åhl et al. hypothesized that the observed larger particles at longer HRTs provides greater opportunity to form aggregates that have larger particle sizes. This explained well the formation of larger particles but it does not

explain why the solids produced by the longer HRT systems show poorer settling characteristics. This may have resulted from the formation of non-ideal flocs.

6.6 ESEM of MBBR Carriers

ESEM images were taken at three magnifications: 15x, 50x and 1000x, to characterize the biofilm attached to the AnoxKaldness K1. Figure 6.8 shows ESEM images at a magnification of 15x. These images along with Figure 6.9 show a decrease in biofilm thickness with increasing HRT. Figure 6.9 shows the actual thickness measurements of the biofilm on the internal wall of the media and Figure 6.10 illustrates the morphology and the structural changes in the attached biofilm by HRT variation.

The average biofilm thicknesses (based on twenty measurements) at HRTs of 1, 1.5 and 2 hours on the carriers were 483±53, 382±33 and 251±29 μm, respectively. Other than the factors discussed in Chapter 5 (i.e. hydrodynamics of the system, nutrient loading, DO concentration and SALR), HRT also has a notable effect on the thickness of the produced biofilm (Cunningham et al., 2001). Based on preliminary MBBR trials in the early stages of the current study, at HRTs of 4 and 6 hours no biofilm growth was observed on the carriers. This observation suggests that at long HRTs the biofilm thickness is reduced to zero as long HRTs promote suspended growth conditions preferentially over attached growth conditions.

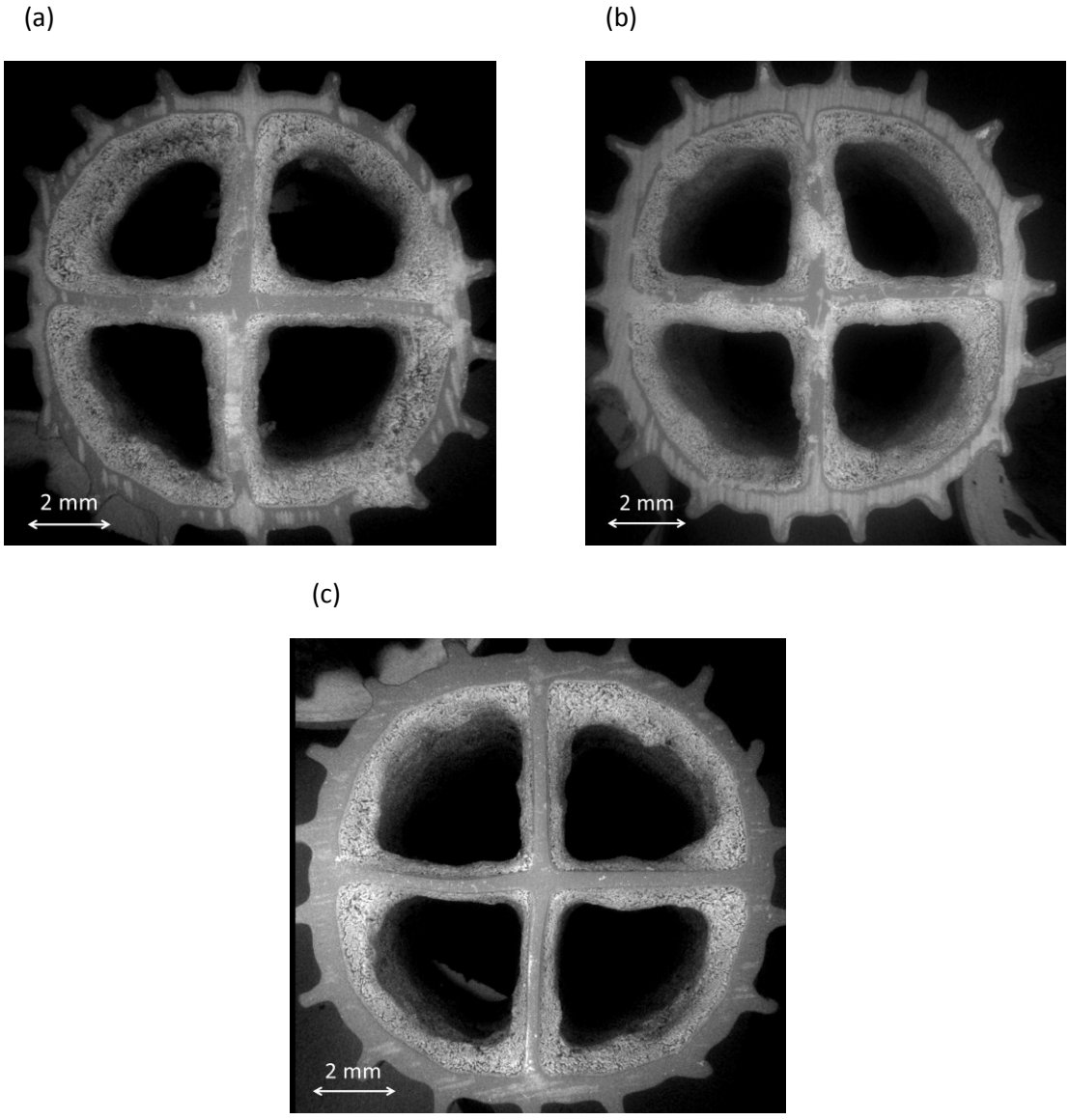

Figure 6.8 ESEM of MBBR reactors at various HRTs acquired at- 15x (a) HRT 1 hour (b) HRT 1.5 hours and (c) HRT 2 hours

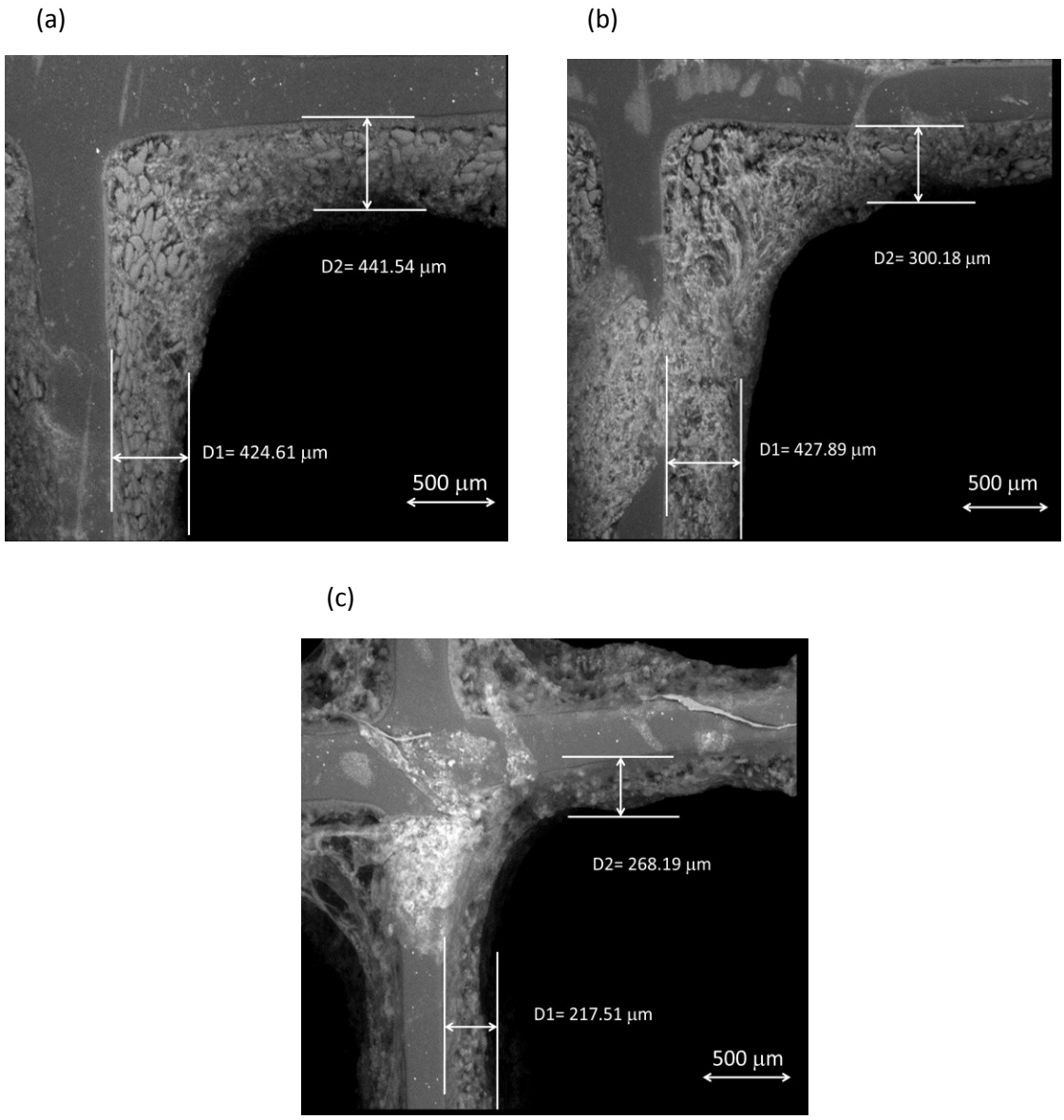

Figure 6.9 ESEM of MBBR reactors at various HRTs acquired at- 50x (a) HRT 1 hour (b) HRT 1.5 hours and (c) HRT 2 hours

Figure 6.10 shows the effect of HRT on the morphology of the biofilm. As discussed in Chapter 5, the biofilm produced on the media in the reactor with the HRT of 1 hour had string-like morphology with small vacancies within the bacterial matrix and at HRTs of 1.5 and 2 hours the carriers housed mushroom-shaped biofilms with some string-like.

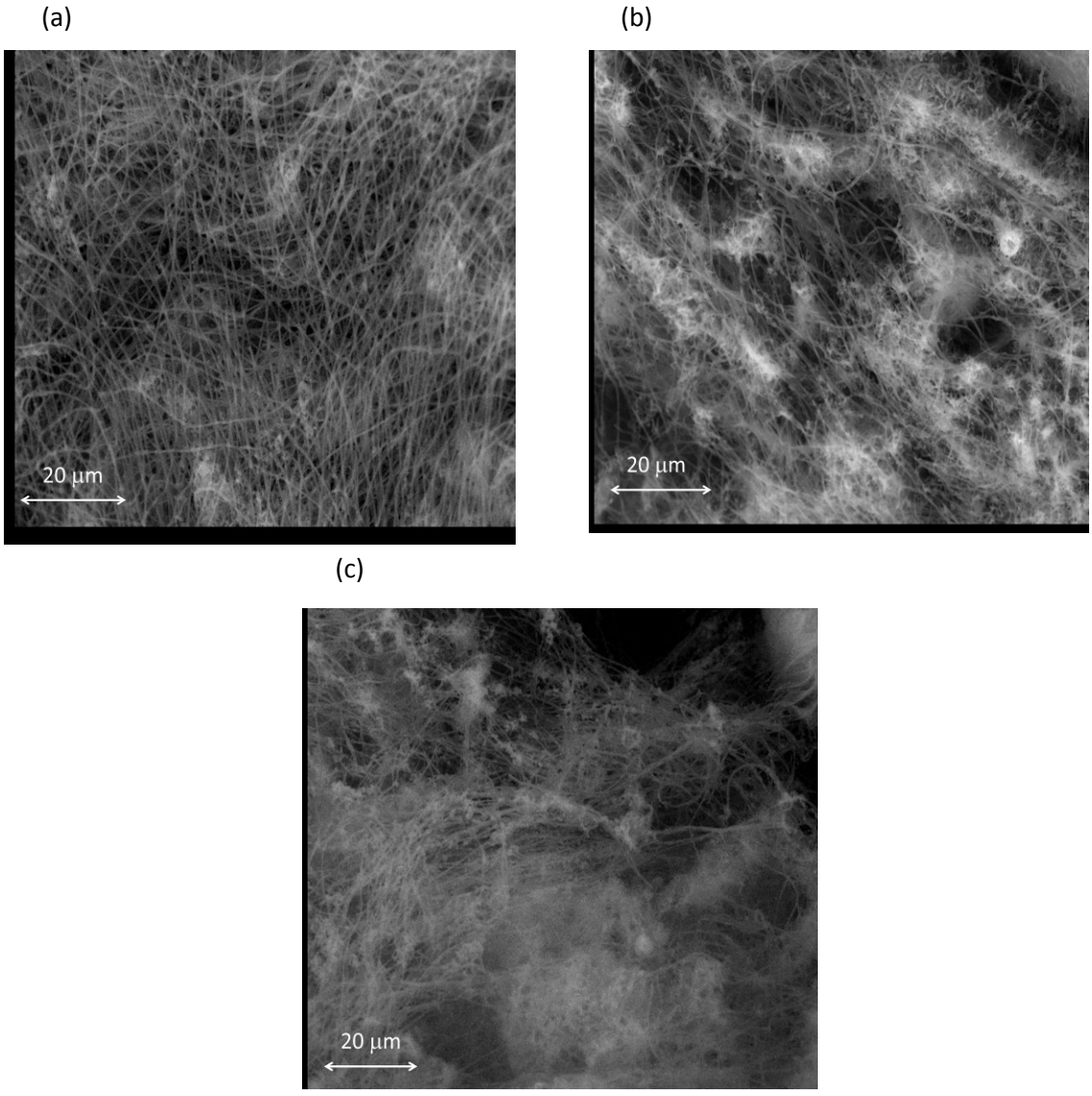

Figure 6.10 ESEM of MBBR reactors at various HRTs acquired at- 1000x (a) HRT 1 hour (b) HRT 1.5 hours and (c) HRT 2 hours

6.7 Biomass Yield and Solid Production Comparison in Two Different MBBR Experimental Phases

The produced solids in MBBR reactors at different SALRs and HRTs are shown in Table 6.7. The produced solids by the MBBR reactors increase as the SALR or HRT increases. The biomass yield is also shown in Table 6.4. The net biomass yield for MBBR reactors was calculated from Equation 5.2 and Equation 5.3 to convert $Y_{net,MBBR}$ to $Y_{true,MBBR}$. The results show that the biomass yield in MBBR reactors is maintained between 0.3 and 0.5 throughout the study.

Table 6.7 Solid production and biomass yield of MBBR reactors operated at various HRTs and SALRs

Reactor	**Solid Production (mg TSS/day)**	**Biomass Yield (g VSS/g COD)**
MBBR, HRT 1 hour	1660±20	0.310±0.03
MBBR, HRT 1.5 hours	2262±140	0.460±0.04
MBBR, HRT 2 hours	2130±180	0.380±0.03
MBBR, SALR 9 gCOD/m^2·d	434±20	0.400±0.03
MBBR, SALR 32 gCOD/m^2·d	1760±80	0.330±0.02
MBBR, SALR 64 gCOD/m^2·d	2900±250	0.330±0.03

Chapter 7

Conclusions and Recommendations

The AS and MBBR laboratory reactors were operated in this study to evaluate the settling characteristics and particles size distribution of the biologically-produced solids in MBBR systems. AS reactor results were used as a baseline, conventional treatment system data set, to compare with the MBBR data.

7.1 Conclusions

- Although changing the SRT of the AS reactors from 5 to 15 days did not change the COD removal levels, the mixed liquor of the 15 days SRT reactor settled very well, while that of the other reactors at SRTs of 5 and 10 days did not. This is based on the SVI and DI values that indicate poorer settling with decreasing SRTs.
- Increasing the MBBR organic SALR from 9 to 64 g COD/m^2·d, slightly decreased the COD removal percentage but also produced more solids with poorer settling characteristics, based on observed SVI and DI measurements. While increasing the MBBR reactors HRT from 1 to 2 hours, increased the COD removal rate and the quantity of solids produced, this change produced poorer settling biologically-produced solids.
- The volume based particle size distribution analysis of the AS reactors shows that at SRT 5 days, there is a larger percentage of larger particles while at SRT of 15 days the percent volume shifted to the smaller particle size ranges and at

intermediate SRT (10 days) the percent volume is distributed in both smaller and larger particle size ranges. Therefore, the particle size distribution seems to trend towards larger particles at lower SRTs.

- The volume-based particle size distribution analysis for the MBBR reactors demonstrates a shift towards larger sized particles at higher SALRs and longer HRTs.
- The AS reactors operated at an SRT of 15 days showed that settlement for 30 minutes almost completely removed particles at all the size ranges except for particles in the range of 2-30 μm, while 10 and 5 day reactors produced very poor settling particles > 400 μm and in the range of 2-400 μm based on the volume particle size distribution.
- Based on the volume particle size distribution, the MBBR reactors (at all investigated SALRs and HRTs) the poorest settling particles were in the 10-60 μm and 260-380 μm size ranges.
- The ESEM images show that the thickest biofilm coverage on the carriers was observed at the highest SALR of 64 $gCOD/m^2 \cdot d$ while the thinnest biofilm coverage occurred at the intermediate SALR value used in this study of 32 $gCOD/m^2 \cdot d$. Also, the images showed that by increasing the HRT from 1 to 2 hours, the average thickness of the biofilm on the carriers also increases.
- Generally, the lower SVI values in MBBR reactors showed that the biologically-produced solids in these reactors tend to settle better than that of the AS reactors. On the other hand, DI values showed less of a relative change due to increased SALRs and HRTs in the MBBR reactors as compared to increased SRTs in the

AS reactors. Therefore, changing the operating parameters in MBBR reactors has shown less of an evident impact on the settling characteristics of biologically-produced solids.

- The MLSS measurement for AS reactors and TSS measurements for MBBR reactors showed that the solids produced (mg TSS/day) by MBBR reactors are at least 8 times less than AS reactors. As the cost of sludge treatment is a significant portion of the total cost, running MBBR systems with proper operating parameters can be an economical alternative to small-scale AS systems.

7.2 Recommendations

The following recommendations are presented below to improve the biologically-produced solids removal in MBBR systems based on lab-scale reactor experiments of this study:

- Further experimental work that studies filtration of MBBR and AS effluents with a proper membrane or filter would help to develop a better understanding of the removal potential of the biologically-produced solids.
- The characterization of the settling characteristic of AS and MBBRs presented in the study should be repeated with real wastewater in order to determine the highly important aspect of influent particle interaction with the biologically-produced particles.
- A detailed study about MBBR particles detached from carriers and the morphology of produced biofilm on the carriers is informative. This will help to

find a relationship between settling characteristics and particle size distribution of solids with morphological and thickness characteristics of biofilms on carriers.

- An analysis of the particle size distribution analysis of particles smaller than 2 μm to determine the contribution of submicron and colloidal matters in settling characteristics of biologically-produced solids.
- Implementation of an experimental work for lower HRTs than 1 hour and higher HRTs than 2 hours would be helpful to find out the impact of HRT on the settling characteristics and particles size distribution of particles better as the present study was limited by reactor feeding and keeping the SALR constant such that the HRT changed only in the range 1-2 hours.
- Investigation of how other parameters (such as carrier size and percent fill) could affect the settling characteristics and particles size distribution in MBBR reactors will be helpful. In other words, this study can specify that which parameter can affect the settling characteristics and the particle size distribution of solids more than the other parameters.
- Implementation of a research on the effect of other factors such as chemical constituents, microbial population and physical properties of particles on their particle size distribution and settling characteristics in MBBR reactors will provide helpful information.

References

Abbas W. (2004), Disc Filtration and Floc Strength, Master of Science Thesis, Lund University, Sweden.

A˚hl R.M., Leiknes T.O., Ødegaard H., (2005). Tracking particle size distributions in a moving bed biofilm membrane reactor for treatment of municipal wastewater, Water Science and Technology, 53 (7), 33-42.

American Public Health Association, (2005). Standard methods for examination of water and wastewater, 21nd edition.

Andreadakis A., (1993) Physical and chemical properties of activated sludge floc, Water Research, 27 (12), 1707-1714.

Andreottola, G., Foladori, P., Ragazzi M., (2000). Upgrading of a small wastewater treatment plant in a cold climate region using an MBBR system, Water Science and Technology, 41(1), 177-185.

Aygun A., Nas B. and Berktay A., (2008). Influence of high organic loading rates on COD removal and sludge production in moving bed biofilm reactor, Environmental Engineering Science, 25(9), 1311-1316.

Barr, T.A., Taylor, J.M., Duff, S.J.B., (1996). Effect of HRT, SRT and temperature on the performance of activated sludge reactors treating bleached kraft mill effluent. Water Res. 30, 799–810.

Bisogni J., Lawrence A.W., (1971). Relationship between biological solids retention time and settling characteristics of activated sludge, Water Res., 5 (9), 753-763.

Bhattacharyya, Bimal C.; Banerjee, Rintu, (2007). Environmental Biotechnology, Oxford University Press.

Brightwell Technologies Inc., MFI Technology. http://www.jazdlifesciences.com/pharmatech/company/Brightwell-Technologies%20Inc/MicroFlow-Imaging-MFI%20Technology.htm?supplierId=30002617&productId=1019977 (Accessed on June 10th 2012).

Canada Gazette, (2010). Wastewater systems effluent regulations, 144 (12). http://www.gazette.gc.ca/rp-pr/p1/2010/2010-03-20/html/reg1-eng.html (Accessed 3 March 2012).

Carnes B. and Eller J., (1972). Characterization of wastewater solids, Water Pollution Control Federation, 44 (8), 1498-1517.

City of Ottawa, ROPEC wastewater treatment plant. http://ottawa.ca/en/env_water/water_sewer/sewer_septic/treatment/ropec/index.html (Accessed on 10th June 2012).

Cunningham A., Lennox J. and Ross R., (2011), Biofilm: The Hypertextbook, http://www.hypertextbookshop.com/biofilmbook/v004/r003/index.html (Accessed on June 10th 2012).

Da-Hong L. and Ganczarczyk J. J., (1991). Size distribution of activated sludge flocs, Research Journal WPCF, 63(5), 806-814.

Davis M, (2010). Water and Wastewater Engineering, WEF process for the water quality professional, first edition, published by McGraw-Hill.

Delatolla R., Tufenkji N., Comeau Y., Gadbois A., Lamarre D. and BerkD., (2009). Kinetic analysis of attached growth nitrification in cold climates, Water Science and Technology 60 (5), 1173-1184.

Delatolla R., Tufenkji N., Comeau Y., Lamarre D., Gadbois A., Berk D., (2009). In situ characterization of nitrifying biofilm: minimizing biomass loss and preserving perspective. Water Res, 43, 1775-87.

Droste R., (1997). Theory and practice of water and wastewater treatment, J. Wiley, New York.

Eckenfelder W., (1979). Principles of water quality management, Krieger Publishing Company, Springer, Edition 1.

Environment Canada, Hydromantis Inc.; AXOR Experts-Conseils Inc.; Ecole Polytechnique, Montréal, Québec, (2003). NH_3 treatment processes for the removal of ammonia from municipal wastewater.

Environmental Protection Agency, (1997). Wastewater treatment manuals: primary, secondary and tertiary treatment, Dublin, Ireland.

Forster C.F., (1983). Particle size analyses in relation to the operation of the activated sludge process, Environmental Technology, 4 (6), 239-246.

Guellil A., Thomas F., Block JC., Bersillon JL., Ginestet P., (2001). Transfer of organic matter between wastewater and activated sludge flocs. Water Research; 35(1), 143-50.

Hilligardt D. and Hoffmann E., (1997). Particle size analysis and sedimentation properties of activated sludge flocs, Water Science and Technology, 36 (4), 167–175.

Huang X., Wei CH., Yu K., (2008). Mechanism of membrane fouling control by suspended carriers in a submerged membrane bioreactor, Journal of Membrane Science, 309 (1-2), 15, 7-16.

Ivanovica I. & Leiknesa T.O., (2012). Particle separation in moving bed biofilm reactor: applications and opportunities, Separation Science and Technology, 47 (5).

Ivanovic I., Leiknes T., Ødegaard H., (2008). Fouling control by reduction of submicron particles in a BF-MBR with an integrated flocculation zone in the membrane reactor, Separation Science and Technology, 43 (7), 1871-1883.

Janczukowicz W., Szewczyk M., Krzemieniewski M., Pesta J., (2000). Settling properties of activated sludge from a sequencing batch reactor (SBR), 10 (1), 15-20.

Jirka, A.M.; Carter, M.J., (1975). Analytical Chemistry, 47(8), 1397 pages.

Jonathan C. Palm, David Jenkins and Denny S. Parker, (1980). Relationship between organic loading, dissolved oxygen concentration and sludge settleability in the completely-mixed activated sludge process, Water Pollution Control Federation, 2484-2506.

Keefer C. E. and Meisel J., (1951). Activated sludge studies. Part III Effect of pH of sewage on the activated sludge process, Sewage ind. Wastes 23, 982-991.

Klausen M., Heydorn A., Ragas P., Lambertsen L., Aaes-Jørgensen A., Molin S., Tolker-Nielsen T., (2003). Biofilm formation by Pseudomonas aeruginosa wild type, flagella and type IV pili mutants, Molecular Microbiology, 48 (6), 1511-1524.

Lee W., Kang I., Lee CH., (2006). Factors affecting filtration characteristics in membrane coupled moving bed biofilm reactor, Water Research, 40, 1827-1835.

Leiknes T., Ødegaard H., (2007). Wastewater reclamation and reuse for sustainability, the development of a biofilm membrane bioreactor, Desalination, (1-3, 5), 135-143.

Liao B.Q., Allen D.G., Leppard G.G., Droppo I.G., Liss S.N., (2002). Interparticle interactions affecting the stability of sludge flocs, Journal of Colloid and Interface Science, 249 (2), 372-380.

Little B., Wagner P., Ray R., Pope R., Scheetz R., (1991). Biofilms: an ESEM evaluation of artifacts introduced during SEM preparation. J. Ind. Microbiol. 8, 213-222.

McQuarrie, James P. Boltz, Joshua P., (2011). Moving bed biofilm reactor technology: process applications, design, and performance, Water Environment Research, 83(6), 560-575(16).

Melin E., Leiknes T., Helness H., Rasmussen V. and Ødegaard H., (2005). Effect of organic loading rate on a wastewater treatment process combining moving bed biofilm and membrane reactors, Water Science & Technology, 51 (6-7), 421-430.

Metcalf & Eddy Inc. , Tchobanoglous G., Burton F., Stensel D., (2003). Wastewater engineering: treatment and reuse, McGraw-Hill Science/Engineering/Math; 4th edition.

Niku S. and Schroeder E., (1981). Factors affecting effluent variability from activated sludge processes, Water Environment Federation, 53 (5), 546-559.

Ødegaard H., (2000). Advanced compact wastewater treatment based on coagulation and moving bed biofilm processes, Water Science & Technology, 42 (12), 33-48.

Ødegaard H., (2006). Innovations in wastewater treatment: the moving bed biofilm process, Water Science and Technology 53 (9), 17-33.

Ødegaard, H., Gisvold, B., Helness, H., Sjøvold, F. and Liao, Z. (2000). High rate biological/chemical treatment based on the moving bed biofilm process combined with coagulation. In: Chemical water and wastewater treatment VI, Springer Verlag, Heidelberg, 245- 255.

Ødegaard H., Gisvold, B., Strickland, J., (2000). The influence of carrier size and shape in the moving bed biofilm process, Wat. Sci & Tech., 41 (4-5), 383-391.

Ødegaard H., Rusten, B. and Westrum, T., (1994). A new moving bed biofilm reactor – Applications and results, Wat. Sci. Tech., 29 (10-11), 157-165.

Ragsdale & Associates, (2004) Wastewater System Operator's Manual, http://ragsdaleassociates.com/WastewaterStudy.htm (Accessed on June 10th 2012).

Rahimi Y., Torabian A., Mehrdadi N., Habibi-Rezaie M., Pezeshk H., Nabi-Bidhendi GR., (2010). Optimizing aeration rates for minimizing membrane fouling and its effect on sludge characteristics in a moving bed membrane bioreactor. Hazard Mater. 28, 186 (2-3), 1097-102.

Richardson, J. F. & Zaki, W. N., (1954). Sedimentation and fluidization. Trans. Inst. Chem. Engrs 32, 35-53.

Rusten B., Eikebrokk B., UlgenesY., Lygren E., (2006). Design and operations of the Kaldnes moving bed biofilm reactors, Aquacultural Engineering 34 (3), 322-331.

Rusten, B., Hem, L., Odegaard, H., (1995). Nitrogen removal from dilute wastewater in cold climate using moving bed biofilm reactors, Water Environment Research 67 (1), 65-74.

Sears K., Alleman J., Barnard J. and Oleszkiewicz J., (2006). Density and activity characterization of activated sludge flocs, Journal of Environmental Engineering, 132, (10) 1235-1242.

SEM laboratory at Carleton University. http://sem.carleton.ca/ (Accessed on 10 June 2012).

Shahriari H., Droste R., (2003). M.A.Sc Thesis, Evaluation and modeling of a membrane activated sludge system. University of Ottawa, Ottawa, Canada.

Sombatsompop K., Visvanathan C., Benaim R., (2006). Evaluation of biofouling phenomenon in suspended and attached growth membrane bioreactor systems, Desalination, 201, 138-149.

Stanley W., (1949). Factors affecting the efficiency of activated sludge plants, Sewage Works Journal, 21 (4), 625-640.

Sunner N., Evans C., Siviter C., Bower T., (1999). The two-stage moving bed/activated sludge process: An effective solution for high-strength wastes, Water and Environmental Management Journal, 13 (5), 353-358.

Tuntoolavest M., Miller L. and Grady C.P., (1983). Factors affecting the clarification performance of activated sludge final settlers, Water Pollution Control Federation, 55 (3).

US EPA Office of Prevention, Pesticides, and Toxic Substances (1998). OPPTS 870.3220, Chemical safety and pollution prevention; Fate, transport and transformation test guidelines, 712-C-98-301.

US EPA Office of Wastewater Management, Mark Rossow, (2004). Primer for municipal wastewater treatment systems, US, Washington DC.

Wang R., Wen X., Qian Y., (2005). Influence of carrier concentration on the performance and microbial characteristics of a suspended carrier biofilm reactor, Process Biochemistry, 40 (9), 2992-3001.

Wanner J., (1994). Activated sludge bulking and foaming control technomic Pub., 327 pages.

Water Environment Federation, (2010). Design of municipal wastewater treatment plants MOP 8, fifth edition, published by McGraw-Hill.

Wessman F., H. Johnson CH., and AnoxKaldnes, Inc., (2006). Cold weather nitrification of lagoon effluent using an MBBR treatment process, Proceedings of the Water Environment Federation, WEFTEC: Session 61 through Session 70 (13), 4738-4750.

Wilen B.-M.; Balmer P., (1999). The effect of dissolved oxygen concentration on the structure, size and size distribution of activated sludge flocs Water Research, 33 (2), 391-400 (10).

Wu J., Jiang X., Wheatley A., (2009). Characterizing activated sludge process effluent by particle size distribution, respirometry and modelling, Desalination 249, 969-975.

Appendix A

Influent and Effluent COD Measurement

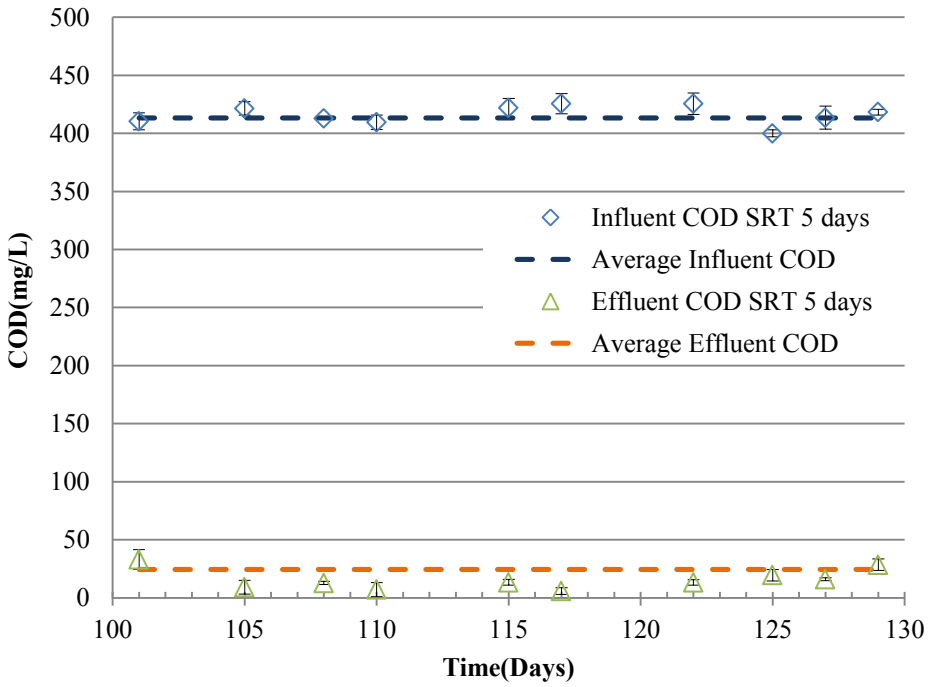

Figure A-1 Activated sludge reactor SRT 5 days: influent and effluent COD

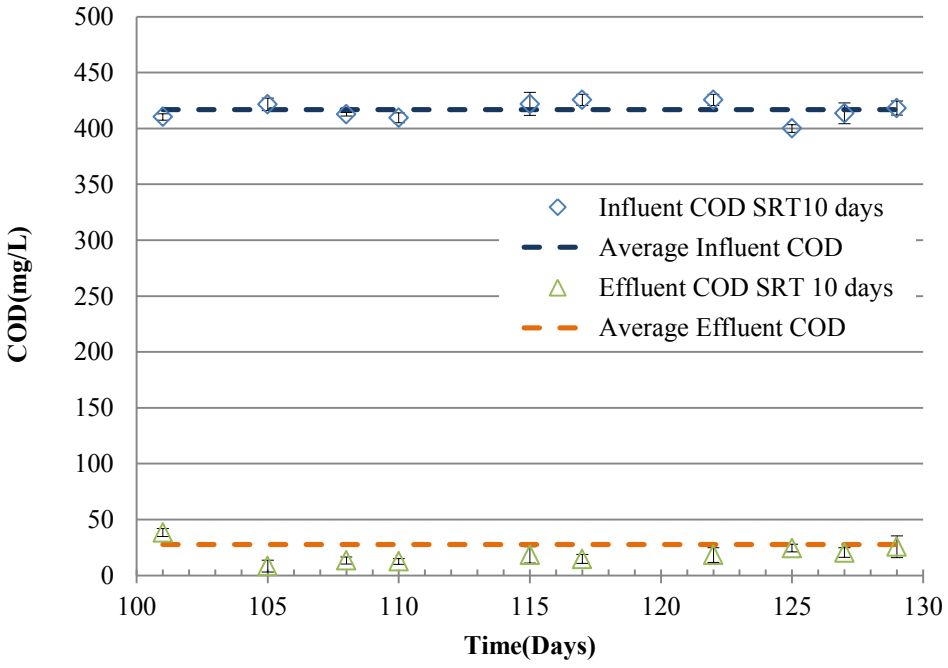

Figure A-2 Activated sludge reactor SRT 10 days: influent and effluent COD

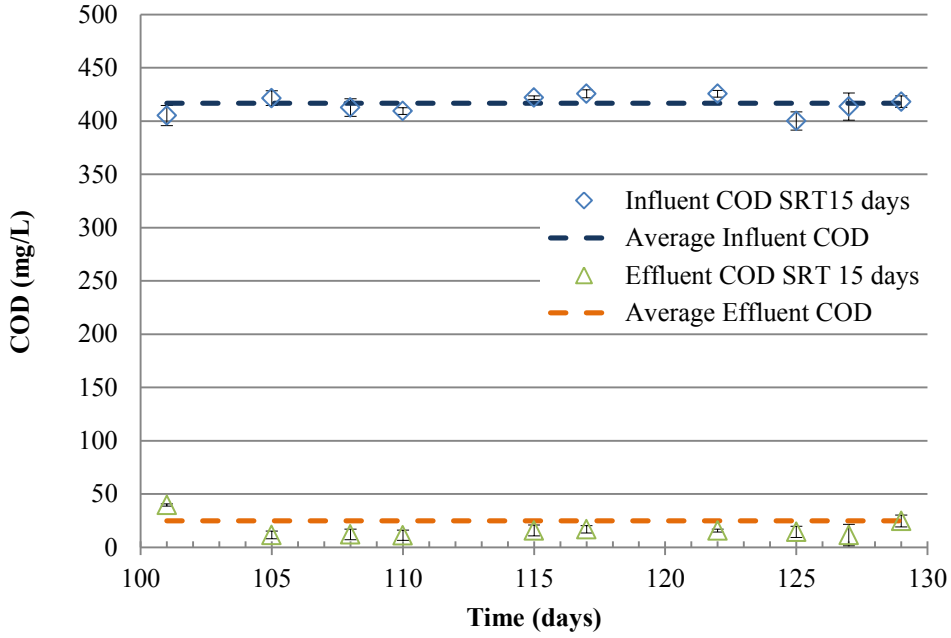

Figure A-3 Activated sludge reactor SRT 15 days: influent and effluent COD

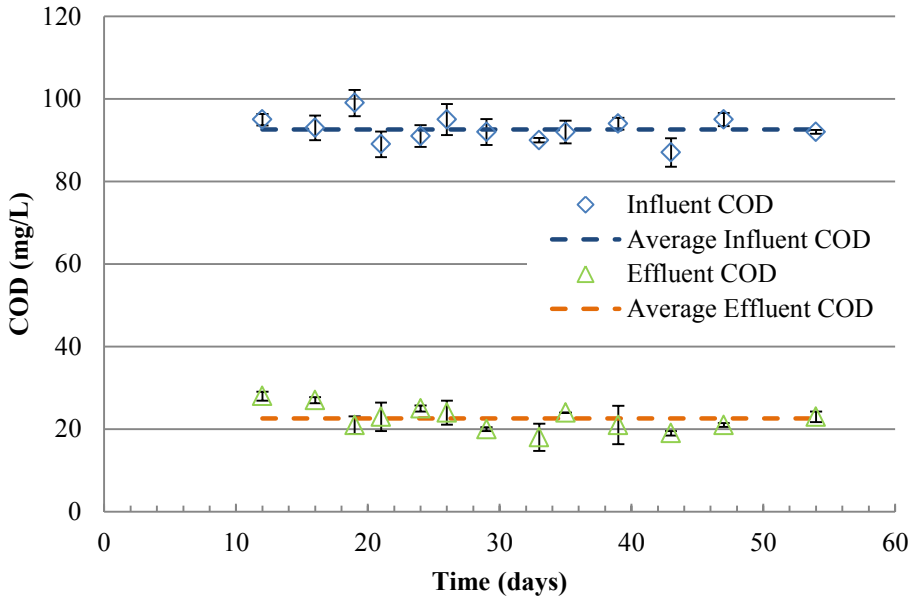

Figure A-4 MBBR reactor SALR 9 gCOD/m^2·d: influent and effluent COD

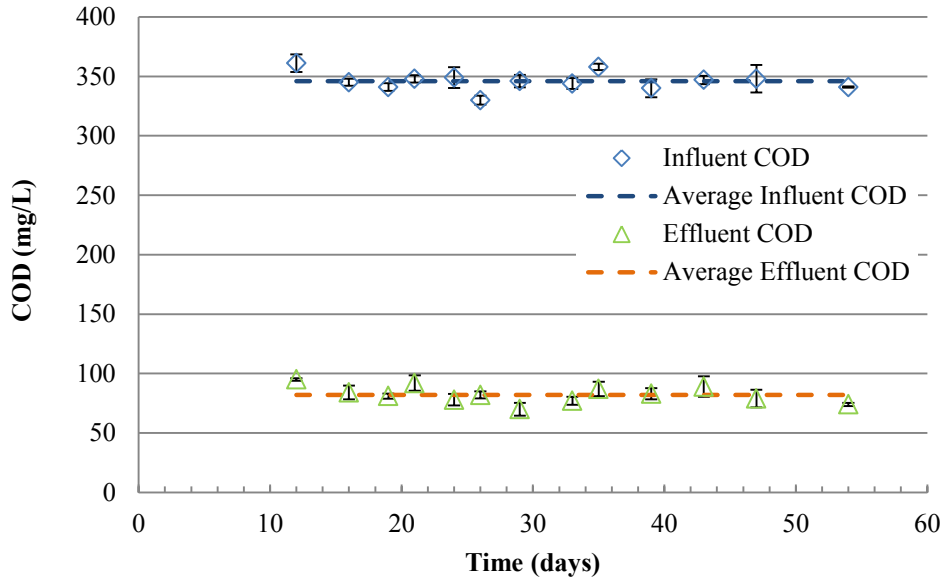

Figure A-5 MBBR reactor SALR 32 gCOD/m^2·d: influent and effluent COD

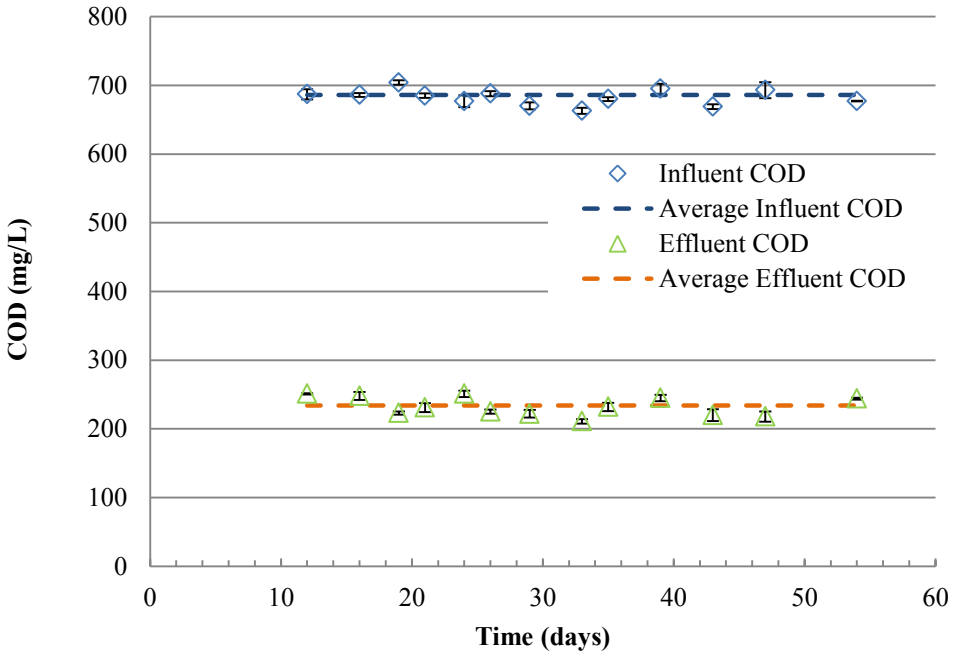

Figure A-6 MBBR reactor SALR 64 gCOD/m^2·d: influent and effluent COD

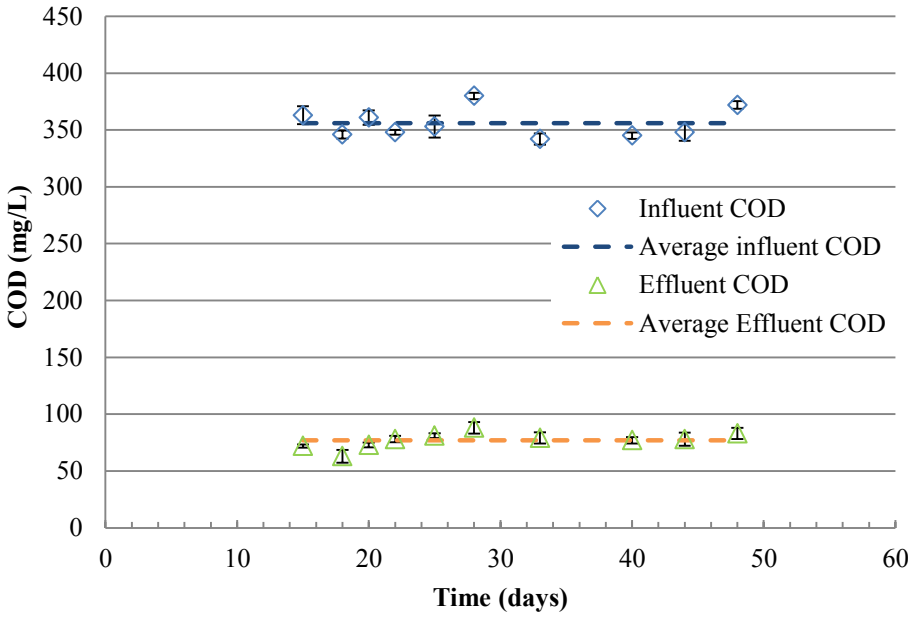

Figure A-7 MBBR reactor HRT 1 hour: influent and effluent COD

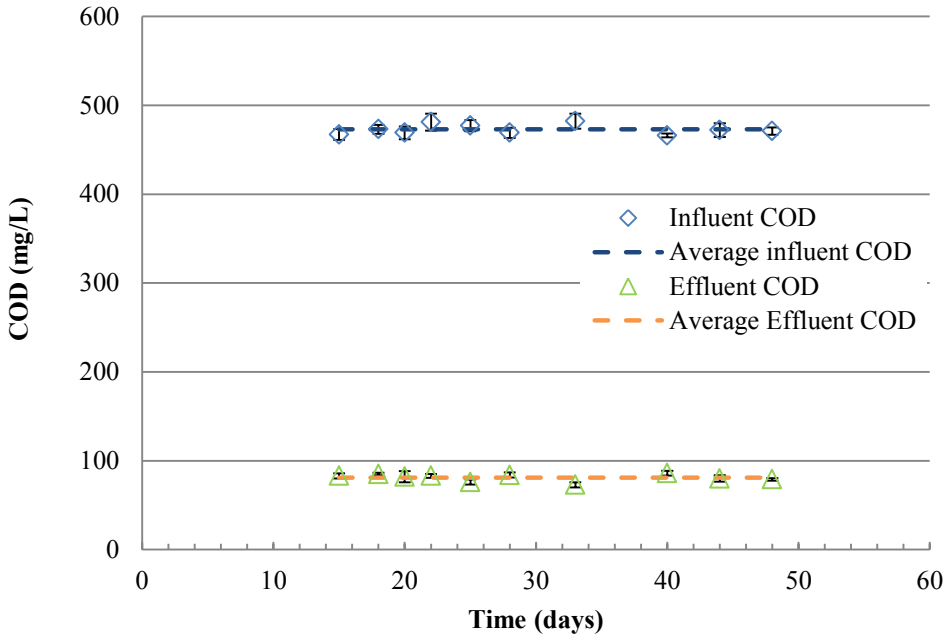

Figure A-8 MBBR reactor HRT 1.5 hours: influent and effluent COD

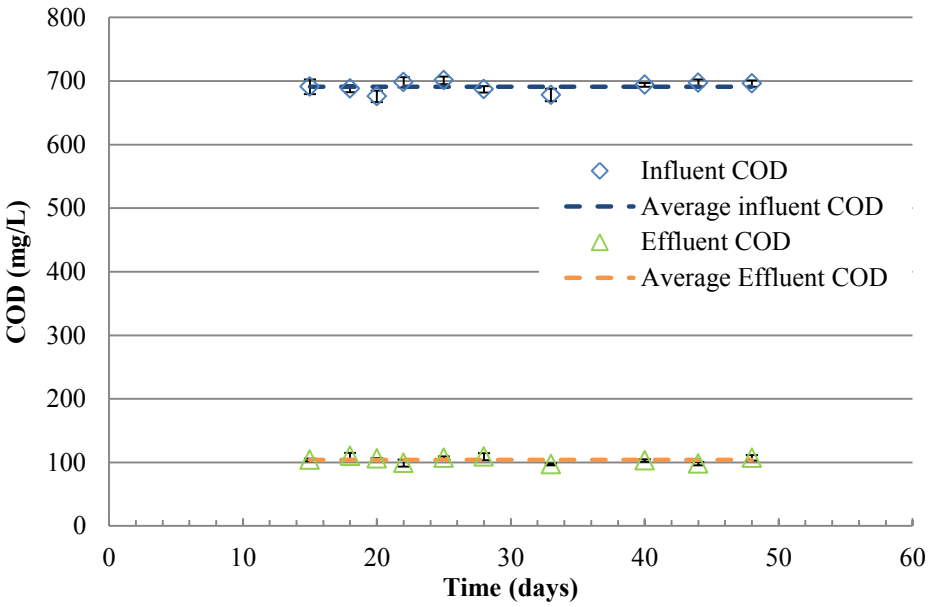

Figure A-9 MBBR reactor HRT 2 hours: influent and effluent COD

Appendix B

TSS Measurement

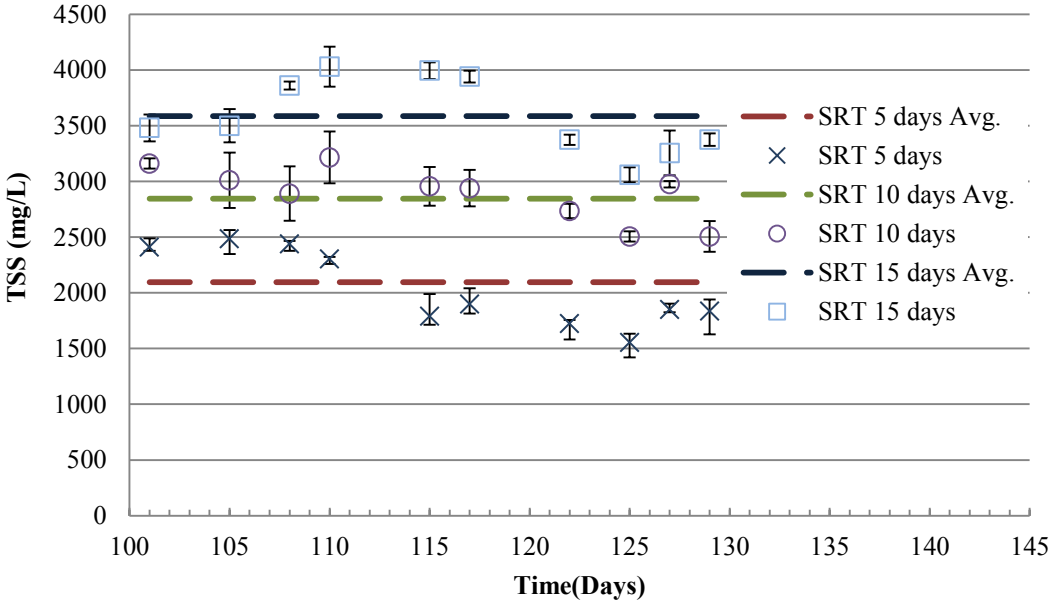

Figure B-1 Activated sludge reactors: MLSS concentrations at various SRTs

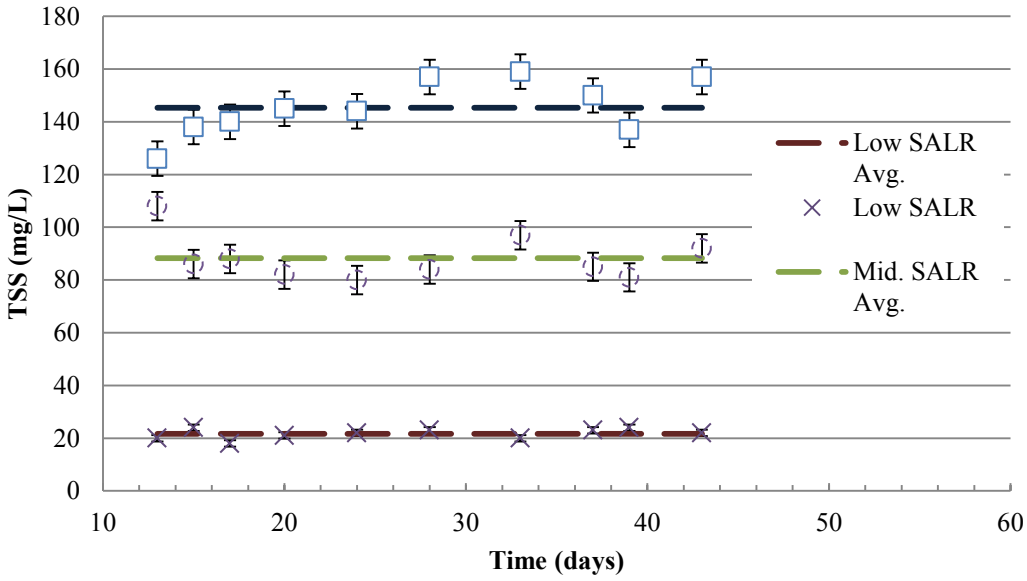

Figure B-2 MBBR reactors: TSS concentrations at various SALRs

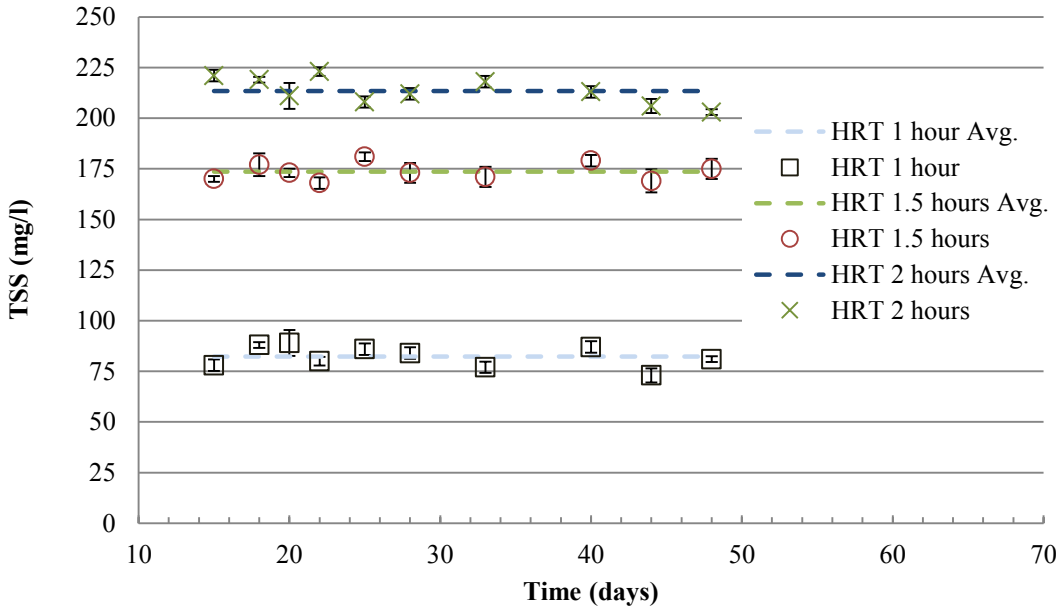

Figure B-3 MBBR reactors: TSS concentration for different HRTs

Appendix C

SVI and DI Measurement

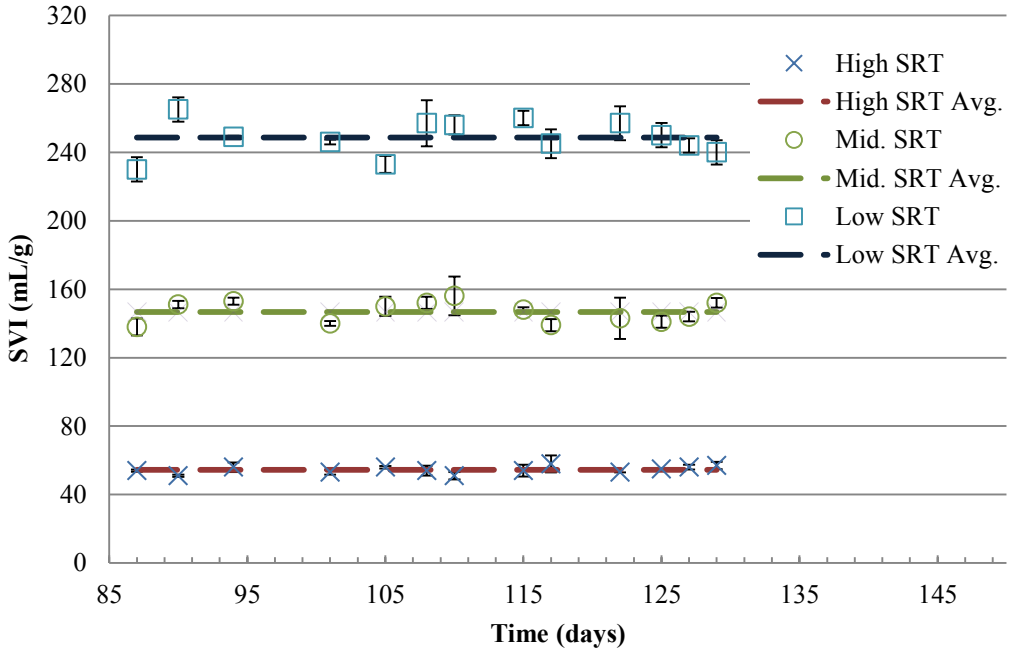

Figure C-1 Activated sludge reactors: SVI values for different SRTs

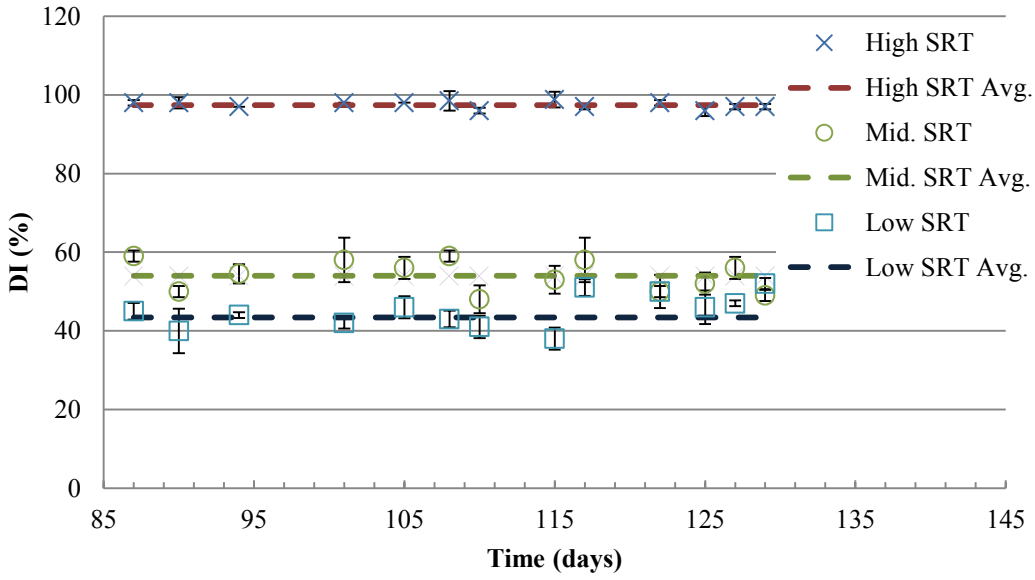

Figure C-2 Activated sludge reactors: SVI values for different SRTs

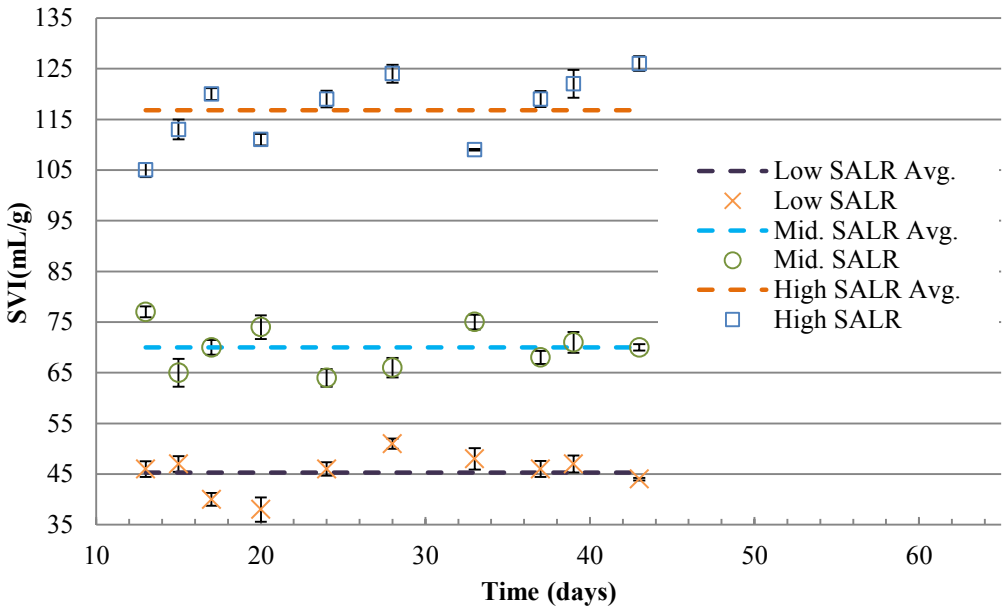

Figure C-3 MBBR reactors: SVI values for different SALRs

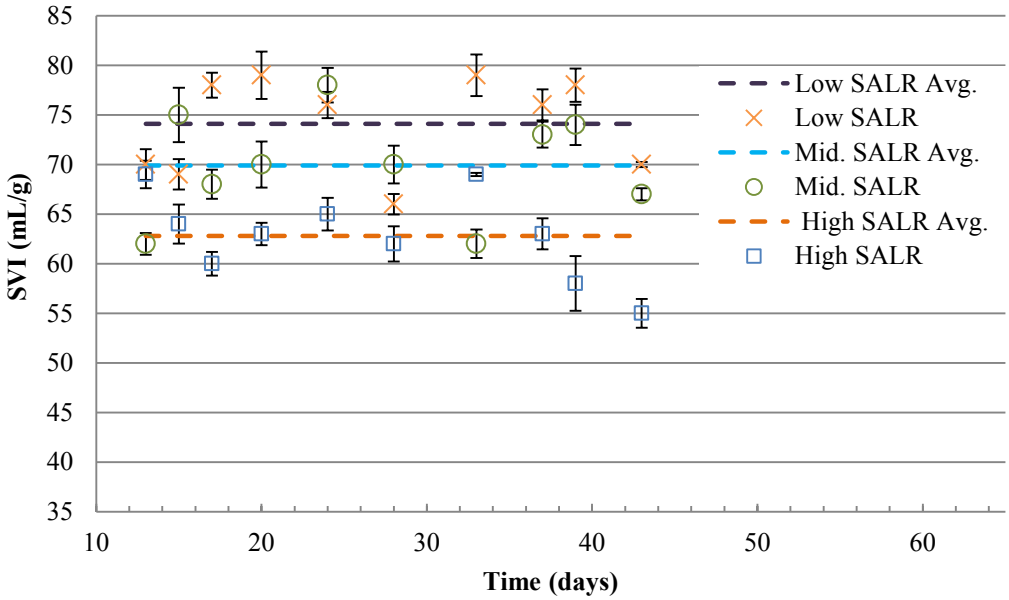

Figure C-4 MBBR reactors: DI values for different SALRs

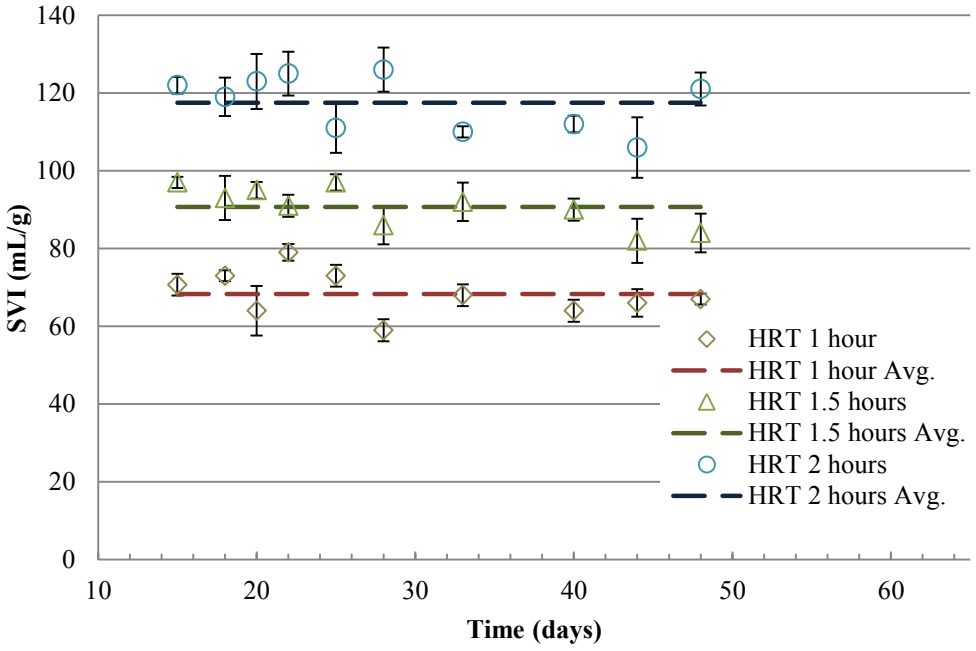

Figure C-5 MBBR reactors: SVI values for different HRTs

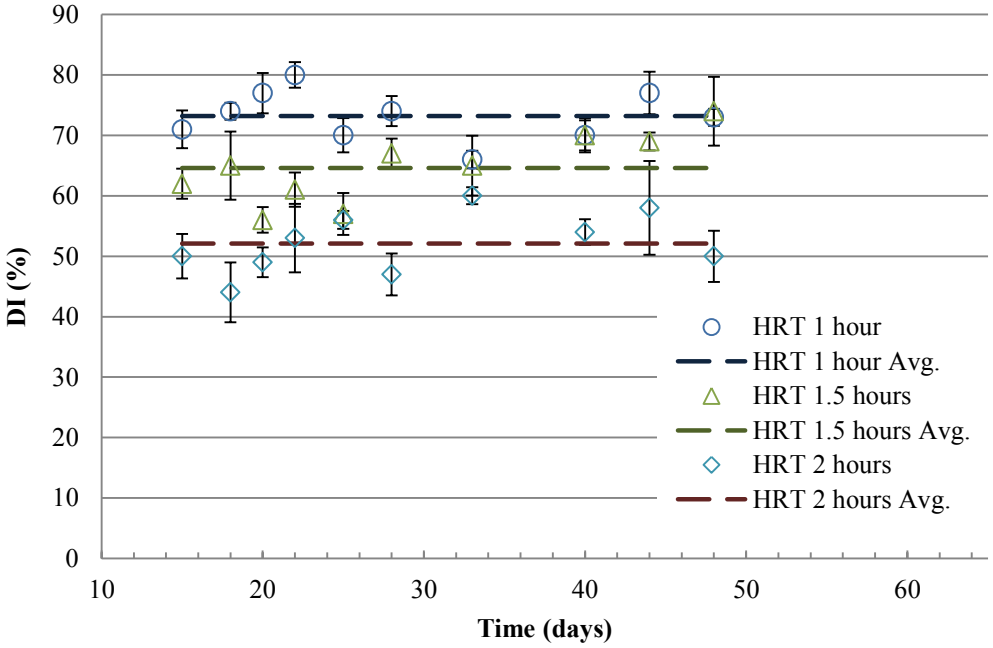

Figure C-6 MBBR reactors: DI values for different HRTs

Appendix D

Density of Biological Solid Calculation

Table D-1 Density calculation for AS biological solids at various SRTs

AS Reactors SRT (days)	(ρ= 1000 mg/ml) **TSS_{DPA} (mg/L)**	(ρ= 1050 mg/ml) **TSS_{DPA} (mg/L)**	(ρ= 1100 mg/ml) **TSS_{DPA} (mg/L)**	(ρ= 1150 mg/ml) **TSS_{DPA} (mg/L)**	(ρ= 1200 mg/ml) **TSS_{DPA} (mg/L)**	**$TSS_{Experimental}$ (mg/L)**
5	2007.00	2107.35	2207.70	2308.05	2408.40	2029.00
10	2075.00	2178.75	2282.50	2386.25	2490.00	2889.00
15	3166.00	3324.30	3482.60	3640.90	3799.20	3587.00
Average Error (%)	13.66	11.92	10.90	10.88	12.80	0.00

Table D-2 Density calculation for MBBR biological solids at various SALRs

MBBR Reactors SALR (g COD/m^2·d)	(ρ= 1000 mg/ml) **TSS_{DPA} (mg/L)**	(ρ= 1050 mg/ml) **TSS_{DPA} (mg/L)**	(ρ= 1100 mg/ml) **TSS_{DPA} (mg/L)**	(ρ= 1150 mg/ml) **TSS_{DPA} (mg/L)**	(ρ= 1200 mg/ml) **TSS_{DPA} (mg/L)**	**$TSS_{Experimental}$ (mg/L)**
9	19.13	25.10	26.29	27.49	28.68	22.00
32	69.19	72.60	80.30	83.95	87.60	88.00
64	140.60	147.7	152.50	159.50	166.44	145.00
Average Error (%)	12.48	11.15	11.14	13.18	15.20	0.00

Table D-3 Density calculation for MBBR biological solids at various HRTs

MBBR Reactors HRT (hrs)	(ρ= 1000 mg/ml) **TSS_{DPA} (mg/L)**	(ρ= 1050 mg/ml) **TSS_{DPA} (mg/L)**	(ρ= 1100 mg/ml) **TSS_{DPA} (mg/L)**	(ρ= 1150 mg/ml) **TSS_{DPA} (mg/L)**	(ρ= 1200 mg/ml) **TSS_{DPA} (mg/L)**	**$TSS_{Experimental}$ (mg/L)**
1	75.10	78.85	82.61	86.36	90.12	82.00
1.5	141.00	148.05	155.10	162.15	169.20	174.00
2	197.10	206.95	216.81	226.66	236.52	213.00
Average Error (%)	11.61	7.19	4.46	6.18	7.90	0.00